Probabilistic and Deterministic Analysis of Earth Dams

In this book, the program of SLIDE (version6.0) depending on two approaches; Deterministic and probabilistic analysis have been used to analyze slope stability and seepage of Mandali earth dams under different load conditions. The limit equilibrium method according to Bishop and Morgenstern-Price is applied to define the potential slip surface and to calculate the factor of safety of the dam slopes. The results obtained from deterministic analysis showed that the factor of safety decreases when increase the value of unit weight of the soil. The decrease also with varying proportions ratio for the increase of seismic load coefficients values and drawdown ratio for rapid drawdown condition. The factor of safety for drains increases when water level decreased with varying Proportions for the increase the value of cohesion of soil and angle of internal friction. For probabilistic analysis, the results showed that the probability of failure is equal to (55.2 %). Also sensitivity analysis is made to investigate the effect of each design parameter and shows that the parameters have sharp effects on the factor of safety of side slopes.

Nabaa Noori Shamsaldeen B.Sc. Civil Engineering, Iraq, University of Kufa, Faculty of Engineering,Civil Department,2008. M.Sc. Hydraulic Structures Engineering, Iraq, University of Kufa, Faculty of Engineering, Civil Department, 2014.

NOOR PUBLISHING

978-3-330-85016-3

Mandali Dam as a Case Study

Shamsaldeen, Khassaf, Abdoul-Hameed

NOOR PUBLISHING

Nabaa Noori Shamsaldeen

Saleh Issa Khassaf

Maha R. Abdoul-Hameed

Probabilistic and Deterministic Analysis of Earth Dams

Nabaa Noori Shamsaldeen
Saleh Issa Khassaf
Maha R. Abdoul-Hameed

Probabilistic and Deterministic Analysis of Earth Dams

Nabaa Noori Shamsaldeen
Saleh Issa Khassaf
Maha R. Abdoul-Hameed

Probabilistic and Deterministic Analysis of Earth Dams

Noor Publishing

Impressum / Imprint
Bibliografische Information der Deutschen Nationalbibliothek: Die Deutsche Nationalbibliothek verzeichnet diese Publikation in der Deutschen Nationalbibliografie; detaillierte bibliografische Daten sind im Internet über http://dnb.d-nb.de abrufbar.

Bibliographic information published by the Deutsche Nationalbibliothek: The Deutsche Nationalbibliothek lists this publication in the Deutsche Nationalbibliografie; detailed bibliographic data are available in the Internet at http://dnb.d-nb.de.

Coverbild / Cover image: www.ingimage.com

Verlag / Publisher:
Noor Publishing
ist ein Imprint der / is a trademark of
OmniScriptum GmbH & Co. KG
Bahnhofstraße 28, 66111 Saarbrücken, Deutschland / Germany
Email: info@omniscriptum.com

Herstellung: siehe letzte Seite /
Printed at: see last page
ISBN: 978-3-330-85016-3

Republic of Iraq
Ministry of Higher Education
and Scientific Research
University of Kufa Faculty of Engineering
Department of Civil Engineering

DETERMINISTIC AND PROBABILISTIC FOR EARTH DAMS ANALYSIS: CASE STUDY MANDALI DAM

By

Nabaa Noori Bashboosh Shams Aldeen

بسم الله الرحمن الرحيم

ومن يتوكل على الله فهو
حسبه أن الله بالغ أمره قد
جعل الله لكل شيء قدرا

صدق الله العلي
العظيم

سورة الطلاق من الآية(3)

ACKNOWLEDGEMENT

In the name of Allah the most compassionate the most merciful.
Praise be to Allah and pray and peace be on his prophet Mohammad and Kinsfolk His home.

First of all, Many thanks and praise are devoutly offered to my Creator, the almighty **ALLAH**, the most beneficent, the most gracious and most merciful, who gave me the ability and the desire to complete this study despite of all the hurdles and constraints in the way of its completion.

I would like to express my sincere appreciation and deepest gratitude to **Prof. Dr. Saleh I. Khassaf** and **Dr. Maha Rasheed Abdoul-Hameed** whom I have the honor to work under their supervision and guidance. Their constructive suggestion, patience and continuous encouragement are highly acknowledged throughout this research. Special thanks are devoted to **Asst. Lec. Uday Alturrfy** and **Mr. Haider Sabah ALkhafajy** for their assistance and care during my work.

I record my sincere gratitude to my family and friends for their encouragement, support; and efforts in order to achieve this work.

Finally, I am grateful to all those who participate in providing me the help and assistance to complete this research.

Noori Bashboosh Shams Aldeen ***Nabaa***

2013

ABSTRACT

In this research, the finite element method (using **SLIDE** (version6.0) computer program) depending on two approaches; **Deterministic** and **probabilistic** analysis have been used to analyze slope stability and seepage of earth dams under different load conditions. The limit equilibrium method according to Bishop and Morgenstern-Price presented by computer program is applied to define the potential slip surface and to calculate the factor of safety of the dam slopes. The effects of each design parameter and load conditions on this factor of safety are studied.

Deterministic analysis includes ground water parameters (phreatic surface location with types of drain and flow vectors), soil properties (shear strength parameters), and load condition (rapid drawdown, distributed load, and seismic force) and probabilistic analysis (probability of failure, reliability index and sensitivity analysis).

The results obtained from deterministic analysis showed that the factor of safety decreases prorate (6.32%) for the increase of the value of unit weight of the soil. Prorate is (28.67%) for the increase of the value of the seismic load coefficients and prorate is (48.754%) for the increase of the drawdown ratio for rapid drawdown condition. The factor of safety increases between (0.83% - 15.40%) for horizontal drain, (2.03% -15.53%) toe drain and (12.09% -16.428%) chimney drain when water level decreased. Prorate is (67.78%) for the increase the value of cohesion of soil, and prorate (57.95%) for increase of the value of angle of internal friction.

For probabilistic analysis, the results showed that the probability of failure is equal to (55.2 **%**). Also sensitivity analysis is made to investigate the effect of each design parameter and shows that the parameters have sharp effects on the factor of safety of side slopes. Stability of upstream side decreases gradually from the

beginning of drawdown to a ratio of drawdown ratio equal to 0.78 at which the most dangerous state may occur.

In case of zoned earth dams, taking Mandali Dam as a case study, the finite element method performed by **SLIDE** program is used to analyze the seepage problem, total head, pressure head distribution, position of phreatic surface and flow vectors for three cross sections at different distance along length of the dam for three major cases, maximum, normal, and minimum water level. The results of side slope stability was investigated under different load conditions analyses show that a critical condition would happen in the upstream side in case of rapid drawdown condition and seismic load. However, the Dam would be closely safe under the other two cases considered (drawdown condition and seismic load), resulting in a minimum safety factor of (1.167) with seismic load coefficient 0.09. For transient groundwater analysis results make a guide that at time (50000 hours, 6 years) Mandali Dam reaches to steady state condition.

Contents

List of Figures

List of Tables

List of Symbols

Symbol	Description
b	Slice width ,(L)
C	Cohesion of soil,(FL^{-2})
C_V	Coefficient of variation of the safety factor, (= σ / μ)
$\bar{c}$	Effective cohesion of soil,(FL^{-2})
E	Interslice normal forces (F)
EL	Horizontal interslice force (from left side of slice),(F)
ER	Horizontal interslice force (from right side of slice),(F)
Ff	Factor of safety with respect to force equilibrium
Fm	Factor of safety with respect to moment equilibrium
FOS	Factor of safety
$FOS_{min.}$	Minimum factor of safety
H	Height of dam ,(L)
HCV	Highest conceivable value of the random variable
i	Hydraulic gradient
K	Hydraulic conductivity. ,(LT^{-1})
Kx	Hydraulic conductivity in x direction .(LT^{-1})
Ky	Hydraulic conductivity in y direction .(LT^{-1})
D	Drawdown of reservoir level. (L)
D/H	Drawdown ratio in the reservoir,(dimensionless)
LCV	Lowest conceivable value of the random variable
l	The inclined width of slice, (L)
NUM.FAILED	Number of Analyses with Safety Factor < 1.
NUM.TOTAL	Total number of analyses (samples)
N	Effective normal force, (F)
n	Number of slices
P	Pressure (FL^{-2})
P	Normal force on the base of the slice,(F)
PF	Probability of failure
R	Radius of slip surface ,(L)
S	Shear strength, (FL^{-2})
U	Velocity component in x-direction. (LT^{-1})
u	Pore water pressure, (FL^{-2})
$\bar{u}$	Initial pore water pressure before drawdown, (FL^{-2})
V	Velocity component in y-direction. (LT^{-1})
Vs	Seepage velocity through porous media. (LT^{-1})
W_i	Weight of the slice,(F)
X	Interslice shear forces,(F)

Symbol	Description
X_L	Vertical component on interslice forces (from left side of slice)
X_R	Vertical component on interslice forces (from right side of slice)
Z	Elevation head (L)
Δu	Change in pore water pressure due to rapid drawdown
γ	Unit weight of soil
θ	Slope angle of slice
β	Reliability index
γ_w	Unit weight of water. (F/L^3)
σ	Normal effective stress
τ	Shear stress
f(x)	Function
λ	Scaling factor
ϕ	Angle of internal friction of soil
μ_{FOS}	Mean safety factor
σ_{FOS}	Standard deviation of safety factor.
β_{LN}	Lognormal Reliability Index
$\bar{\phi}$	Effective angle of internal friction of soil
θ_i	Slope of slice.

Chapter One

Introduction

1.1 General

Dams are structures that serve to store water for use during periods of drought or to protect land areas, represent one of the civilizations oldest engineered structures. In current times, dams are an essential component of water supply systems, hydroelectric power facilities, and flood-control projects. Dams can also serve to create reservoirs for recreational and navigational use and for sediment retention. A dam frequently serves as a multipurpose facility.

The earth dam is the first type of dams built by human to control and manage the water resources and figure (1.1) shows one of the earth dams. The earth dam is developed with the development of engineering science in the domain of hydraulic and geotechnical. The earth dam should be designed such that the failure does not occur and should be safe and stable in slope stability during construction and throughout its life.

For slope stability analysis of earth dam two types of analysis are used:

- Deterministic analysis: where all parameters (C,ϕ, γ, and seismic force) are accurately known, hence there will be aunique output. Deterministic problems are easier to deal with and are referred to as a certainty design.
- Probabilistic analysis: where many of the involved parameters cannot be evaluated with a high certainty. Therefore there will be several outputs and the engineer should choose the right output. These can be solved by using probabilistic approach and are referred to as uncertainty problems.

In the present research, two approaches are depended: Deterministic and probabilistic analysis will analyze seepage and slope stability for one of the zoned earth dam in Iraq (**Mandali Dam as case study)** by using computer programs of analyzing **SLIDE** (version6.0)

Figure (1.1) The Earth Dam

1.2 Types of Failure of Earth Dams

For earth dams, the term "failure" is defined herein as an occurrence of excessive erosion or deformation of the embankment that may result in an uncontrolled release of reservoir water or damage to appurtenant structures. To assess the safety of a dam and the possibility of failure, the different potential failure mechanisms must be recognized. Failure mechanisms are grouped into four general categories: slope stability, piping, overtopping, and foundation failures, as shown in Figure (1.2) below.

In the present work, side slope stability against failure will be analyzed under different loads and water conditions.

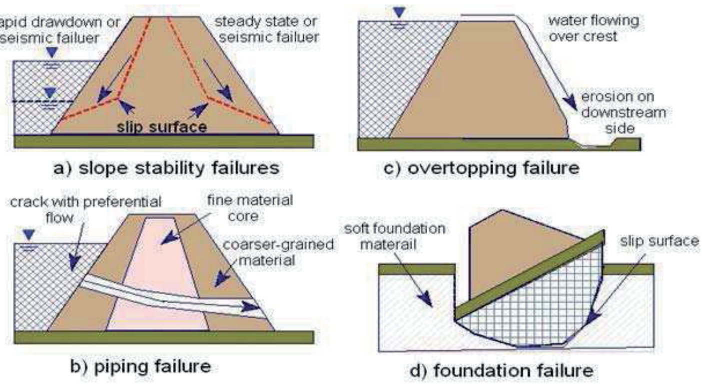

Figure (1.2) Failure Mechanisms for Earth Dams (**USBR,** 2001**).**

1.3 Seepage through Earth Dams

The seepage study through the body of earth dams is important during the dam design stage to calculate the losses from reservoir, pore water pressure distributions used primarily in the analysis of stability against shear failure, and position of the free surface which is used as boundary condition in the analysis of the side slope stability **(Sherard et al., (1963)).**

In the present work the finite element numerical model will be used to investigate the unconfined seepage problem and position of phreatic surface in a zoned earth dam.

1.4 Stability Analysis of Earth Dams

There are three types of slope stability failures for earth dams: (steady-state, seismic and rapid-drawdown). For the steady-state case, failure occurs on the downstream side of the dam under conditions of steady-state seepage. This type of failure may occur as a result of an increase in pore water pressure in the dam. For the rapid-drawdown case, failure occurs on the upstream side of the embankment as a result of a sudden lowering of the reservoir level. For the seismic case, the driving force on the soil mass increases due to a horizontal earthquake force, where as the resisting force may be reduced if portions of the embankment or foundation liquefy. Liquefaction can occur during an earthquake in loose, saturated, sandy soils. During liquefaction, the soil particles are rearranged into a denser configuration, which tends to displace pore water. Since the pore water cannot vacate the pore spaces immediately, the pore water pressure temporarily increases. If this increase is sufficient, the soil particles become supported by the pore water, which has no shear strength. As a result, the shear strength of the soil approaches zero. When performing a seismic slope stability analysis, it may be found that at times during the earthquake when ground shaking is at a maximum, the Factor of Safety falls below 1.0 and some deformation occurs **[USBR,** (2001)**].**

1.5 Objectives of the Study

The objectives of the present study are:

1. Conducting a probabilistic and deterministic analysis of earth dam. For deterministic analysis study the effect of a ground water parameters (phreatic surface location with types of drain, rainfall infiltration and factor of safety), material properties (cohesion of soil, angle of internal friction, unit weight of soil), and loading condition (seismic load coefficient, distributed load, tension cracks and rapid drawdown in water level) on the stability of an earthen dam. Probabilistic analysis will give the probability of failure, reliability index and sensitivity analysis

2. Analyzing a zoned earth dam [**Mandali Dam as case study**] including seepage analysis under different water conditions and transient groundwater analysis , slope stability analysis for steady state condition, rapid drawdown condition, and seismic load condition for deterministic analysis
3. Probabilistic analysis to find the probability of failure, reliability index and sensitivity analysis of a zoned earth dam[**Mandali Dam**].

1.6 Layout of the Study

To meet the above mentioned objectives, the present study is divided into the following chapters:

Chapter One: (Introduction) presents a general introduction to stability of earth dam's problem.

Chapter Two: (Basic Concepts and Literature Review) offer a summary about the theories to solve problems of seepage analysis through earth dams and slope stability analysis of earth dams.

Chapter Three: This chapter contains a comparison between the results of SLIDE V.6.0 (computer program) and other programs and techniques to check the reliability of this program.

Chapter four: display a parametric study carried out to demonstrate the effect of some design parameters (Ground water, material properties, load parameters, and dynamic load parameters).

Chapter five: Re- analysis and evaluation of the stability of one Iraqi zoned earth dam [Mandali Dam as case study] under different load condition.

Chapter Six: (Conclusions and Recommendations) presents the conclusions drawn from this study and the recommendations for future works.

Chapter Two

Basic Concepts and Literature Review

This chapter presents the necessary background and theory concerning stability and seepage. Therefore consideration must be given to a number of different topics. Firstly, descriptions of seepage theories in soil mechanics and secondly, brief descriptions of the theories of stability. Most of the previous studies on the seepage through earth dams and slope stability analysis under static and pseudo static will be reviewed in this chapter.

2.1 Theoretical Seepage Analysis

The study of seepage through earth dams is one of the important analyzes in dam design in order to calculate the quantity of water losses from the reservoir. It should give estimation to the pore water pressure distribution, locating the position of the free surface which is used in the analysis of the dam stability against the shear failure. Finally, studying the hydraulic gradient gives a general idea about the potential piping.

Seepage analysis forms an important and basic part of geotechnical engineering. It may be required in volume change prediction, ground water contamination control, slope stability analysis, and the design of earth structures such as dykes or dams. [Fredlundet.al.,2001]

2.2 Steady-State Seepage through Earth Dams

The most critical conditions are likely to occur with the reservoir full under steady state seepage and those resulting, during and after rapid drawdown of the reservoir water level. In order to assess the factor of safety of a potential slip surface, the distribution of pore pressure in the dam must be known. Failures of earth or rockfill dams can result from excessive leakage from piping at the toe, or from slope failures on the dam face in upstream and downstream side. All the three cases can be analyzed with the aid of a steady-state flow net.

2.3 The Equation of Flow through a Porous Medium

The flow of water through saturated porous medium is generally governed by Darcy's Law [**Harr**, (1962)];

$$Vs = ki \qquad \dots (2\text{-}1)$$

where:

Vs : Seepage velocity through porous media. (L/T)

k : Hydraulic conductivity. (L/T)

i : Hydraulic gradient = $-\dfrac{\partial H}{\partial s}$

H : Piezometric head. (L)

S : Distance along the flow line. (L)

Darcy's Law is considered to be of great importance in studying agreat number of practical problems since it is applicable to flow through porous media of two and three dimensions.

2.4 The General Equation of Steady Seepage Flow

The two-dimensional anisotropic components of seepage through porous media according to the general Darcy's Law form are [**Freeze** and **cherry**, (1979)].

$$U = kxIx = -kx\frac{\partial H}{\partial x} \qquad \dots \quad (2\text{-}2a)$$

$$V = kyIy = -ky\frac{\partial H}{\partial y} \qquad \dots \quad (2\text{-}2b)$$

where

U: velocity component in x-direction. (L/T)

V: velocity components in y-direction. (L/T)

k_x, k_y: Hydraulic conductivity in x, y directions respectively. (L/T)

H: Piezometric head ($H = \frac{P}{\gamma_w} + z$). (L)

P: pressure (F/L^2).

γ_w: Unit weight of water. (F/L^3) and.

z: elevation head (L).

The continuity equation for two-dimensional and incompressible, irrotational flow is:

$$\frac{\partial U}{\partial x} + \frac{\partial V}{\partial y} = 0 \quad \text{… (2-3)}$$

Substituting Darcy's equation (2-2) in equation (2-3) gives:

$$\frac{\partial}{\partial x}\left(k_x \frac{\partial H}{\partial x}\right) + \frac{\partial}{\partial y}\left(k_y \frac{\partial H}{\partial y}\right) = 0 \quad \text{… (2-4)}$$

For homogenous and isotropic soil, the hydraulic conductivity is equal every where in all directions: $k_x = k_y$

Then equation (2-4) becomes:

$$\frac{\partial^2 H}{\partial x^2} + \frac{\partial^2 H}{\partial y^2} = 0 \quad \text{… (2-5a)}$$

Equation (2-5a) is called Laplace Equation and it is similar to Laplace Equation of velocity potential for ideal fluid flow or non-viscous, irrotational flow.

Laplace equation represents the condition of steady-state laminar flow and different methods to find the piezometric head of the flow domain can be used.

For homogenous and anisotropic soil the hydraulic conductivity is equal every where and not equal in all directions, i.e.: $k_x \neq k_y$

Then Laplace equation becomes:

$$kx\frac{\partial^2 H}{\partial x^2}+ky\frac{\partial^2 H}{\partial y^2}=0 \qquad \text{… (2-5b)}$$

where:

kx : Hydraulic conductivity in the horizontal direction.

ky : Hydraulic conductivity in the vertical direction.

2.5 Methods for Solution of Laplace's Equation

In order to do a seepage analysis, a general model describing the phenomena of seepage must be available. Supplied with specific boundary conditions and soil properties, this model can be used to determine head and flow distribution and seepage quantities. Laplace equation is the mathematical basis for several models or methods used in seepage analysis.

Solutions to steady-state, laminar flow, seepage problems must solve Laplace's equation. Several methods have been developed to solve exactly or approximately Laplace's equation for various cases of seepage, The following methods are the most widely used methods according to **[Lambe** and **Whitman, 1969]**. One of the most widely used methods, the flow net, can be adapted to many of the under seepage and through-seepage problems found in dams and other projects involving hydraulic structures.

2.5.1 Models

Models which scale or simulate the flow of water in porous media can provide a good view for what is occurring during seepage and allow a physical view for the reaction of the flow system to changes in head, design geometry, and other assumptions. These models are: sand models, electrical analogies and viscous flow models

2.5.2 Graphical Method

The flow net sketching was first suggested by Forchheimer and further developed by A.Casagrande (1937)**, [Lambe** and **Whitman**, 1969**].** The solution of seepage equation (2.5a) in two dimensions may be presented by two families of curves intersecting one another orthogonally and forming a pattern of curvilinear squares. The two families of lines are known as equipotential lines, or lines joining points of equal total head, and streamlines

2.5.3 Analytical Method

Exact solutions to the Laplace equation may be obtained by various analytical methods.

The simplest theoretical solution are suggested by Kozeny (1931**)** who considered the problem of seepage throughout an earth dam with a parabolic upstream face, resting on an impervious base and having a horizontal toe drain located on the down stream portion of the dam. The flow net for the section consists of a system of confocal parabolas [**Lambe and Whitman**, 1969].

Casagrande,(1940)**[**Quoted from **Al-Qaisi,** (1999)**]**,developed approximations Kozeny's solution to include dams with trapezoidal toe drains and slope drains and suggested an adjustment to account for a straight upstream face.

Unconfined flow in dams was also studied by Numerov [reported by **Harr 1962**] who obtained solution in graphical form but, unfortunately, its application is still not straightforward.

2.5.4 Numerical and Computer Methods

As a result of many difficulties that appear through analytical methods, approximate and experimental methods, it was resorted to numerical methods in order to get the required results with good accuracy. These results could be compared with analytical solutions by applying various boundary conditions for simple problems beside the development of computer systems. These methods are: finite difference, finite volume, finite elements, boundary elements, and analytical elements method. Computer models are used to make acceptable approximations for the Laplace equation in complex flow conditions. The three primary methods of numerical solution are finite difference, finite element and boundary element. All can be used in one, two, or three-dimensional modeling. Several computer programs for these methods are available. In the present work the finite element method will be used.

2.5.4.1 Finite- Element Method

This method is also based on grid pattern (not necessarily rectangular) which divides the flow region into discrete elements and provides (N) equations with (N) unknowns. Material properties, such as permeability, are specified for each element and boundary conditions (heads and flow rates) are set. A system of equations is solved to compute heads at nodes and flows in the elements. The finite element has several advantages over the finite difference method for more complex seepage problems. These include [U.S. Army Crops. of Engineers, 1986]:

- Complex geometry including sloping layers of material can be easily accommodated.
- By varying the size of elements, where seepage gradients or velocity are high zones can be accurately modelled.
- Pockets of material in a layer can be modelled

The finite element method was first applied to boundary value field problems by Zienkiewicz and Cheung (1966). Later their method was extended to obtain a solution for steady state seepage in an anisotropic foundation under a concrete dam [**Zienkiewics et al.**, 1966].

Zhang et al., (2000) have pointed out that in problems of steady seepage, it is not necessary to determine the iteration process or the enter free surface, but only the elevation of the release point. It is shown by the finite element mesh in several examples.

Subuh, (2002) presents a mathematical model and applies it for analyzing two–dimensional steady state seepage through stratified and isotropic earth dams. A numerical solution using finite elements method (Galerkin method) is employed to predict the piezometric head distribution, seepage quantity, pore water pressure, and locating the free surface profile.

Al- Labban,(2007) utilizes the finite element method to solve the governing equations of flow through earth dams. Eight node isoparametric elements are used to model the dam and its foundation, while mapped infinite elements are used to model the problem boundaries. The computer program Geo-Slope is used in the analysis through a sub-program named SEEP/W. The program is verified by analyzing three problems which were previously solved using the flow net.

AL- Jairry,(2010) presents an application of finite element analysis, using CivilFEM/ANSYS software, to predict two dimensional steady state water seepage through an earth dam of two soil zones resting on impervious base. Seepage characteristics (quantity and length of seepage surface) produced at downstream are investigated against permeability coefficient ratio changing of the two soil zones, and based on results of the solution/. It has been found that seepage quantity and velocity downstream are very sensitive to any change of permeability ratio of the two soil zones forming the dam.

Pakhshandehroo et al.,(2011) have modeled the earth dam by a finite element mesh. The pore water pressure in the dam was investigated following its construction and first and second impoundments. The overall trend in monitored pore water pressure is well modeled by the transient analysis. The result shows that the six month time period between impoundments is long enough for the pore water pressure to reach equilibrium everywhere throughout the core except where considerable initial construction induced pore water pressure is observed. Therefore, it is concluded that pore pressures in the core of earth fill dams may not achieve steady state conditions even several months after the dam construction and impoundments.

2.6 Stability Analysis

Slope stability analysis using computers is an easy task for engineers when the slope configuration and the soil parameters are known. However, the selection of the slope stability analysis method is not an easy task. Effort should be made to collect the field conditions and the failure observations in order to understand the failure mechanism, which determines the slope stability method that should be used in the analysis. Therefore, the theoretical background of each slope stability method should be investigated in order to properly analyze the slope failure and assess the reliability of the analysis results.

Two dimensional slope stability methods are the most common used methods among engineers due to their simplicity. However, these methods are based on simplifying assumptions to reduce the three-dimensional problem to a two-dimensional problem .Therefore the accuracy of the analysis results varies according to the used method.

A stability analysis of earth dams and banks requires consideration of the coupled effects of:

- Loads such as body weight, surcharge, and forces caused by sequential construction.

- Seepage forces due to steady or transient flow of water. Often, for simplicity, the effects of external and seepage forces are uncoupled and superimposed [**Li** and, **Desai**, 1983].

2.6.1 Conventional Methods of Slope Stability Analysis

Most of the methods currently utilized in slope stability analysis are based on the equilibrium limit approach. The essential assumption of this approach is the validity of well known Moher-Coulomb failure criterion which defines the shear strength of soil as follows:

$$S = c + \sigma \tan\varphi \qquad \text{......................... (2.6)}$$

Where (c), (ϕ) and (σ) are cohesion intercept, angle of internal friction, and the normal stress respectively. The method of limit equilibrium assumes that the shear strength of the soil is partially mobilized along an assumed failure surface which may be a straight line, circular arc, logarithmic spiral curve or any other irregular surface. The method, however, defines the factor of safety (FOS) as the ratio of available shear strength (S) and the developed shear stress (τ):

$$FOS = \frac{S}{\tau} \qquad \text{................(2.7)}$$

Equation (2.7) is a form of definition introduced by Bishop (1955) which has gained fairly wide acceptance. The factor of safety (FOS) is taken as the ratio of the total shear strength available on the slip surface to total shear stress mobilized (τ) in order to maintain equilibrium [**Spencer**, 1967]. The interest lies in materials that are saturated with groundwater; in such a case, equation (2.6) takes the form:

$$S = c + (\sigma - u)\tan\varphi \qquad \text{................(2.8)}$$

In which (u) is the pore water pressure. For the mentioned definition, the method of slices appears as a good approach for obtaining an accurate solution for any shape of failure [**Whitman**, and **Bailey**, 1967].

2.6.2 Method of Slices

In the method of slices, the soil mass above the slip surface is divided into a number of vertical slices and the equilibrium of each of these slices is considered. The actual number of the slices depends on the slope geometry and soil profile. However, breaking the mass up into a series of vertical slices does not make the problem statically determinate. In order to get the factor of safety by using the method of slices, it is necessary to make assumptions to remove the extra unknowns and these assumptions are the key roles of distinguishing the methods.

Most computer programs are using the methods of slices, as they can handle complex slope geometries, variable soil and water conditions and the influence of external boundary loads. Therefore, they are the most commonly used methods in slope stability analysis [**Al-Bataineh,** 2006]. Some of the most popular and significant methods are described hereinafter.

It is very important to define the techniques that are used to select the shape of the slip surface and the location of the critical slip surface. The **U.S. Army Corps of Engineers,(2003a)** recommend that the shape and location of the critical slip surfaces are subjected to the limitations bellow:

- **Shape of the Slip Surface.** All of the limit equilibrium methods require a potential slip surface to be assumed in order to calculate the factor of safety. Calculations are repeated for a sufficient number of trial slip surfaces to ensure that the minimum factor of safety has been calculated. For computational simplicity the candidate slip surface is often assumed to be circular or composed of a few straight lines.

- **Location of the Critical Slip Surface:** The critical slip surface is defined as the surface with the lowest factor of safety. Because different analysis procedures employ different assumptions, the location of the critical slip surface can vary somewhat among different methods of analysis. The critical slip surface for a given problem analyzed by a given method is found by a systematic procedure of generating trial slip surfaces until the one with the minimum factor of safety is found. Searching schemes vary with the assumed shape of the slip surface and the computer program used.

2.6.2.1 Ordinary Method of Slices

This method is also referred to as "**Fellenius**' method. It is the simplest method of slices to use. The method assumes that the resultant of the interslice forces acting on any slice is parallel to its base, therefore the interslice forces are neglected (Fellenius, 1936). Only moment equilibrium is satisfied. In this respect, factors of safety calculated by this method are typically conservative. Factors of safety calculated for flat slopes and/or slopes with high pore pressures can be on the conservative by as much as 60 percent, when compared with values from more exact solutions (**Whitman** and **Baily**, 1967). For this reason this method is not used much nowadays. [**Al-Bataineh,** 2006].

2.6.2.2 Simplified Bishop Method

This method was first described by Bishop (1955). The simplified version of the method is developed further by Janbu et al**.** (1956). Ihis method neglects the inter-slice shear force since it assumes that the resultant of the inter-slice forces acting on each slice has a horizontal line of action and associated with circular slip surfaces, violates the equilibrium equation of horizontal force so it is an approximate method.(**Lambe** and **Whitman**, (1969)).

Whitman and **Bailey** (1967*)* indicate that the error in the values of factor of safety obtained by this method of analysis is usually less than 5%. The value of safety factor by using the simplified method, FOS, can be calculated from:

$$FOS = \frac{\sum_{i=1}^{i=n}\left[\bar{c}\Delta x_i + (W_i - u_i\Delta x_i)\tan\bar{\phi}\right]\left[1/M_i(\theta)\right]}{\sum_{i=1}^{i=n} W_i \sin\theta_i} \qquad \ldots (2\text{-}9)$$

where:

$$M_i(\theta) = \cos\theta_i\left(1 + \frac{\tan\theta_i \tan\bar{\phi}}{FOS}\right) \qquad \ldots (2\text{-}10)$$

The $\bar{c}$ and $\bar{\phi}$ are effective shear strength parameters for the soil at the base of the slice

n: number of slices

W_i : weight of the slice.

θ_i : slope of slice.

u_i : the average pore water pressure at the bottom of the slice is equal to $u_i = h_i * \gamma_w$

h_i: height of the water in the piezometer placed at the bottom of the slice.

Equation (2-9) is to be solved by trial and error method since FOS appears on both sides of the equation. However the convergence of trial is very rapid. Also $M_i(\theta)$ can be found from Figure (2.1). The two methods above [ordinary method and simplified Bishop method] are presented in Figure (2.2) which shows the differences between the two method

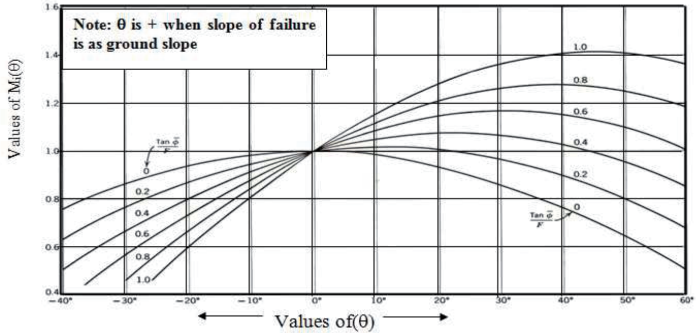

Figure (2.1) Values of $M_i(\theta)$ **(After Janbu, 1973)**

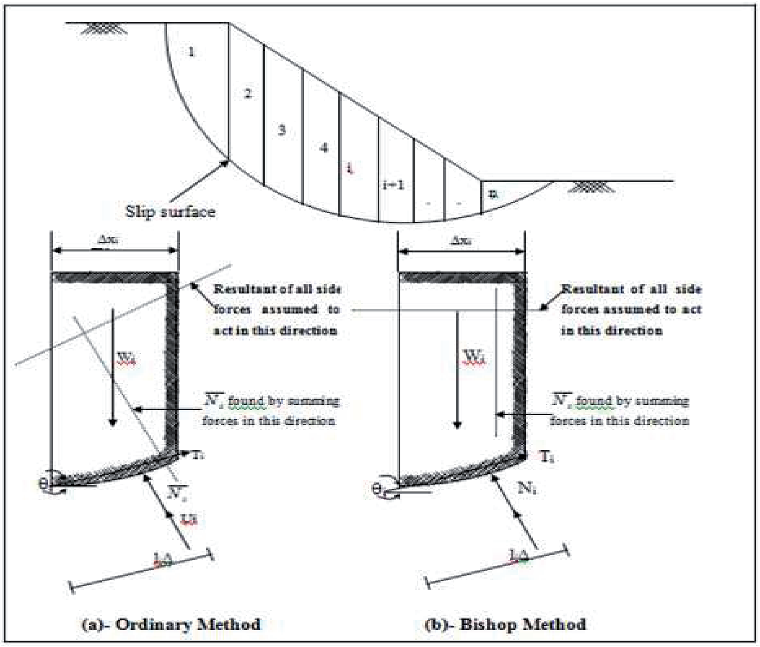

Figure (2.2) General Slip Surface and Forces Acting on Typical Slice according to **[Lambe** and **Whitman,** 1969**].**

2.6.2.3 Morgenstern and Price's Method

This method is developed by **Morgenstern** and **Price** (1965). It is considerd not only the normal and tangential equilibrium but also the moment equilibrium for each slice in circular and non-circular slip surfaces. In this method, a simplifying assumption is made regarding the relationship between the interslice shear forces (**X**) and the interslice normal forces (**E**) as:

$$X = \lambda \cdot f(x) \cdot E \qquad \text{.........} \quad (2.11)$$

Where, f(x) is an assumed function that varies continuously across the slip and (λ) is an unknown scaling factor that is solved for as part of the unknowns.

The unknowns that are solved for in the Morgenstern and Price method are the factor of safety (FOS), the scaling factor (λ), the normal forces on the base of the slice (P), the horizontal interslice force (E), and the location of the interslice forces (line of thrust). Once the above unknowns are calculated using the equilibrium equations, the vertical component of the resultant force on the interslice forces (X) is calculated from equation (2.11).

An alternative derivation for the Morgenstern-Price method is proposed by **Fredlund** and **Krahn** (1977). They have shown that almost identical results may be obtained using their general formulation of the equations of equilibrium (GLE) together with Morgenstern and price's assumption about the interslice shear forces (equation 2.11). The solution satisfies the same elements of the static case but the derivation is more consistent with that used in the other methods of slices and also presents a complete description of the variation of the factor of safety with respect to (λ).

According to **Fredlund** and **krahn** (1977), the normal force is derived from the vertical force equilibrium equation, as shown in figure (2.3).

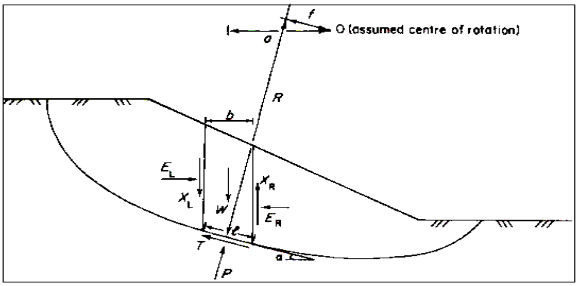

Figure (2.3), General Method of Slices (**Fredlund** and **Krahn**, 1977)

$$P = \frac{\left[W - (X_R - X_L) - \frac{1}{f}\left(c^{-} l \sin\alpha - ul \tan\phi^{-} \sin\alpha \right) \right]}{m_\alpha} \qquad \text{. . . . . (2.12)}$$

where:

P: Normal force on the base of the slice

W: Weight of slice

X_R : Vertical component of the resultant force on the interslice (from right side of slice)

X_L : Vertical component of the resultant force on the interslice (from left side of slice)

Two factors of the safety equations are computed, one with respect to the moment of equilibrium (Fm) and the other with respect to the force of equilibrium (Ff). The moment of equilibrium equation is taken with respect to a common point as:

$$F_m = \frac{\sum [\ c^{-} l + (P - ul) \tan\phi^{-}\ ] R}{\sum (Wd - P_f)} \qquad \text{. . . . . (2.13)}$$

For circular slip surfaces: $f = 0$, d = Rsinα and R = constant;

$$F_m = \frac{\sum \left[c^{-} l + (P - ul) \tan\phi^{-} \right]}{\sum W \sin\alpha} \qquad \text{. . . . . (2.14)}$$

The factor of safety with respect to force equilibrium is:

$$F_f = \frac{\sum\left(c^{-} l + (P - ul)\tan\phi^{-}\right)\cos\alpha}{\sum P\sin\alpha} \quad \text{. . . . .} \quad (2.15)$$

On the first iteration, the vertical shear forces (X_R and X_L) are set to zero. On subsequent iterations, the horizontal interslice forces are first computed from:

$$(ER - EL) = P\sin\alpha - \frac{1}{f}\left[c^{-} l + (P - ul)\tan\phi^{-}\right]\cos\alpha \quad \text{. . . . .} \quad (2.16)$$

where:

ER: Horizontal interslice force (from right side of slice)

EL: Horizontal interslice force (from left side of slice)

l: The inclined width of slice

u: Pore water pressure

P: Normal force on the base of the slice

Then the vertical shear forces are computed using an assumed (λ) value and *f*(x). Once X_R and X_L are determined, the normal force P on the base of each slice is then calculated and the value of λ for which $F_m = F_f$ can then be found iteratively as shown in figure (2.4).

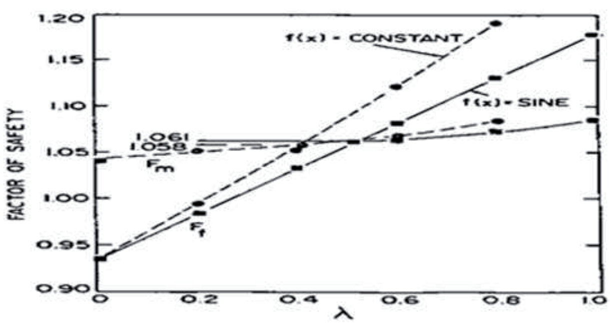

Figure (2.4) Variation the FOS with Respect to Moment and Force Equilibrium vs. λ for the Morgenstern-Price Method [**Fredlund** and **Krahn**, 1977].

In summary, Morgenstern and Price's Method

- considers both interslice forces,
- assumes a interslice force function, f(x),
- allows selection for interslice force function,
- computes FOS for both force and moment equilibrium**. (Aryal,2006)**

This method of slope stability analysis, which is valid for slip surfaces of any arbitrary shape, is considered as the more general rigorous method [**Baker**, 1980]. Its generality stems from the fact that no stringent restriction is imposed neither on the direction or location of the interslice forces nor on the shape of the slip surface analyzed [**Al-Jorany**, 1996].

For these reasons, the Morgenstern – Price method is chosen among all the other methods to be used in the limit equilibrium computation procedure presented in this work.

In addition to the methods mentioned previously for the analysis of slope stability by the using slices method, there are other methods available, e.g., Spencer's Method, Janbu's Simplified Method, Janbu's Generalized Procedure of Slices (GPS), and Sarma's Method.

Obaid (2002) used a computation procedure by which the most critical slip surface and its relevant minimum factor of safety is obtained. He uses this computation procedure to re-analyze the stability of upstream side slope of a zoned earth dam (Al-Qadisiya Dam, nowadays it is called Haditha dam) and finds that the dam is safe under the different water level condition (minimum, maximum, and normal water levels).

Al-Bataineh (2006) presents the various methods of two-dimensional limit equilibrium analysis which differ from each other in two regards. Different methods use different assumptions to make up the balance between the number of equations of equilibrium and the number of unknowns. Different methods use different assumptions regarding the location and orientation of the internal forces between the assumed slices. The following paragraphs are reviews on some previous studies presented by different researches in field of stability of earth dam under rapid drawdown condition and seismic load (earthquake).

Khattab (2008) presentes the stability and the factor of safety against Mosul embankment sliding by considering possible rapid drawdrown and earthquake conditions and using three methods. Unsaturated condition is considered assuming the shear strength parameter (ϕ_b) to be (0, 0.5ϕ,ϕ). GEO – SLOPE OFFICE was used as the analytical tool to simulate both seepage, slope stability, and earthquake. The main results indicate that the minimum slope stability factor of safety are reached using Bishop method .It was achieved during 8 days water drawdown and within the second day which indicates the most critical case.

Tran (2008) developed a numerical model to analyze the stability of the Tieng main dam in rapid drawdown condition for two cases before and after rehabilitation, using limit equilibrium and finite element methods. Changes of stress-strain behaviours and pore pressure, failure mechanism, and factor of safety of the upstream slope are investigated. In this study he find that the stability of the upstream slope is dramatically decreased but still being stable during rapid drawdown condition.

Lakehal et.al.,(2011) applied the modified method of Bishop,when an attempt is made to construct sets of nomgrams for the calculation of the safety factor of homogeneous earth dams under long term stability. It allows the user to get the optimal safety factor of the dam immediately according to the material classification and the parameters of design, height and slope.

Kamanbedast and Delvari ,(2012) presents attempt soil stability of Dam has been done with using Ansys. Therefore, result wore compared whit Geo studio Software result. Firstly, Dam were studied with using their Analysis method, then Seepage are predicated the seepage Rate in Ansys, 18% percent is lower than Geo studio results. Besides, Slope Stability is studied and different behavior of Dam is simulated. Safety factor values (for two software) had distinctive difference. For instance calculated safety factor, according to the Bishop method, for upstream slope for Geo studio, value equal 1.5 are determinate.

Patel and **Sanghvi** (2012) have presented examines static and dynamic slope stability analysis of "Kaswati Dam" which are located in Bhuj region by using of geo-studio 2007. Static slope stability analysis is done by Bishop's simplified method and dynamic slope stability analysis is done by time history method. In static upstream slope stability analysis that can achieve minimum factor of safety is 2.922 and dynamic upstream slope stability analysis that can achieve minimum factor of safety is 1.137. In static downstream slope stability analysis that can achieve minimum factor of safety is 2.109 and dynamic downstream slope stability analysis that can achieve minimum factor of safety is 1.095. In dynamic analysis of upstream slope 38% factor of safety decreases with compare to static analysis. In dynamic analysis of downstream slope 50% factor of safety decreases with compare to static analysis

2.7 Probabilistic and Sensitivity Analyses

In a traditional slope stability analysis, it is assumed that the values of all model input parameters are exactly known. For a given slip surface, a single value of safety factor is calculated. This type of analysis can be referred to as a **deterministic** analysis.

For most real world, for the slope stability problems the values of many input parameters are not very well known. Therefore, a **probabilistic** approach to the analysis of slope stability can be useful. In a probabilistic slope stability analysis, certain statistical distributions to the model input parameters, such as material properties (cohesion, unit weight, angle of internal friction), support properties (reinforcement of side slope), loads (seismic load), and water table location must be assigned.

Assigning a statistical distribution to one or more model input parameters, allows to calculate the degree of uncertainty in the value of the parameters. Input data samples are randomly generated based on the defined statistical distributions. A given slip surface may then have many different calculated for values of safety factor. This results in a distribution for safety factors, from which a probability of failure for the slope can be calculated.

In a **sensitivity** analysis, individual input parameters are varied between minimum and maximum values. This result in a plot of safety factor versus the parameter value, which allows determining which input parameters have the greatest effect on safety factor, and which parameters do not.

In probabilistic methods, the possibility that values of shear strength and other parameters may vary is considered. It provides a means of evaluating the degree of uncertainty associated with the computed factor of safety. Although probabilistic techniques are not required for slope analysis or design, these methods allow the designer to address issues beyond those that can be addressed by deterministic methods, and their use is encouraged. Probabilistic methods can be utilized to supplement conventional deterministic analysis with little additional effort. [**U.S. Army Crops. of Engineers, 2003b**]

There are several different statistical distributions available for defining random variables. In most cases, a normal distribution will be used. The normal (or

Gaussian) distribution is the most common probability density function (PDF), and is generally used for probabilistic studies in geotechnical engineering [**Duncan** and **Stephen**, **2005**].

Elouni and **kheder**,(2006) the reliability analysis has been performed on El Houareb embankment dam(Tunisia). Here, the basic assumption, which considers soil properties of the embankment dam which are statistically homogeneous, has been followed. Special attention has been paid to the global probability of failure. The calculated global probability of failure value is found to be close to the value associated with the critical ellipsoid failure mechanism. Hence, the concept of global probability of failure is coherent should be considered later, as the probability of failure of the project.

Karami and **Roozbahan**i ,(2010) studied the reliability analysis performed on Kalan embankment dam of Malayer, Iran by a numerical procedure or locating the surface of minimum reliability index for the earth slope. Here, basic assumption, which considers soil properties of the embankment dam are statistically homogeneous, has been followed.

Taha et.al.,(2010) presents the slope stability problems which are solved by using both deterministic and probabilistic approaches and can be characterized as optimization problems. In the deterministic approach, the factor of safety is the function to be minimized while for probabilistic analysis, the reliability index is considered to be the objective function. The search for the minimum factor of safety or the reliability index is a very complicated optimization problem, and many successful optimization methods have been employed to solve this problem. This work presents a survey of the literature on the various optimization methods applied to solving slope stability problems.

Khan F.and **Malik A.**(2013) show that in their analysis the pseudostatic case is critical for Naulong Dam located on Mula river at Sunth, about 30Km from

Gandava town in Tehsil. A probability and sensitivity analysis is carried out for some of the cases to assess probability of failure. The materials in the zoned embankment are assigned some variation for the probability analysis which showed that some slip surfaces have a probability of failure which is much greater than an acceptable limit. From the sensitivity analysis it is concluded that the variation in friction angle of the shell material affects the factor of safety more than any other material parameter and variation tried. To get a probability of failure within selected limits the probability analysis is carried out on revised downstream slopes to see the difference in probability of failure after the slopes are flattened from 1.75H:1V to 2H:1V and 2.25H:1V.

In the present work takes a zoned earth dam [**Mandali Dam as case study**] to study seepage and stability analysis for steady and drawdown condition. It is important to study the seepage through the body of earth dams, the pore water pressure distribution and position of the free surface that effect of stability and study transient groundwater analysis. For slope stability analysis of earth dams, two types of analysis are used the deterministic analysis and the probabilistic analysis to define the potential slip surface and calculate the factor of safety of the dam slopes.

Chapter Three

Application of Computer Program (SLIDE V .6.0)

3.1 Introduction

This chapter presents the information about program and its verification of the results that obtained from the program and compares it with the analytic and laboratory result. The cases taken in the program about seepage and the slope stability then comparing with other researchers

SLIDE is a 2D limit equilibrium slope stability program for evaluating the safety factor or probability of failure, of circular or non-circular failure surfaces in soil or rock slopes. *Slide* analyzes the stability of slip surfaces using vertical slice limit equilibrium methods. Slide also includes finite element seepage analysis through earth dams built right into the program.

Although the Slide groundwater analysis is geared towards the calculation of pore pressures for slope stability problems, it is not restricted to slope geometry configurations. The Groundwater modeling and analysis capabilities in *Slide* can be used to analyze an arbitrary 2-dimensional groundwater problem for saturated / unsaturated steady state flow conditions.

SLIDE V.6.0 is slope stability software to include built-in steady state unsaturated groundwater analysis capabilities using finite element method, full details of this program are shown in appendix-**A**. Comparing the results of computer program (**SLIDE V.6.0)** with other results of programs for both seepage of water through earth dams and slope stability analysis are very important, thus it should be done before using the program. The main aims of the comparison are to check the reliability of the theoretical aspects utilized in this program and then to examine the proper working of this program with previous work.

3.2 Verification of Computer Program (slide V.6.0)

This part is an analysis for **two** types of problems:

- Verification of the seepage through earth dams where two different seepage examples are considered. The first example is analyzed by (**Megan, (2002))** and the second example is analyzed by (**Al-Labban,(2007)).**

- Verification of slope stability. For slope stability analysis problems two different slope profiles are considered. The first example is taken from **Duncan and Wright (2005)** and the second example is an analysis of one of the planned James Bay dikes. The model is taken from **Duncan and Wright (2005)**

3.2.1 Seepage Analysis Problems

3.2.2 Laboratory Embankments Model

Two laboratory embankments models are designed and constructed by Powertech Labs Incorporated to study the influence of a pervious zone on the measured self potential response to steady state seepage flow. The embankments are constructed of pure quartz silica sand (Ottawa sand) graded according to ASTM C33-93 and compacted in layers at approximately 5% moisture content within a Plexiglas tank, Figure (3.1) show the dimensions of the problem. Seepage is induced by means of an upstream reservoir maintained at constant levels of 22.5 cm and 18.0 cm. Two embankment configurations were tested at these reservoir levels which are a homogeneous dam and a dam containing an upstream defect. A pervious zone extending the full 15 cm crest length of the embankment is introduced using a 3.75 cm layer of concrete sand placed 4 cm above the base. The defect extends from the upstream face of the dam to a distance of 60cm from the upstream toe, as indicated in Figure (3.1) below. The hydraulic conductivity for Ottawa sand and defect zone are ($4.5*10^{-4}$ cm/s) and ($5.5*10^{-4}$ cm/s), respectively.

The hydraulic head distribution within each embankment is monitored by means of six manometers connected to ports located at the side of the tank, as indicated in Figure (3.1) below. Electrical self potential (SP) measurements are recorded automatically using a series of gel-filled electrodes placed in contact with the soil along the upstream and downstream faces of the dam. Hydraulic and electrical readings are monitored until the system is stabilized and then recorded for a period of five days under steady-state flow conditions.

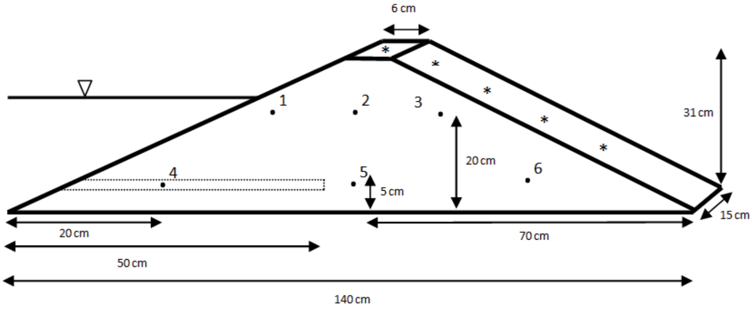

*Not to scale

Figure (3.1) Laboratory Embankment Dimensions with Manometer and Electrode Measurement Locations, **(After Megan, 2002).**

3.2.3 Experimental Studies

A 141×5×31 cell mesh has been made by **Megan (2002)** to model the laboratory dams under steady-state flow conditions using three dimensional self potential (3DSP). Measured and modelled hydraulic head data are compared at each port location, as shown in table (3.1) for the two embankment configurations at both reservoir levels. Figure (3.2) and figure (3.3) display the results of the 3-D numerical seepage analyses taken through a central cross-section of each embankment. These cross-sections are representative of the numerical solution in all cells parallel to the crest.

Two laboratory embankments are modelled by **SLIDE** program in the present work. Finite element analysis approach is used to model the seepage through the embankment. The numbers of elements used are 1531 with three nodded triangular elements having 828 nodes. The results of the finite element analysis to the total head distribution for two different cases of water conditions (reservoir level, 22.5cm and 18.0cm) and for two different embankments (homogenous embankment, non homogenous with defect zone) are shown in Figures(3.2) and (3.3) .

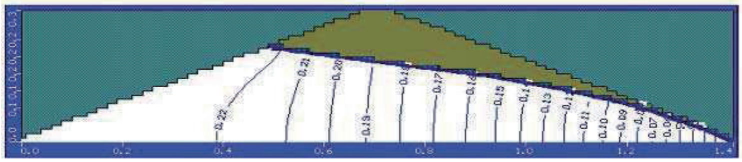

a- **Model by Megan**

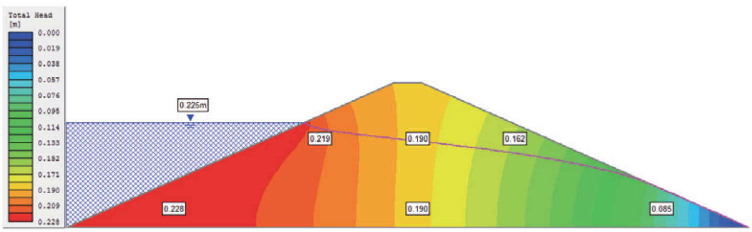

b- **Model by Slide**

Homogeneous Dam , water level 22.5 cm

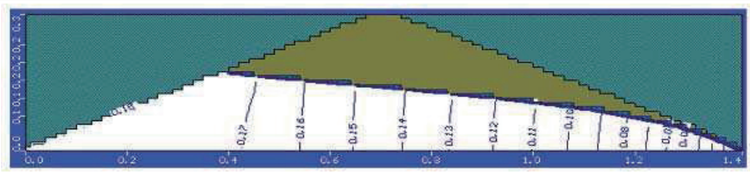

c- **Model by Megan**

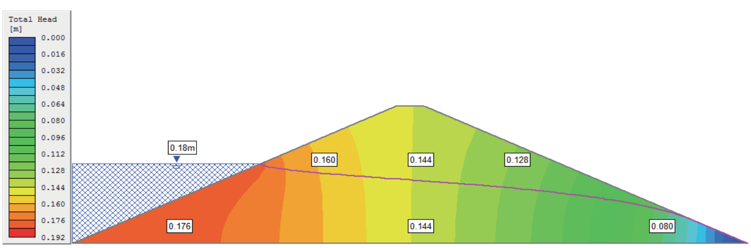

d- **Model by Slide**

Homogeneous Dam, water level 18 cm

Figure (3.2) Total Head Distribution as Obtained in the Present Work by **SLIDE** Program and **Megan, (2002)** for Homogeneous Dam

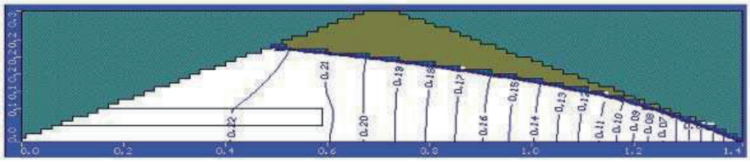

a- Model by Megan

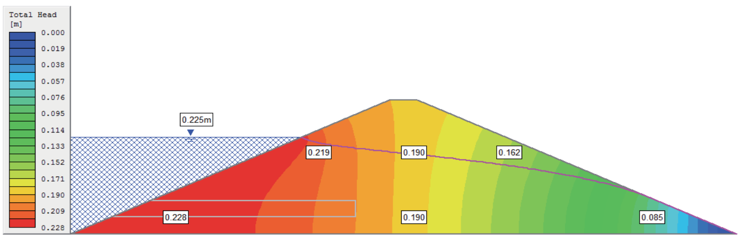

b- Model by Slide

Dam with up stream defect, water level 22.5 cm

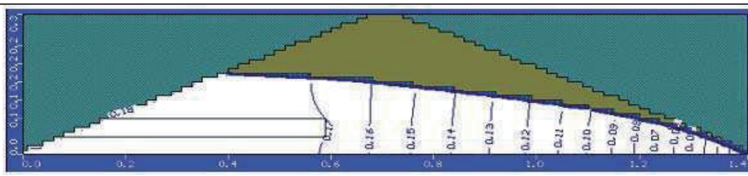

c- Model by Megan

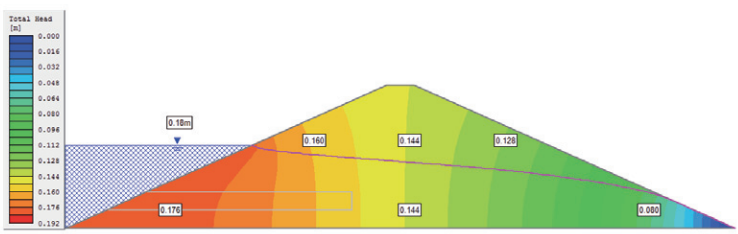

d- Model by slide

Dam with up stream defect, water level 18 cm

Figure (3.3) Total Head Distribution as Obtained in the Present Work by **SLIDE** Program and **Megan, (2002)** for Dam with up Stream Defect.

Figures (3.2) and (3.3) show results at different values of total head distribution for two different cases of water conditions and embankments. Each embankment is monitored by means of six manometers modelled by 3-D numerical seepage analyses and **SLIDE** program in the present work.

Measured and modelled hydraulic head data are compared at each port location, as shown in Table (3.1) for the two embankment configurations at both reservoir levels.

Table (3.1) Comparison between Measured Data of Laboratory Work by (Megan,2002) and the Result of Slide Program

Measure points	22.5 cm water level						18.0 cm water level					
	Total head cm of water						Total head cm of water					
	Homogeneous			Upstream defect			Homogeneous			Upstream defect		
	Measured	Model 3D	SLIDE results	Measured	Model 3D	SLIDE results	Measured	Model 3D	SLIDE results	Measured	Model 3D	SLIDE results
1	22.5	22.1	21.9	22.2	22.2	21.9	-	-	-	-	-	-
2	18.5	19.0	19.0	20.2	19.7	19.0	-	-	-	-	-	-
3	-	-	-	-	-	-	-	-	-	-	-	-
4	22.8	22.5	22.8	22.1	22.4	22.8	18.2	18.0	17.6	17.5	18.0	17.6
5	18.6	18.7	19.0	20.2	19.4	19.5	15.1	14.4	14.4	15.0	15.6	14.4
6	10.1	8.8	8.5	9.8	9.2	8.5	8.6	7.7	8.0	7.8	7.9	8.0

***(-) the values represent to the total head upper free surface**

Table (3.1) shows a comparison between the total heads computed by the **SLIDE** program model and numerical analysis of **Megan, (2002)** at different points through the dam. In the table the values of total head distribution that lays upper water surface will be neglected so they are not included in the table.

The table describes the well agreement between the measured data and the results of the **SLIDE** program model, and a good agreement between the results of **SLIDE** program and the results of 3D numerical analysis of **Megan, (2002).**

3.2.4 Earth Dam with a Rock Toe Filter on Impervious Foundation

Figures (3.4) and (3.5) show the dimensions of the problem and the flow net for the seepage through a homogeneous earth dam with a rock toe drain as published by (**Lambe and Whitman, (1979)**).

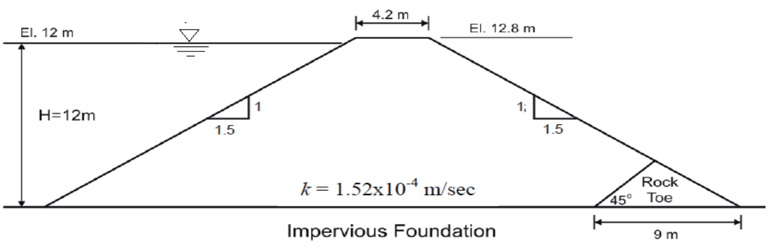

Figure (3.4): The Dimensions of a Dam with Rock Toe Filter (From Lambe and Whitman, 1979).

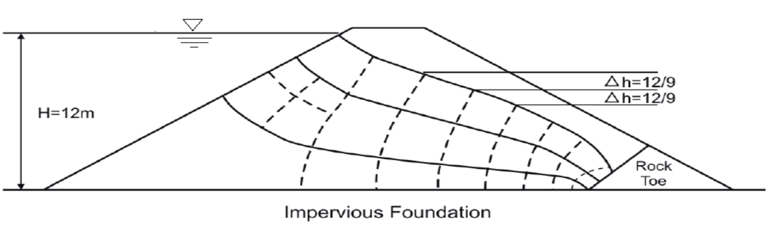

Figure (3.5): The Flow Net Solution, (After Lambe and Whitman, 1979).

Al- Labban ,(2007) presents analyzed seepage through the unconfined earth dam by using SEEP/W. The finite element mesh used for the analysis is shown in Figure (3.6). The mesh includes higher-order eight-noded elements near the toe. The upstream boundary nodes are designated as head boundaries with total head equals to the water level in the reservoir (12 m). The bottom node along the contact between the dam and toe drain is designed as a zero pressure head boundary.

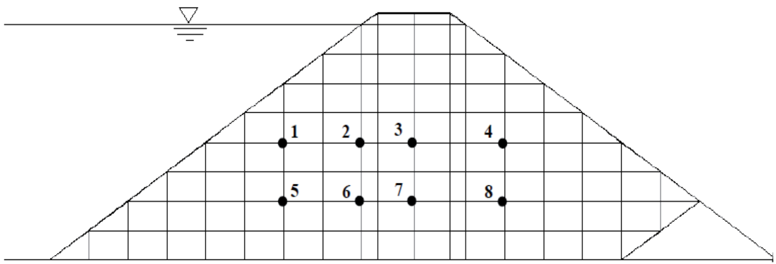

Figure (3.6): Point Select to Comparison in the Present Work by **SLIDE** Program

Figure (3.7) shows (a) the SEEP/W results with contours of equal head and (b) the resulting flow vectors. There are 10 contours at intervals of (12/9) and beginning at a minimum value of (0). The number of contours in (b) is the same as the number of equipotential lines in the flow net, and the head loss in both cases is (12/9) meters per contour.

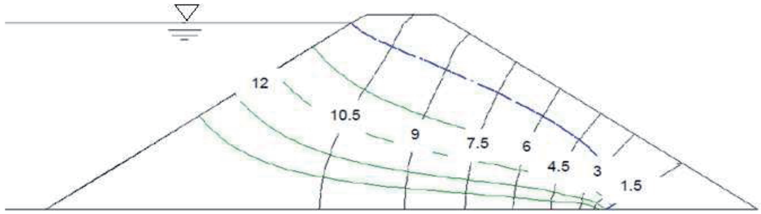

a- The Phreatic Line, Flow Net and Contours of Total Head.

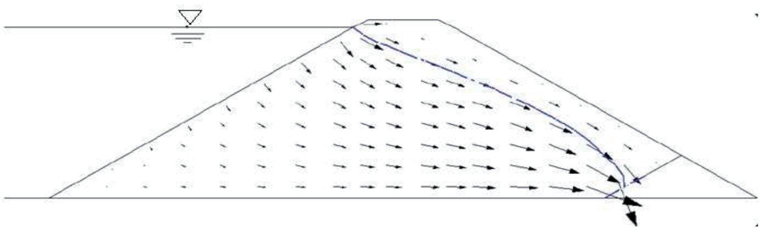

b- The Vectors of Flow.

Figure (3.7): The Results of the SEEP/W Analysis Program Taken through Earth Dam Presented by **Al- Labban ,(2007).**

Earth dam with a rock filter toe of the steady state are modelled by **SLIDE** program in the present work. Finite element analysis approach was used to model the seepage through the Earth dam. The numbers of elements used are 1448 with three nodded triangular elements having 779 nodes. The results of the finite element analysis by the program of the total head distribution for earth dam with a rock toe filter (reservoir level, 12m) are shown in Figure (3.8).

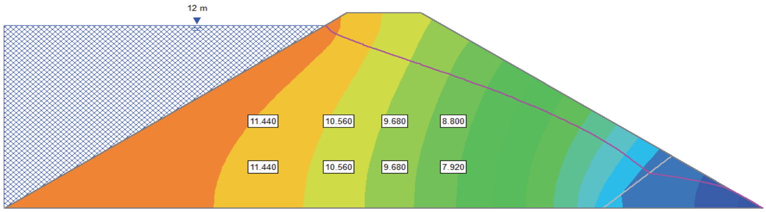

Figure (3.8) Total Head Distribution (m) as Obtained in the Finite Element Method (Slide Program).

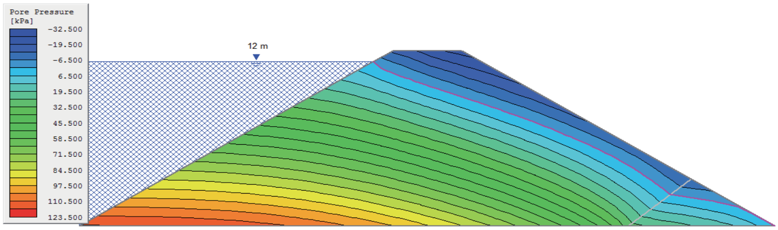

Figure (3.9) Pore Pressure Distribution (m) as Obtained in the Finite Element Method (Slide Program).

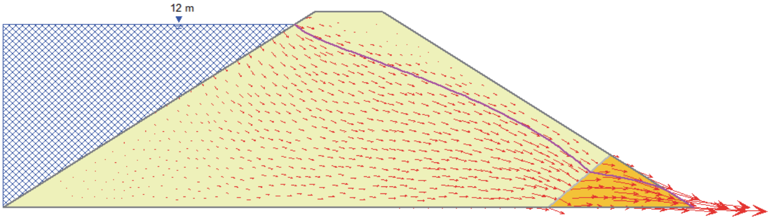

Figure (3.10) the Vectors of Flow as Obtained in the Finite Element Method (Slide Program).

Table (3.2) shows a comparison between the total heads computed by the finite element method, **SLIDE** program and the flow net at different points through the dam.

Table (3.2): Comparison between the Total Heads Computed by the Finite Element Method (**slide** program) and the Flow Net

Total head (m)				Total head (m)			
Points	Flow net Solution	SEEP/W results	SLIDE results	Points	Flow net solution	SEEP/W results	SLIDE results
1	10.73	11.47	11.44	5	10.43	11.17	11.44
2	9.63	10.45	10.56	6	9.35	10.13	10.56
3	8.67	9.48	9.68	7	8.43	9.16	9.68
4	6.65	7.39	8.80	8	6.2	6.94	7.92

3.3 Slope Stability Analysis

3.3.1 Example No.1(Duncan and Wright (2005))

Asymmetric earth embankment dam resting on a layered soil foundation with ponded water of height 23.057m on the left side is shown in Figure (3.11). The left face and right face of the dam is constructed using shell material. The soil properties are shown in Table (3.3).

The asymmetric earth embankment dam modelled by **SLIDE** program is adopted in the present work and the finite element analysis approach is used to model the Slope Stability Analysis. This example studies two cases: the global critical slip surface is of interest in Case 1 and the critical slip surface tangent at height 4.573m is of interest in Case 2.

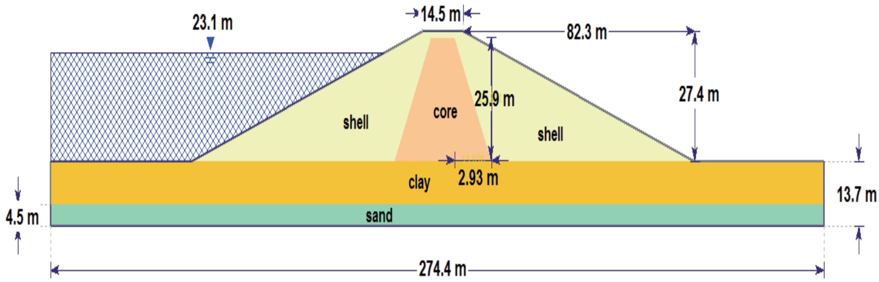

Figure (3.11) The Dimensions of a Symmetric Earth Embankment Dam (From Duncan and Wright. 2005)

Table (3.3): Material Properties (**Duncan and Wright. 2005**)

Material	k (m/s)	c (kN/m^2)	φ (^{0})	γ (kN/m^3)
Outer Shell	5.091×10^{-5}	0	34	19.632
Clay Core	5.091×10^{-9}	4.788	26	19.161
Foundation Clay	5.091×10^{-8}	0	24	19.318
Foundation Sand	5.091×10^{-6}	0	32	19.946

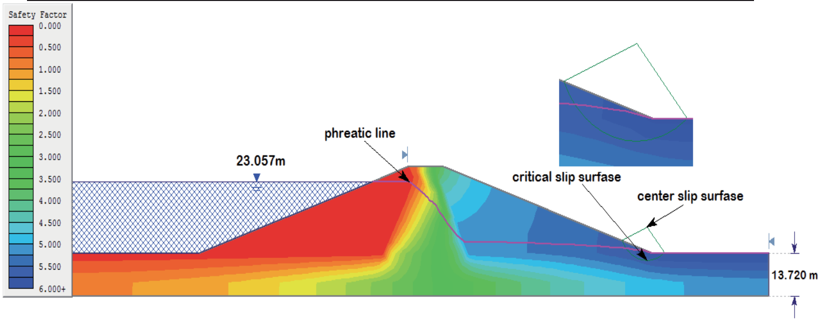

Figure (3.12) (Circular) Critical Slip Surface by (SLIDE V.6.0) Program case 1

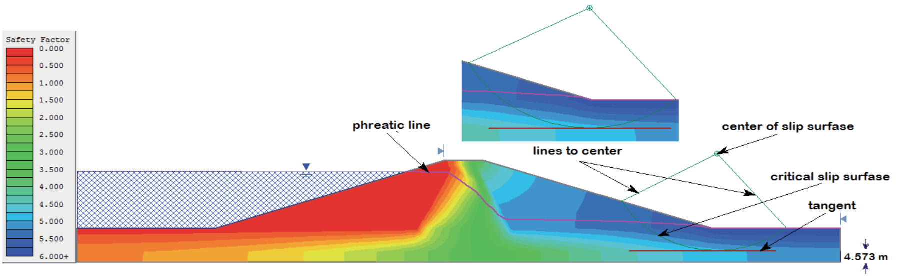

Figure (3.13) (Non-circular) Critical Slip Surface by (**SLIDE V.6.0**) Program Case2

Table (3.4) shows Comparison of factor of safety values obtained by different methods of slope stability analysis in slide program and comparison with value of factor of safety from (Duncan and Wright. 2005).

Table (3.4) Comparison of Different Solutions to Example No.1

Method	Factor of Safety by **slide** program		Max. different between FOS calculated and FOS known Percent%	
	critical slip surface (circular)	critical slip surface (non-circular)	(circular)	(non-circular)
Simplified Bishop Method	1.186	1.355	6.84	1.09
Janbu's Method(Rigorous)	1.132	1.231	1.98	10.14
Janbu's Method (simplified)	1.076	1.291	3.06	5.76
Spencer's Method	1.193	1.361	7.47	0.656
Morgenstern-Price-Method	1.19	1.363	7.20	0.510

The factor of safety of symmetric earth embankment dam for circular critical slip surface is (1.11) and for critical slip surface tangent at height 4.573m is 1.37, as obtained by **Duncan and Wright ,(2005)**

3.3.2 Example No.2 (Duncan and Wright (2005) - James Bay Dike)

Figure (3.14) shows the planned cross section of James Bay Dike. The table (3.5) show the material properties

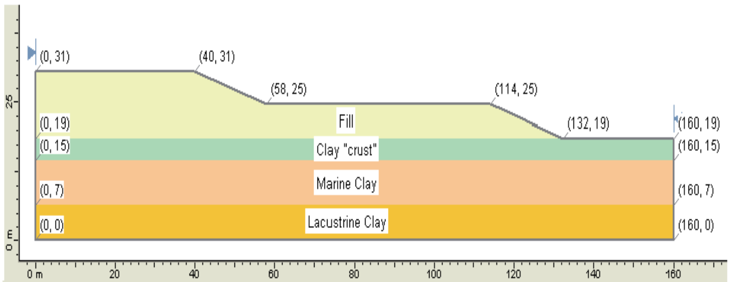

Figure (3.14) The planned cross section of James Bay Dike

Table (3.5): Material Properties (**Duncan and Wright (2005))**

Material	c (kN/m^2)	φ (^{0})	γ (kN/m^3)
Fill	0	30	20
Clay “crust”	41	0	20
Marine Clay	34.5	0	18.8
Lacustrine Clay	31.2	0	20.3

For side slope stability, **James Bay Dike** used two types of slip surface circular slip surfaces and non-circular slip surfaces to estimate the factor of safety by using bSLOPE which produces a slope stability code based on a MATLAB code written by Mohammed Tabarroki. Figure (3.15) show the results of factor of safety by James Bay Dike

In the present research, two cases are studied the first case assumes that the critical slip surface is circular and the second case assumes that the critical slip surface is non-circular. The critical slip surface is located using auto refine search in case 1 and is located using block search in case 2 as shown in figures (3.16) and (3.17).

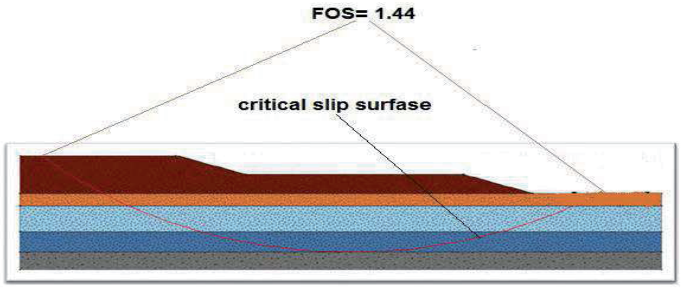

a- Circular

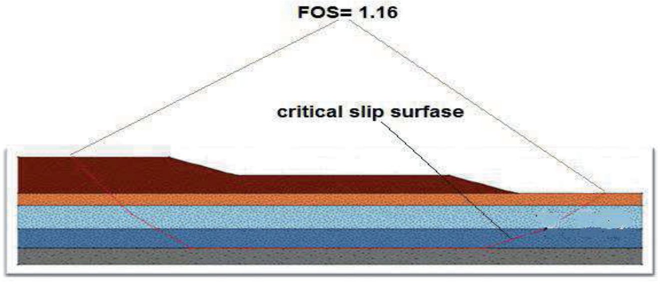

b- Non-circular

Figure (3.15) Failure Surface through Cross- Section by James Bay Dike

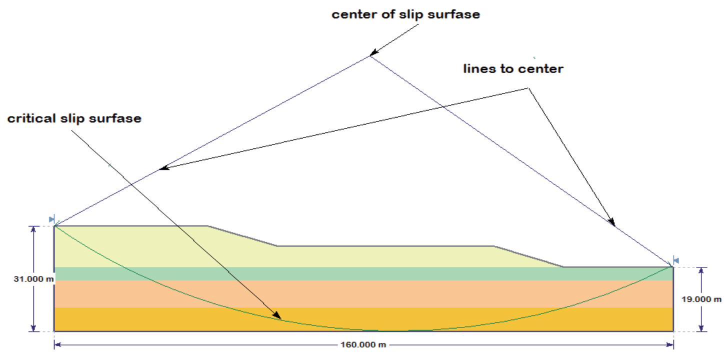

Figure (3.16) (Circular) Critical Slip Surface by (**SLIDE V.6.0**) Program Case1

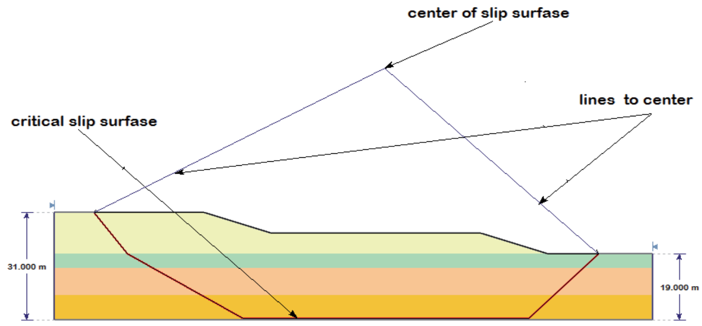

Figure (3.17) (Non-circular) Critical Slip Surface by (**SLIDE V.6.0**) Program Case2

Table (3.6) shows comparison of factor of safety values obtained by different methods of the slope stability analysis in the slide program and comparison with the value of the factor of safety from Duncan and Wright. 2005

Table (3.6) Comparison of Different Solutions to Example No.2

Method	Factor of Safety				Max. different between FOS calculated and FOS known Percent%	
	Critical slip surface (circular)		Critical slip surface (non-circular)			
	Result of slide	Result by James Bay Dike	Result of slide	Result by James Bay Dike	(circula)	(non-circular)
Simplified Bishop Method	1.437	I.44	1.141	-	0.896	2.47
Janbu's Method(Rigorous)	1.453	-	1.101	1.16	0.206	5.89
Janbu's Method (simplified)	1.364	-	1.180	-	5.931	0.854
Spencer's Method	1.433	-	1.201	-	1.172	2.649
Morgenstern-Price-Method	1.435	-	1.182	-	1.034	1.025

The factor of safety of cross- section for circular critical slip surface was(1.45) and for non-circular critical slip surface was (1.17) these results was obtained by **Duncan and Wright ,(2005).**

The results of **SLIDE** program for example No.1 and example No.2 are given in Tables (3.4) and (3.6). The values of the FOS obtained in the present analysis are according to general limit equilibrium (**Morgenstern-Price-Method),** although other methods of analysis are available. The main reasons which lead to choose this method of analysis have been discussed in the previous chapter. The results indicated a good agreement with the results of **SLIDE** program and this is a good sign to use this program in the present work.

Chapter Four

Parametric and sensitivity analysis

This chapter depends on two approaches; **deterministic** and **probabilistic** analysis shows the effect of some design parameters on the stability of side slope of earth dams. Figure (4.1) shows the layout of this chapter. These parameters are divided into four groups according to their type and as follows:

- Ground water parameters (phreatic surface location with types of drain, Rainfall infiltration and factor of safety).
- Physical parameters (cohesion of dam material, angle of internal friction of dam material and total unit weight of dam material,).
- Dynamic load parameters (seismic load coefficient, distributed load, tension cracks and rapid drawdown in water level).
- The sensitivity effect of the considered design parameters on the factor of safety which shall by investigated by using two analysis approaches, deterministic and probabilistic analyses

The general example problem has been adopted from **(Arora, 2007).** The results are obtained by the **SLIDE V.6.0** computer program.

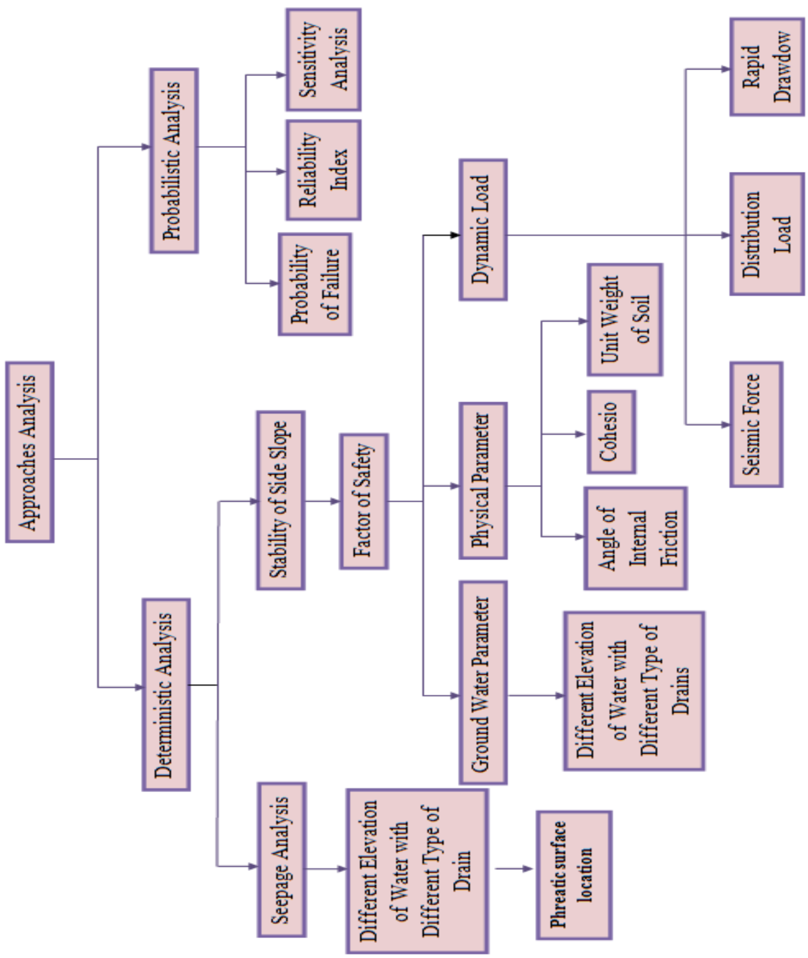

Figure (4.1) Layout of Present Research

4.1 Ground Water Parameters

4.1.1 Effect of the Phreatic Surface

One of the important points in the study stages and during construction of earth dams is seepage through the dam body. Seepage is the continuous movement of water from the upstream face of the dam toward its downstream face. The upper surface of this stream of percolating water is known as the phreatic surface. The phreatic surface should be kept at or below the downstream toe. The position of the phreatic surface influences the stability of the earth dam because of the potential piping due to excessive exit gradient and sloughing that result in the softening and weakening of the soil mass that touch the downstream slope or intersect it.

About 30% of earth dams have failed due to the seepage failure like piping and sloughing. Recent comprehensive reviews by Foster et al. (2000a,b) and Fell et al. (2003) show that internal erosion and piping are the main causes of failure and accidents affecting embankment dams; and the proportion of their failures by piping increased ranges from 43% before 1950 to 54% after 1950.

Seepage should be effectively controlled to preclude structural damage or interference with normal operations. Provision of a drainage system would not only allow easy passage for the seepage flow but also prevent the phreatic line from emerging at the downstream sloping face. Drainage blankets, chimney drains, and toe drains are designed to ensure that they control and safely discharge seepage for all conditions. The design of these features must also provide sufficient flow capacity to safely control seepage through potential cracks in the embankment impervious zone.

Figure (4.2) shows a general example problem for a side slope of the up stream =1:3 (V:H) and the down stream =1:2.5 (V:H) total unit weight (γ) = 20 kN/m^3, angle of internal friction (ϕ) = 28^o, cohesion (c) = 20 kPa.

To study the effect of water level of embankment, different analyses have been made for different elevation of water (27, 22, 17, 12 and 7 m) for the general example problem that has or has not drainage system where other parameters remained constant.

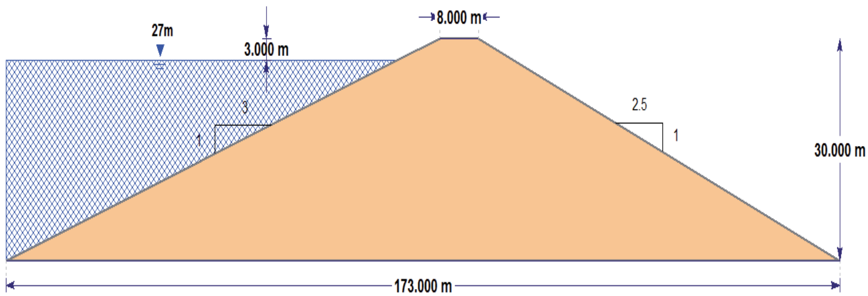

Figure (4.2) General Example as a Basic Problem Used in the Parametric Analysis.

Figure (4.3) show the phreatic line within the earth dam and the factor of safety that has or has not drainage system.

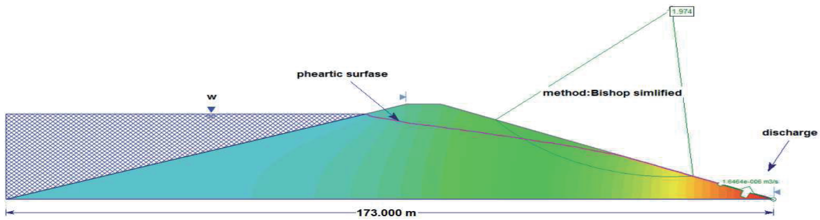

a- No drainage system (FOS=1.974)

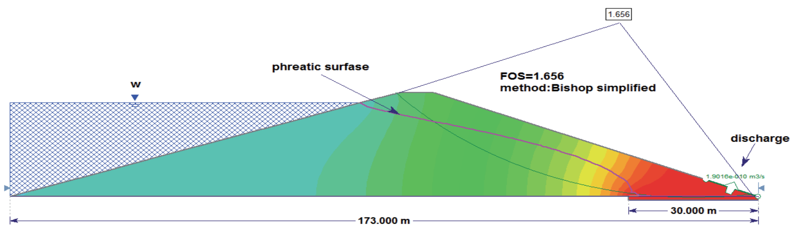

b- Horizontal drainage blanket (FOS=1.656)

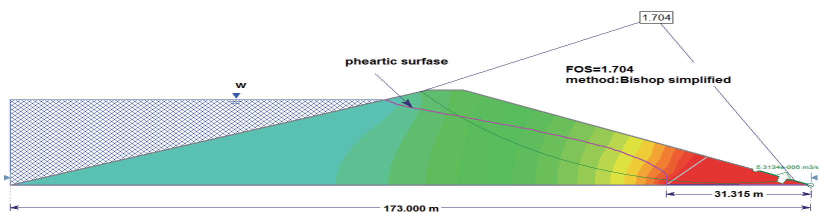

c- Toe drain (FOS=1.704)

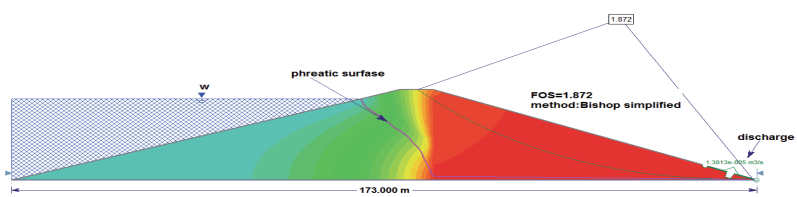

d- Chimney drain (FOS=1.872)

Figure (4.3) Most Critical Slip Surface in Downstream Side for General Example

Figure (4.3) shows that the toe drain installation is just an effort to prevent softening and erosion of the downstream toe and its efficiency attenuate as the dam height increases. When using the horizontal drainage blanket, the phreatic line recedes from the downstream slope and when the chimney drain is installed the phreatic line tends to remain mainly in upstream side so the seepage will not continue throughout the embankment.

Curves in Figure (4.4),(4.5), and (4.6) represent the general example with different values of factor of safety for different values of water level of reservoir (27,25, 22, 17, 12 and 7 m). All of these results are obtained using **SLIDE** program.

Figure (4.4) shows the general example without drainage system. It can be noticed that the phreatic surface would intersect the downstream slope if no drainage is installed and the flow lines will reach the downstream face. Also water level of reservoir decreases the factor of safety increased.

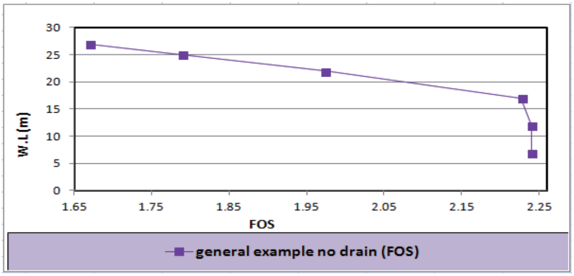

Figure (4.4) Effect of Different Values of water Level of Reservoir on FOS for General Example no Drain.

Figure (4.5) shows the general example of a horizontal drainage blanket in downstream with length 30m and 1m width. It is clear that the horizontal drainage blanket has a potential to recede the phreatic line from the downstream slope. However, horizontal drains may not be completely effective in drawing down phreatic levels in horizontally stratified embankments and because different values water level of reservoir decrease the factor of safety increased.

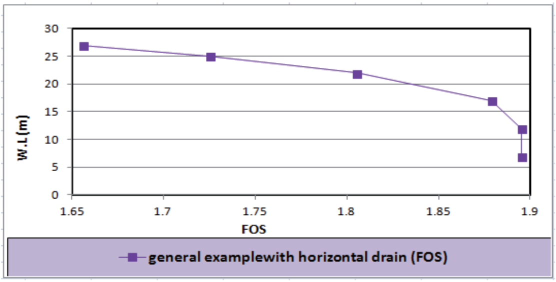

Figure (4.5) Effect of Different Values of Water Level of Reservoir on FOS for General Example with Horizontal Drain.

Figure (4.6) shows the general example with toe drain in downstream with length 9m and slope is 1V: 1H. It can be concluded from this Figure that the installation of a toe drain in dams would be just an effort to prevent softening and erosion of the downstream toe. What the flow volume increases as a result of water table increment in the reservoir, then the performance of the toe drain would be unacceptable and for different water level of reservoir decreased the factor of safety increased. For the chimney drain is installed vertically with a 1m width and 27 m height the chimney drain has restrained the phreatic line almost in upstream side of the dam and the downstream side of the dam is free of pore pressure and for different water level of reservoir decrease the factor of safety remains constant.

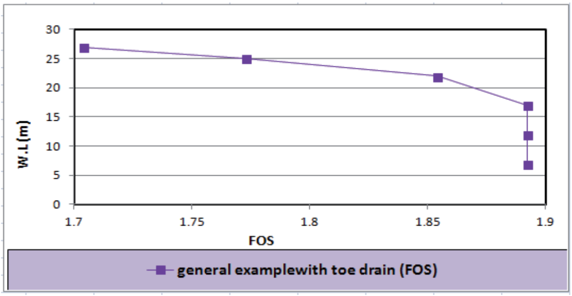

Figure (4.6) Effect of Different Values of Water Level of Reservoir on FOS for General Example with Toe Drain

Table (4.1) shows the values of factor of safety found by using **SLIDE** program with different water level of reservoir. It can be observed from the table that the factor of safety increases with the decreasing of the water level of reservoir.

Table (4.1) the Factor of Safety for Different Position of Water Level of Reservoir.

Input Parameters				Output Parameters			
H(m)	C (kPa)	ϕ^o	γ (kN/m^3)	FOS by **SLIDE** Prog.			
				No drain	horizontal drain	toe drain	chimney drain
27	20	28	20	1.670	1 56	1.704	1.872
25				1.789	1 73	1.725	1.872
22				1.974	1 05	1.854	1.872
17				2.227	1 79	1.892	1.872
12				2.240	1 95	1.892	1.872
7				2.240	1 95	1.892	1.872

4.2 Physical Parameters

4.2.1 Effect of the Angle of Internal Friction

This effect has been studied by considering different values of the angle of internal friction (ϕ = 5°, 10°, 20°, 25°,28°, 34°,and 40°).It has been assessed by considering different values of (ϕ) while other parameters are kept constant (height of embankment = 12 m, slope angle (α) = $\tan^{-1}$ (1/2), total unit weight (γ) = 19.2 kN/m^3, angle of internal friction (ϕ) = 20° and phreatic surface).

Figure (4.7) represent the general example for different cohesion of soil (c) for different values of the angle of internal friction. It can be observed that decreasing the value of cohesion from 20 kPa to16 kPa for different angle of internal friction, the factors of safety are decrease between (16.75% - 7.09%). Also it can be observed that increasing the value of cohesion from 20 kPa to30 kPa for different angle of internal friction, the factors of safety increased between (42% - 17.65%).

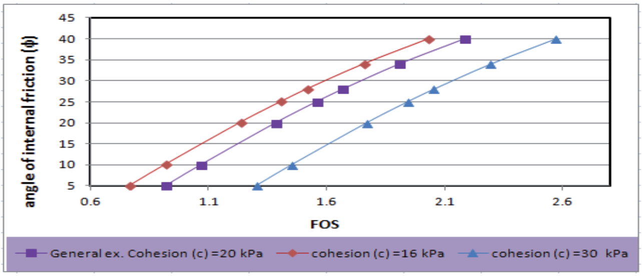

Figure (4.7) Effect of Angle of Internal Friction on FOS for Different Values of Cohesion.

Figure (4.8) represent the general example for different unit weight (γ) for different values of the angle of internal friction. It can be observed that decreasing the value of unit weight (γ) from 20 kN/m^3 to 18 kN/m^3 for different values of angle of internal friction, the factors of safety are increased between (8.26% - 0.73%).

Also, it can be observed that increasing the value of cohesion from 20 kPa to 22 kPa for different value of the angle of internal friction, the factors of safety decreased between (6.63% - 0.59%).

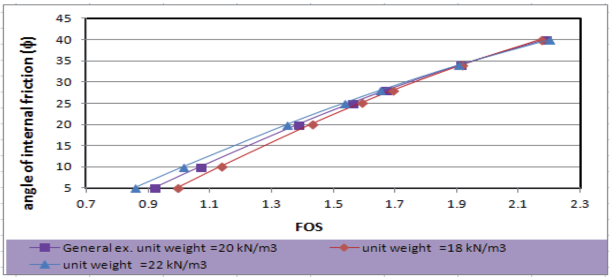

Figure (4.8) Effect of Angle of Internal Friction on FOS for Different Values of Unit Weight of Soil

It can be observed from the curves that the factor of safety increases with the increase of the angle of internal friction of soil. All the tables are shown in appendix-B

4.2.2 Effect of Cohesion

Effect of cohesion has been assessed by considering different values of cohesion (c) while other parameters are kept constant. The considered values are (c = 10, 20, 25, 30, 40 and50 kPa).

Figure (4.9) represents the general example for the different angle of internal friction at different values of cohesion (c = 10, 20, 25, 30, 40, and50 kPa). It can be observed that decreasing the value of angle of internal friction (ϕ) from 28° to 23° for different values of cohesion, the factor of safety decreases between (14.10% - 4.54%) Also, that increases the value of angle of internal friction (ϕ) from 28° to 34°

for different values of cohesion (c) implies that the factors of safety increased between (18.7% - 6.05%).

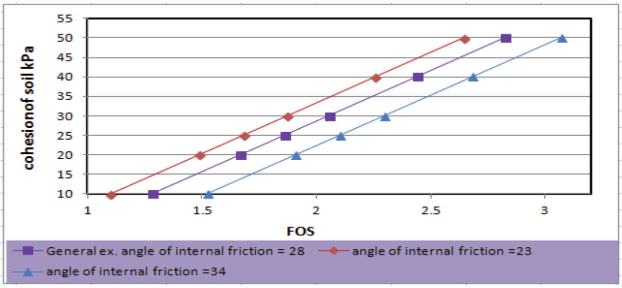

Figure (4.9) Effect of Cohesion on FOS for Different Angles of Internal Friction.

Figure (4.10) represent the general example for different unit weight (γ) at different values of the cohesion(c = 10, 20, 25, 30, 40 and 50kPa). It can be observed that decreasing the value of unit weight (γ) from 20 kN/m^3 to18 kN/m^3 at different values of the cohesion of the soil, the factor of safety increases between (1.63% - 25.20%). Also, it can be observed that increasing the value of unit weight (γ) from 20 kN/m^3 to22 kN/m^3 for different values of the cohesion of the soil, the factor of safety is decreasing between (1.32% - 5.74%).

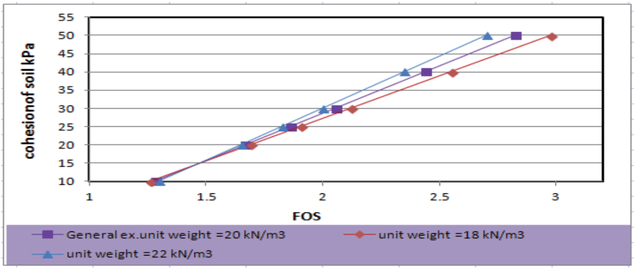

Figure (4.10) Effect of Cohesion on FOS for Different Unit Weights.

It can be noticed from the curves that the factor of safety increases with the increase of the cohesion(c) of the soil. All tables are shown in appendix- B.

4.2.3 Effect of unit weight of soil

To study the effect of unit weight of soil (γ), different analyses have been made for different values of unit weight of soil (γ =14, 16,18,20,22 and 23 kN/m^3) where other parameters remained constant.

Curves in figure (4.11) shows the general example for different cohesion of the soil (c) at different values of unit weight of soil (γ =14, 16,18,20,22 and 23 kN/m^3). It can be observed that decreasing the value of the cohesion from 20 kPa to 16 kPa for different values of unit weight, the factor of safety decreases between (12.64% - 8.15%). Also it can be observed that increasing the value of the cohesion from 20 kPa to30 kPa the factor of safety increased between (31.50% - 20.37%).

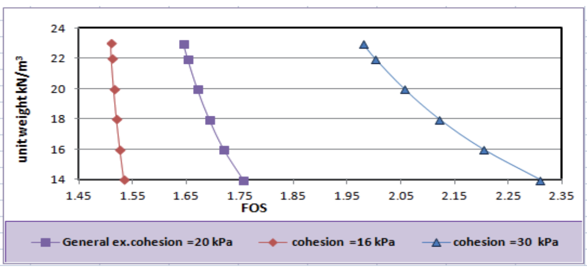

Figure (4.11) Effect of Soil Unit Weight on FOS for Different Values of Cohesion**.**

Curves in figure (4.12) shows the general example for different angle of internal friction (ϕ) at different values of soil unit weigh (γ =14, 16,18,20,22 and 23 kN/m^3). It can be observed that decreasing the value of internal of friction (ϕ) from 28° to 23° for different total unit weight, the factor of safety is decreasing between (7.46% - 11.92%). Also, it can be observed that increasing the value of angle of internal friction (ϕ) from 28° to 34° for different values of unit weight of the soil, the factor of safety is increasing between (9.85% - 15.87%).

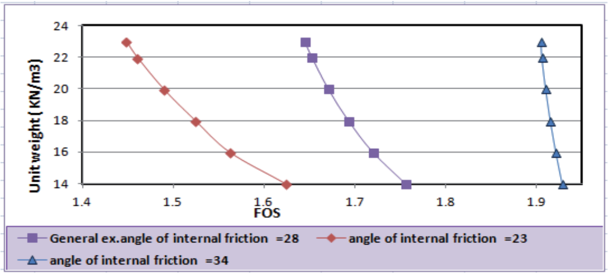

Figure (4.12) Effect of Soil Unit Weight on FOS for Different Angles of Internal Friction.

It can be observed from the curves that an increase in the unit weight lead to increasing the driving force that lead to reduce the factor of safety. All tables are shown in Appendix- B.

4.3 Dynamic Load Parameters

4.3.1 Seismic Load Parameters

Dynamic loads generated by seismic disturbances must be considered in the design of all major dams situated in recognized seismic 'high-risk' regions. The possibility of seismic activity should also be considered for dams located outside those regions, particularly those sited in close proximity to potentially active geological fault complexes.

Seismic activity is associated with complex oscillating patterns of accelerations and ground motions, which generate transient dynamic loads due to the inertia of the dam and the retained body of water. Horizontal and vertical accelerations are not equal, the former being of greater intensity. For design purposes both should be considered operative in the sense least favourable to stability of the dam. Horizontal accelerations are therefore assumed to operate normal to the axis of the dam. **(Novak and Nalluri,(2007)**

If seismic coefficients are defined, a seismic force will be applied to each slice as follows:

Seismic Force = Seismic Coefficient * Slice Weight . . . . (4.1)

From this definition it can be observed that the seismic force increases when slice weight increases.

To study the effect of seismic load coefficients, six different load coefficients (0.05, 0.07, 0.1, 0.13, 0.15 and 0.2) are considered.

Figure (4.13) shows different angles of internal friction of soil (ϕ) for different values of seismic force coefficients (0.05, 0.07, 0.1, 0.13, 0.15 and 0.2). It can be observed that decreasing the value of the internal friction (ϕ) from 28° to 23° for different values of seismic load coefficients, the factor of safety is decreasing between (10.75% - 10.17%). Also, it can be observed that increasing the value of angle of internal friction (ϕ) from 28° to 34° for different values of seismic force coefficients, the factors of safety increased to about (14%).

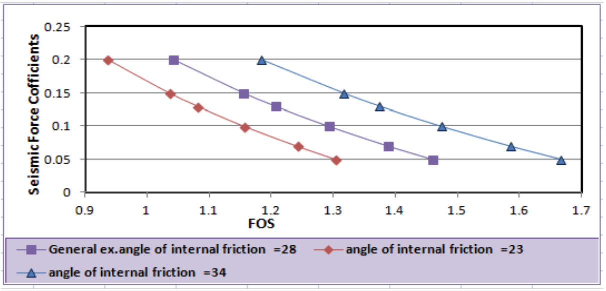

Figure (4.13) Effect of Different Values of Angle of Internal Friction on FOS for Different Values of Seismic Coefficient

Figure (4.14) shows different values of the cohesion of the soil(c) for different values of seismic load coefficients (0.05, 0.07, 0.1, 0.13, 0.15 and 0.2). It can be observed that decreasing the value of the cohesion from 20 kPa to16 kPa for different coefficient of seismic force, the factor of safety is decreasing about (10%). Also, it can be observed that increasing the value of cohesion from 20 kPa to30 kPa at different values of seismic force coefficients, the factors of safety increased to about (24%).

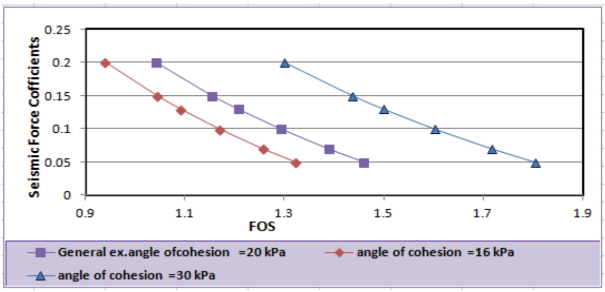

Figure (4.14) Effect of Different Values of Cohesion on FOS for Different Values of Seismic Force Coefficient.

Figure (4.15) shows different values of unit weight of soil(γ) for different values of seismic load coefficients (0.05, 0.07, 0.1, 0.13, 0.15 and 0.2). It can be observed that decreasing the value of the unit weight of the soil from 20 kN/m^3 to18 kN/m^3 for different coefficient of the seismic force, the factor of safety is increasing to about (1.3%) and it can be observed that increasing the value of the cohesion from 20 kN/m^3 to 22 kN/m^3 different values of seismic force coefficients, the factors of safety is decreasing to about (1.1%)

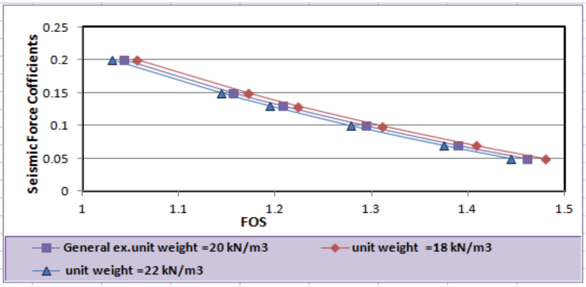

Figure (4.15) Effect of Different Values of Soil Unit Weight on FOS for Different Values of Seismic Force Coefficient.

It can be observed from the curves that the factor of safety decreases with the increase of seismic force coefficients. All tables are shown in appendix- B.

4.3.2 Distributed Load

To study the effect of the distributed load, different analyses have been made for different values of the distributed load (0, 10, 20,30,40,50 and 60 kN/m^2) where other parameters remained constant.

Figure (4.16) shows the general example for different cohesion of the soil (c) for different values of the distributed load (0, 10, 20,30,40,50 and 60 kN/m^2). It can be observed that decreasing the value of the cohesion from 20 kPa to 10 kPa for different values of the distributed load, the factor of safety is decreasing to about (10 %). Also, it can be observed that increasing the value of cohesion from 20 kPa to30 kPa the factors of safety is increasing to about (11%).

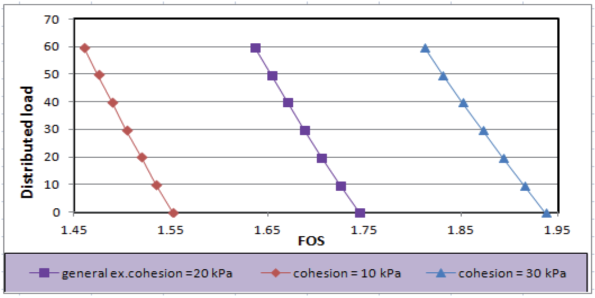

Figure (4.16) Effect of Different Values of Cohesion on FOS for Different values of Distributed Load.

4.3.3 Rapid Drawdown Condition

The drawdown is known as one of the most dangerous conditions for the upstream side slope. When the countervailing upstream water pressure has disappeared, it causes a danger to the upstream slope. The upstream shell cannot stay stable under the hydrodynamic pressure due to rapid drawdown. Soils inside the dam body remain saturated and seepage commences from it towards the upstream slope. Seepage and hydrodynamic pressures create downward forces acting on the upstream slope. Those are adverse to the stability and create a critical condition to the upstream slope. The Rapid Drawdown Condition occurs when a slope that is used to retain water experiences a rapid (sudden) lowering of the water level and the internal pore pressures in the slope cannot reduce fast enough.

Events following a rapid drawdown may be useful, but approximately be divided into four stages as shown in Figure (4.17). If the drawdown time is much less than the time in which consolidation adjustment can occur within the slope, the pore pressures immediately following the drawdown will be equal to the pore pressures before drawdown plus the change in pore pressure due to the change in water load against the slope. In time, consolidation adjustments will occur, but pore pressures will remain high until the excess water drains from the slope and a new equilibrium is reached corresponding to the low level of water against the slope. With free draining soils, such as coarse sands and gravels, the consolidation time will generally be less than any actual drawdown time so that the stage depicted in Figure (4.17b) never occurs and stability of slopes in such soils can be analyzed using a transient flow net as shown in Figure (4.17c). With slowly draining soils, the situation depicted in Figure (4.17b) is critical with regard to stability of slopes [**Lambe** and **Whitman**, 1969].

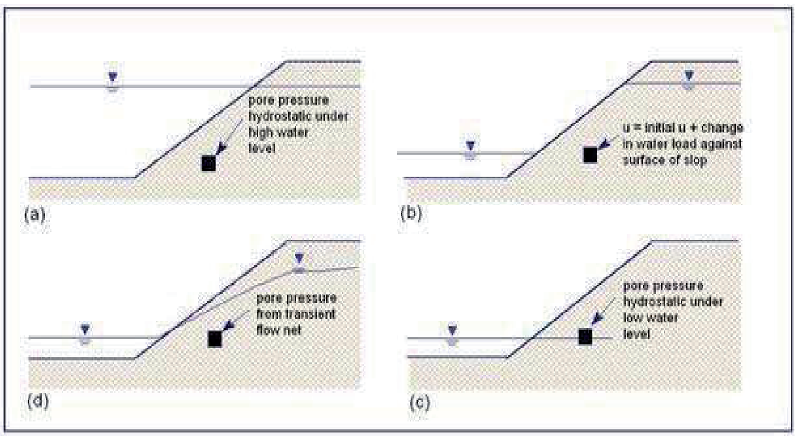

Figure (4.17) Response of Slope to Rapid Drawdown. (a) Initial Equilibrium Condition. (b) after Drawdown but before Consolidation Adjustment. (c) after Consolidation Adjustment. (d) Final Equilibrium Condition. [**Lambe** and **Whitman , 1969**].

The general example is considered to study the effect of some design parameters on the values of the drawdown rate and FOS for upstream side slope. Figure (4.18) shows the general example with same materials properties of the dam (which are the same as in previous analysis in this chapter).

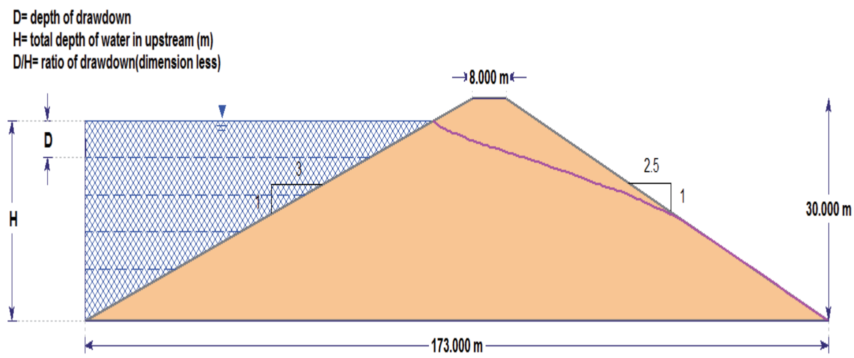

Figure (4.18) General Example with Same Material Properties Used in Previous Analysis.

The stability of upstream side slope under rapid drawdown condition are studied for different ratio of drawdown. FOS for different ratio of (D/H), the ratio of decreases FOS from steady state condition, shown in the table (4.2) below. The factor of safety for steady state condition before drawdown is 3.152.

Table (4.2) Factor of Safety for Upstream Side slope under Rapid Drawdown Condition for Different Depth of Drawdown

Depth of drawdown (m)	D/H Dimension less	FOS	$P\% = \frac{3.152 - FOS}{3.152} * 100$
3	0.12	2.970	5.77%
6	0.23	2.578	18.21%
9	0.34	2.184	30.71%
12	0.45	1.875	40.54%
15	0.56	1.662	47.27%
18	0.67	1.546	50.95%
21	0.78	1.522	51.71%
24	0.89	1.522	51.71%
27	1	1.522	51.71%

P **= ratio of decreases FOS from steady state (%)**

Figure (4.19) shows the general example for different values of depth of drawdown (9, 12, 15,18,21,24 and 27m). It can be observed that increasing of drawdown ratio the factor of safety is decreased. It can be concluded from the curve that the critical degree of FOS during the rapid drawdown can be considered at the drawdown ratio of 0.78, not until the emptying. An explanation of the critical FOS is due to the cohesive strength of the slope and trade-off between soil weight and soil shear strength as the drawdown ratio is varied. The fully submerged slope is more stable than the dry slope, as indicated by a higher FOS.

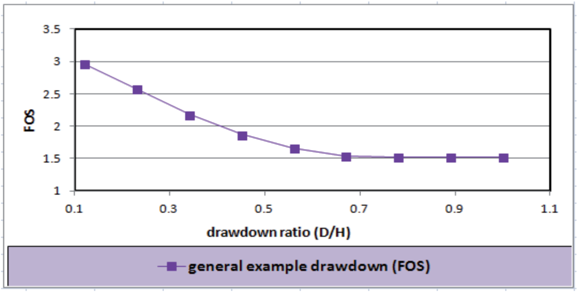

Figure (4.19) FOS for Different Drawdown Ratio.

4.3.3.1 Pore Water Pressure along Slip Surface

The study the changes in pore water pressure along slip surface for different drawdown ratios are illustrated in Figures (4.20) to (4.26).The Figures show the changes in pore water pressure along the slip surface. The initial pore water pressure represents the steady state condition before drawdown and pore water pressure represents final pore water pressure after drawdown. These are defined as:

$$u = \bar{u} + \Delta u \qquad \dots (4.1)$$

where:

u = final pore water pressure.

$\bar{u}$ = initial pore water pressure before drawdown.

Δu = change in pore water pressure due to rapid drawdown.

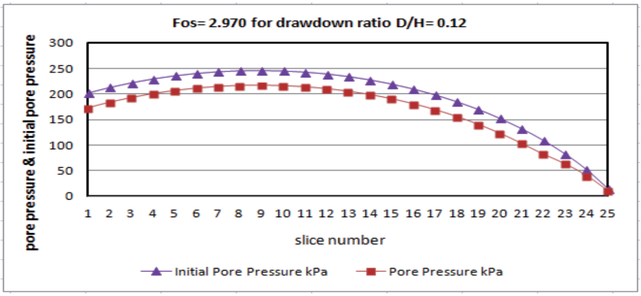

Figure (4.20) Pore Water Pressure and Initial Pore Water Pressure along Slip Surface for Drawdown Ratio = 0.12, FOS = 2.970

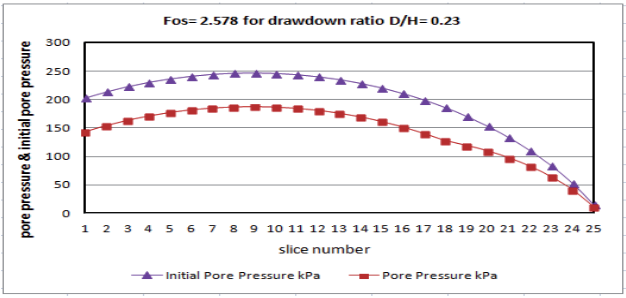

Figure (4.21) Pore Water Pressure and Initial Pore Water Pressure along Slip Surface for Drawdown Ratio = 0.23, FOS = 2.578

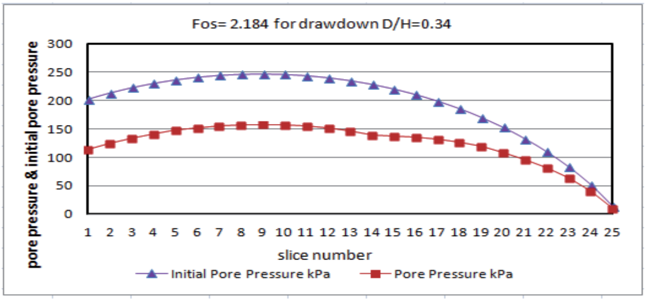

Figure (4.22) Pore Water Pressure and Initial Pore Water Pressure along Slip Surface for Drawdown Ratio = 0.34, FOS = 2.184

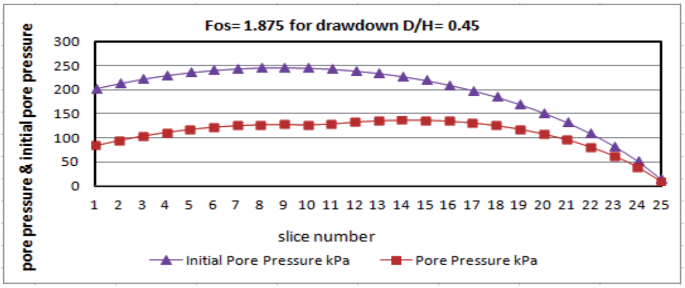

Figure (4.23) Pore Water Pressure and Initial Pore Water Pressure along Slip Surface for Drawdown Ratio = 0.45, FOS = 1.875.

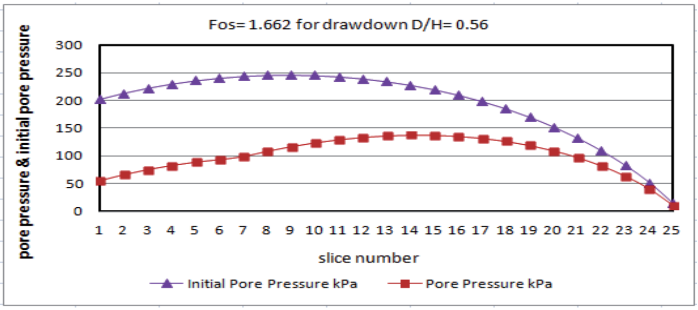

Figure (4.24) Pore Water Pressure and Initial Pore Water Pressure along Slip Surface for Drawdown Ratio = 0.56, FOS = 1.662.

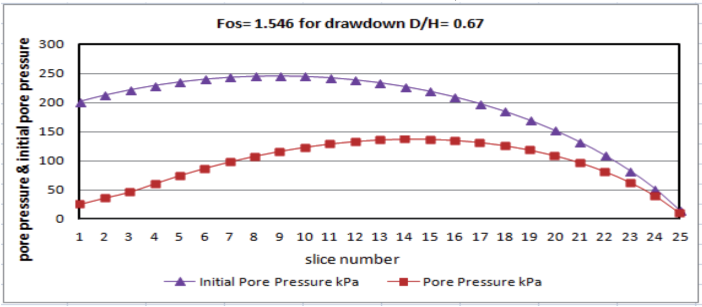

Figure (4.25) Pore Water Pressure and Initial Pore Water Pressure along Slip Surface for Drawdown Ratio = 0.67, FOS = 1.546.

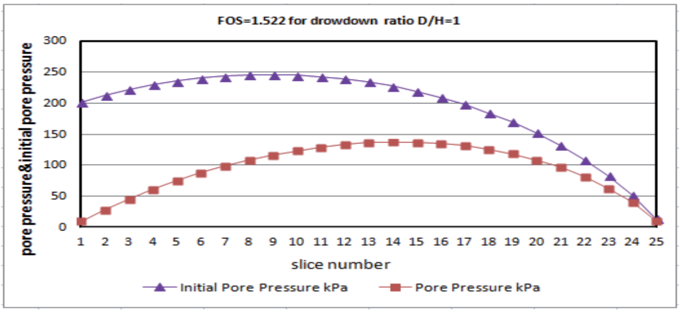

Figure (4.26) Pore Water Pressure and Initial Pore Water Pressure along Slip Surface for Drawdown Ratio =1, FOS = 1.522.

From these curves, it can be seen that the pore water pressure decreases with the increases of drawdown ratio (D/H). This increase in (D/H) will increase the negative pore water pressure in the upstream side slope. In general, the pore water pressure has a large effect on the stability of upstream side slope.

4.3.3.2 Effect of Material Properties on the Drawdown Condition

To study the effect of material properties on the stability of upstream side slope under rapid drawdown condition, five different ratios of drawdown D/H, (0.34, 0.45, 0.56, 0.67, and 1) are considered. This effect has been studied by considering the aforementioned (D/H) values for general example whereas other parameters are kept constant

To study the effect of drawdown, different analyses have been made for different values of drawdown ratio (0.34, 0.45, 0.56, 0.67, and 1) where other parameters remained constant.

Figure (4.27) shows the general example for different cohesion of soil (c) for different values of drawdown ratio (0.34, 0.45, 0.56, 0.67, and 1). It can be observed that when decreasing the value of cohesion from 20 kPa to 10kPa for different values of drawdown ratio then the factor of safety is decreasing between (11.64% - 14.91%). Also, it can be observed that when increasing the value of cohesion from 20 kPa to30 kPa then the factors of safety is increasing between (11.67% - 14.98%).

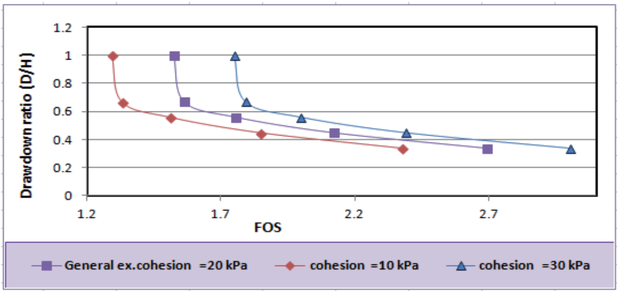

Figure (4.27) Effect of Different Values of Cohesion of Soil on FOS for Different Values of Drawdown Ratio.

Figure (4.28) represents the general example for different angle of internal friction for different values of drawdown ratio (0.34, 0.45, 0.56, 0.67, and 1). It is observed that when decreasing the value of the angle of internal friction (ϕ) from 28° to 22° for different values of cohesion, then the factor of safety is decreasing between (18.44% - 16.81%). Also, it can be observed that when increasing the value of angle of internal friction (ϕ) from 28° to 34° for different of cohesion (c) then the factors of safety increasing between (20.6% - 18.92%).

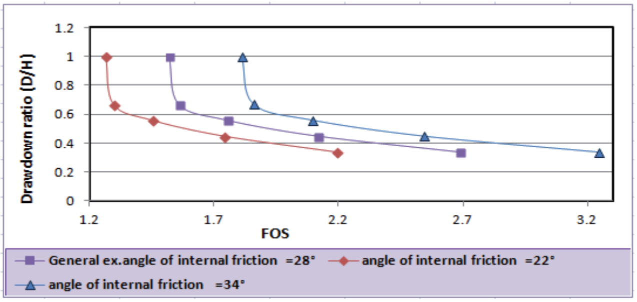

Figure (4.28) Effect of Different Values of Internal Friction of Soil on FOS for Different Values of Drawdown Ratio.

It can be observed from the curves that the factor of safety decreases with the increase of drawdown ratio (D/H). All tables are shown in appendix- B.

4.4 Probabilistic and sensitivity analyses

In order to carry out a probabilistic analysis by using **SLIDE** computer program, at least one (or more) of model input parameters should be defined as random variables. Almost all model input parameters in **SLIDE** can be defined as random variables, for example, material properties, support properties and load magnitudes.

In this analysis, the material properties (cohesion of soil, unit weight of soil and angle of internal friction of soil), and loads (seismic force) will be defined as random variables. This is done by selecting a statistical distribution for each selected parameter (random variable), and entering the appropriate parameters for the distribution (standard deviation, minimum and maximum values, correlation coefficient).

There are some different statistical distributions available for defining random variables. In most cases, the normal distribution will be used. The normal (or

Gaussian) distribution is the most common probability density function (PDF), and is generally used for probabilistic studies in geotechnical engineering [**Duncan** and **Stephen**, **2005**].

In the present work the normal distribution will be used as a statistical distribution for defining random variables. For the normal distribution, 99.73 % of all samples will fall within 3 standard deviations of the mean value. This fact leads to Eq. (4.2), (the "Three Sigma Rule") which allows to estimate the standard deviation for a normally distributed random variable. This Eq. is useful if actual data of the random variables is not available [**Duncan** and **Stephen, 2005**].

$$\sigma = \frac{HCV - LCV}{6} \qquad \ldots\ldots\ldots \quad (4.2)$$

where:

σ = estimated standard deviation

HCV = highest conceivable value of the random variable

LCV = lowest conceivable value of the random variable

In this part of the analysis will be taken the general example in the beginning of this chapter. All parameters defined as random variables and standard deviations of all random variables are shown in Table (4.3).

Table (4.3) Input Data for Probabilistic Analysis, n = 1000

Random variables	Distribution	Mean value	Minimum value	Maximum value	Standard deviation
Cohesion (kN/m2)	Normal	20	10	30	**3.333**
Angle of internal friction(degree)	Normal	28	10	46	**6**
Unit weight(kN/m3)	Normal	20	16	24	**1.333**
Seismic load coefficient	**Normal**	**0.1**	**0**	**0.2**	**0.033**

The primary results of the probabilistic analysis can be displayed by mean of FOS, probability of failure, reliability index (normal) and reliability index (lognormal) and correlation coefficient between random variables; these relations are shown below:

- **Mean FOS:** The mean safety Factor is the mean (average) safety factor, obtained from the probabilistic analysis. It is simply the average of the safety factors calculated for the global minimum slip surface.
- **Probability of Failure:** The probability of failure is defined as the number of analyses with safety factor less than 1 divided by the total number of samples, calculating by equation (4.3).

$$PF = \frac{NUM.FAILED}{NUM.TOTAL} * 100\% \qquad \text{....... (4.3)}$$

where:

PF = probability of failure.

$NUM.FAILED$ = Number of analyses with safety factor < 1.

$NUM.TOTAL$ = Total number of analyses (samples).

- **Reliability Index:** The Reliability Index is an indication of the number of standard deviations which separate the mean safety factor from the critical safety factor (= 1). The Reliability Index can be calculated assuming either a normal or lognormal distribution of the safety factor results. If it is assumed that the safety factors are normally distributed, then Equation (4.4) is used to calculate the Reliability Index.

$$\beta = \frac{\mu_{FOS-1}}{\sigma_{FOS}} \qquad \text{........ (4.4)}$$

where:

β = reliability index.

μ_{FOS} = mean safety factor.

σ_{FOS} = standard deviation of safety factor.

If it is assumed that the safety factors are best fitted by a lognormal distribution, then Equation (4.5) is used to calculate the Reliability Index.

$$\beta_{LN} = \frac{\ln\left[\frac{\mu}{\sqrt{1+Cv^2}}\right]}{\sqrt{\ln\left(1+Cv^2\right)}} \qquad \text{. . . . . (4.5)}$$

where:

β_{LN} = lognormal Reliability Index.

μ = the mean safety factor.

Cv = coefficient of variation of the FOS (= σ / μ), **(Duncan and Stephen, 2005).**

- Correlation coefficient between random variables: The correlation coefficient indicates the degree of correlation between the two variables. A correlation coefficient close to 1 (or -1) indicates a high degree of correlation. A correlation coefficient close to zero indicates little or no correlation.

Results of probabilistic analysis are given in the Table (4.4). Correlation coefficient between shear strength parameters is estimated as close to (-0.5) according to natural of relationship between cohesion of soil and angle of internal friction.

Table (4.4) Results of the Probabilistic Analysis

Probabilistic analysis results	
Parameters	**value**
Factor of Safety, mean	**0.991**
Factor of Safety, standard deviation	**0.1991**
Factor of Safety, minimum	**0.434**
Factor of Safety, maximum	**1.675**
Probability of Failure	**55.200 % (552failed surfaces / 1000 valid surfaces)**
Reliability index (assuming normal distribution)	**-0.047**
Reliability index (assuming lognormal distribution)	**-0.147**

Figure (4.29) shows the results and location of the most critical slip surface for deterministic and probabilistic analyses.

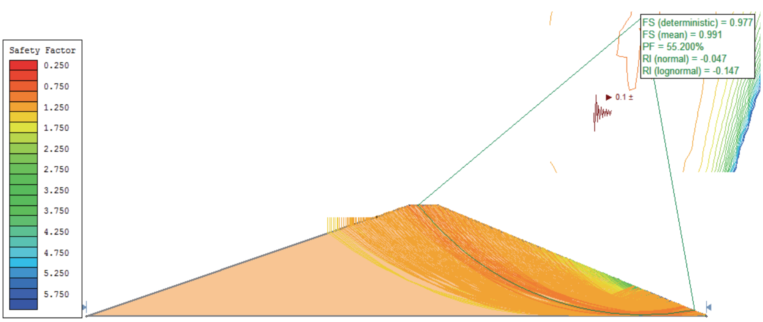

Figure (4.29) Results and Location of the Most Critical Slip Surface for Deterministic and Probabilistic Analyses.

Figures (4.30) present the sensitivity analysis of parameters that affect the factor of safety for general example

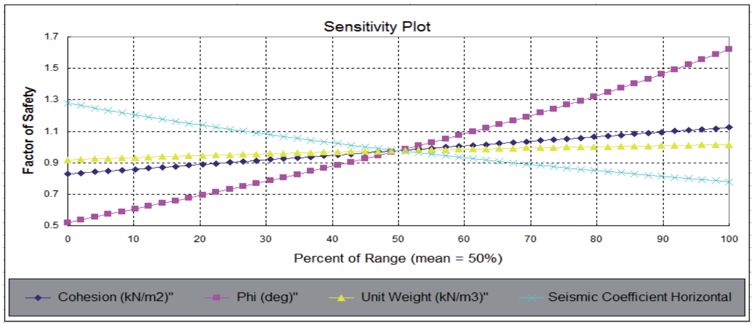

Figure (4.30) Sensitivity Plots of Parameters that Affect FOS.

From figure (4.30) it can be observed that the factor of safety is more sensitive to the friction angle, cohesion and seismic load coefficient (steep curves), while it is least sensitive to the unit (curves are almost flat). Percent of range = 0 represents the minimum value of each variable, and percent of range = 100 represents the maximum value of each variable. It is clear that all the curves were intersected at percent of range = 50%. Percent of range = 50% always represents the mean value of each variable.

Figures (4.31),(4.32),(4.33),and(4.34) shows the relationship between the cohesion of soil, friction angle of the soil, the unit weight of soil and of seismic load coefficient and Safety Factor respectively when this is parameter defined as a random variable.

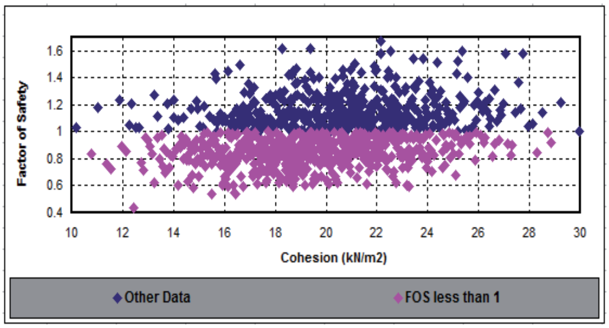

Figure (4.31) Relationship between Cohesion of Soil and Safety Factor for Probabilistic Analysis.

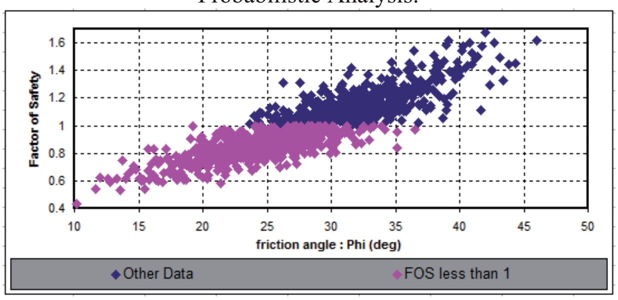

Figure (4.32) Relationship between Friction Angle of Soil and Safety Factor for probabilistic Analysis.

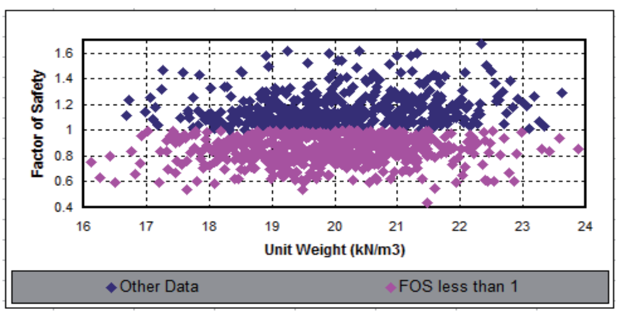

Figure (4.33) Relationship between Unit Weight of Soil and Safety Factor for probabilistic Analysis.

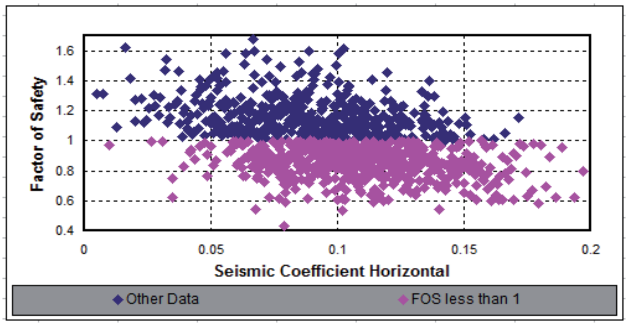

Figure (4.34) Relationship between Seismic Coefficient and Safety Factor for probabilistic Analysis.

It can be observed that the factor of safety is more effected to the friction angle, cohesion and seismic load coefficient and least effected to the unit (curves are almost flat).

Chapter Five

Result and Discussion of the Case Study

The aim of this chapter the deterministic and probabilistic approaches is used to investigate and analyze the effects of different loading conditions and different water level in the reservoir on seepage and slope stability for zoned earth dam **(**Mandali Dam as a case study), as shown in figure (5.1) . The same loading conditions that had been considered by the designer will by studied in this analysis and the results of the computer programs **(SLIDE V.6.0)** will be compared to those obtained by the designer.

After achieving the verification of the computer programming **(SLIDE V.6.0)** that has been presented in this study, the program is approved to be suitable for use to analyze seepage through earth dam and stability analysis of side slope. It is always required to answer the critical question to what extent the side slopes of an existing earth dam are safe. In this respect, the stability of side slopes of one important Iraqi dam will be re-analyzed in this chapter

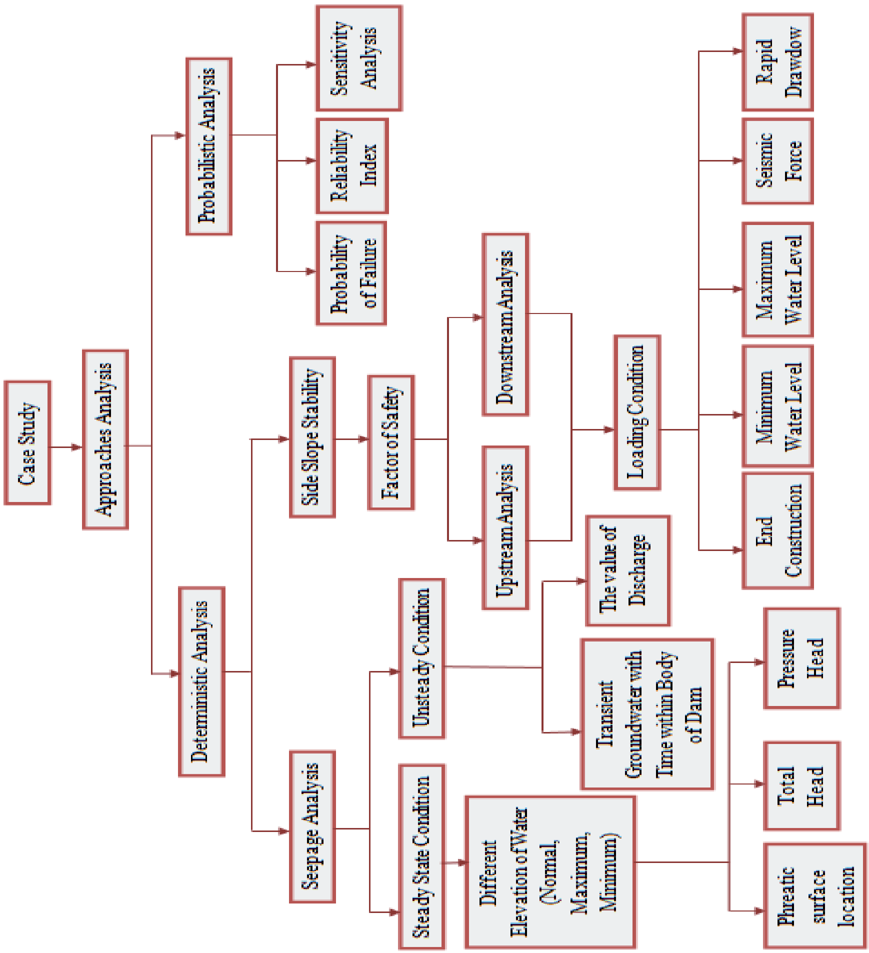

Figure (5.1) Analysis of Case Study

5.1 Zoned Earth Dams Mandali Dam: A Case Study

5.1.1General Description

The Mandali Dam is one of the earth fill dams in Iraq, which have been designed by Directorate General of Dam and Reservoirs. The designer analyzed the stability of the side slope of Mandali Dam under different loading conditions. The main reason behind that is the very conventional methods which utilized in that analysis.

Mandali dam is located on Harran Wadi, in the governorate of Diyala. TheWadi originates in Iran and passes the Iraqi border at north east of Mandali town and the area of the dam is bounded by the following coordinates (373700-378500) N, (554500-565000) E. The dam is a low dam, which acts in most of its parts as a submerged weir. The Wadi bed is gravely and permeable to some depth as it is clear from geological investigation. The type of dam most suitable for this situation is an earth fill dam at the wings and part of the wadi channel with a concrete weir at the center part. Earth fill materials such as clay, gravel, and sand are available in the area in good quantities and quality. The concrete part is in the form of an ogee weir with energy dissipation arrangement and its length is decided by the large design discharge anticipated in the wadi. **(Directorate General of Dams and Reservoire,(2004))**.

5.1.2 Basic Data of Mandali Dam:

Mandali dam with a central core at its total length is about (1316 m) and its maximum height is about (14m). The shell is composed mainly of poorly graded gravel with high percentage of coarse gravel , and the central core. The investigation and laboratory tests show that the available materials are clay at the site as a construction material for core. Figure (5.2) show a typical cross section of Mandali dam.

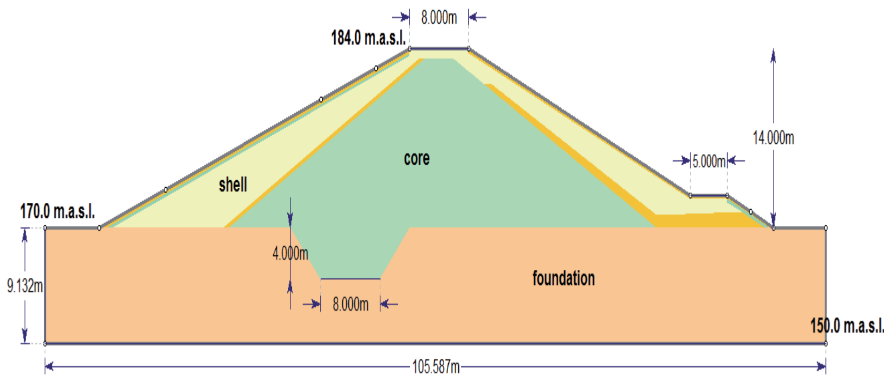

Figure (5.2) Cross Section of Mandali Dam by Programs (SLIDE V.6.0)

Table (5.1) displays the most important laboratory testing properties of the different materials composing of Mandali Dam.

Table (5.1) Material Properties for Mandali Dam **(Directorate General of Dams and Reservoire,(2004))**

Material type	**Parameter**	**Value**
Mealy dolomite (Foundation)	permeability, cm/sec	$(1.09\text{-}9.88)\times10^{-4}$
	Total unit weight, γ_t kN/m^3	21.5
	Cohesion, C kN/m^2	0
	Angle of internal friction ϕ	35
Poorly graded gravel with coarse gravel (shell)	permeability, cm/sec	$(1.37\text{-}2.72)\times10^{-4}$
	Total unit weight, γ_t kN/m^3	18.6
	Saturated unit weight, γ_s kN/m^2	20.5
	Cohesion, C kN/m^2	0
	Angle of internal friction ϕ	44
clay(Core)	permeability, cm/sec	1.15×10^{-6}
	Total unit weight, γ_t kN/m^3	17.6
	Saturated unit weight, γ_s kN/m^2	18
	Cohesion, C kN/m^2	80

5.2 Modeling and Analysis:

Stability analysis of zoned earthen dams is a more sensitive analysis than that of another big building structure because the great mass of the dam has a complex design structure, sensitive to water condition and load condition.

The finite element mesh used in this analysis is shown in Figure (5.3). Three node triangle element are used to describe the domains. The mesh contains 2500 element and 1624 node. The first step in this analysis is concerned with the selection of the numbers of element. These values are selected when the number of element becomes independents of solution. In this case any increment in the number of element dose not effect on the values of the solutions in domain of the analysis the number of elements which are selected from the mesh generation from change in phreatic surface as shown in Figure (5.4).

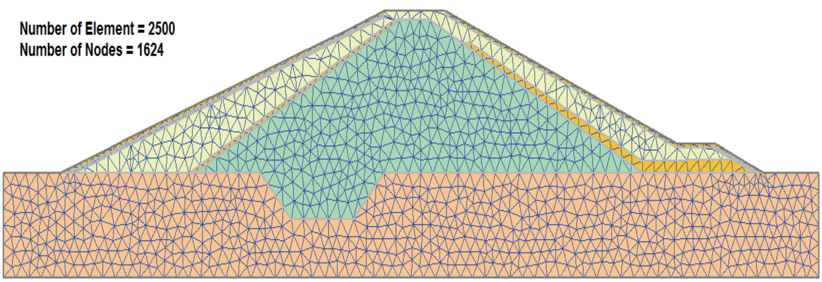

Figure (5.3) Finite Element Mesh for the Mandali Dam

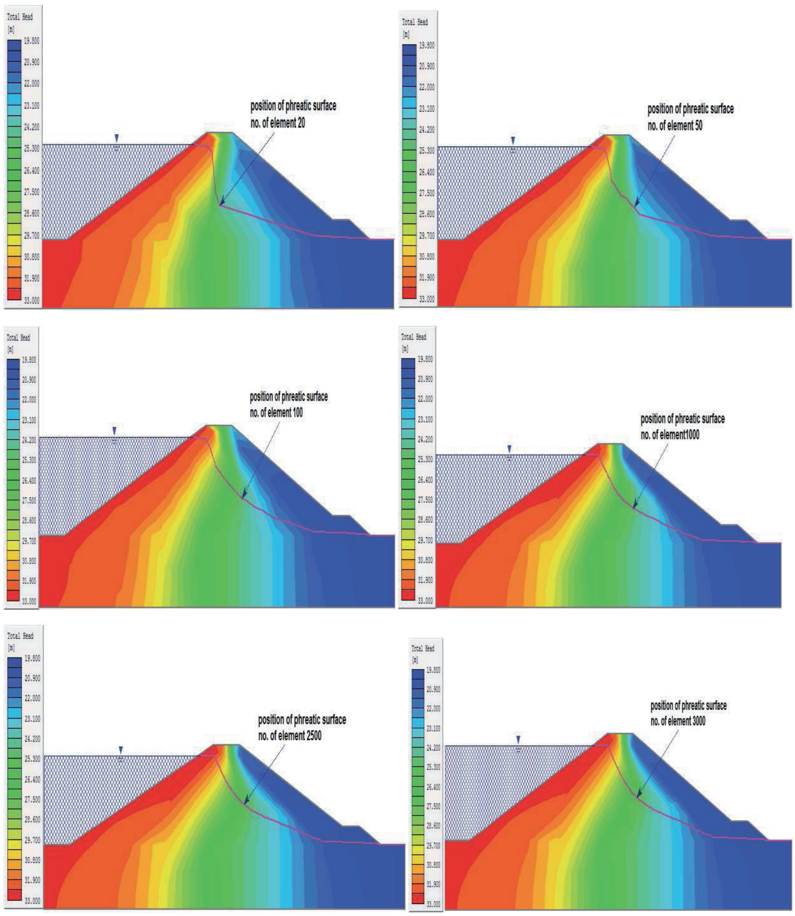

Figure (5.4) Mesh Generation from Change in Phreatic Surface

5.3 Results and Discussion

5.3.1 Seepage Analysis Results

Seepage through Mandali Dam under different water conditions is presented as follows:

- Normal reservoir level (180.0 m.a.s.l.)
- Maximum reservoir level (182.5 m.a.s.l.)
- Minimum reservoir level (173.0 m.a.s.l.)

Figure (5.5) shows three cross sections at different distance along length of the dam they will be considered in the analysis with respect to the different value of water level to find the effect of water level on the pheratic surface, total head and pressure head distribution. However, the total head and pressure head distribution for different value of water level (normal, maximum and minimum) are shown in Appendix- C.

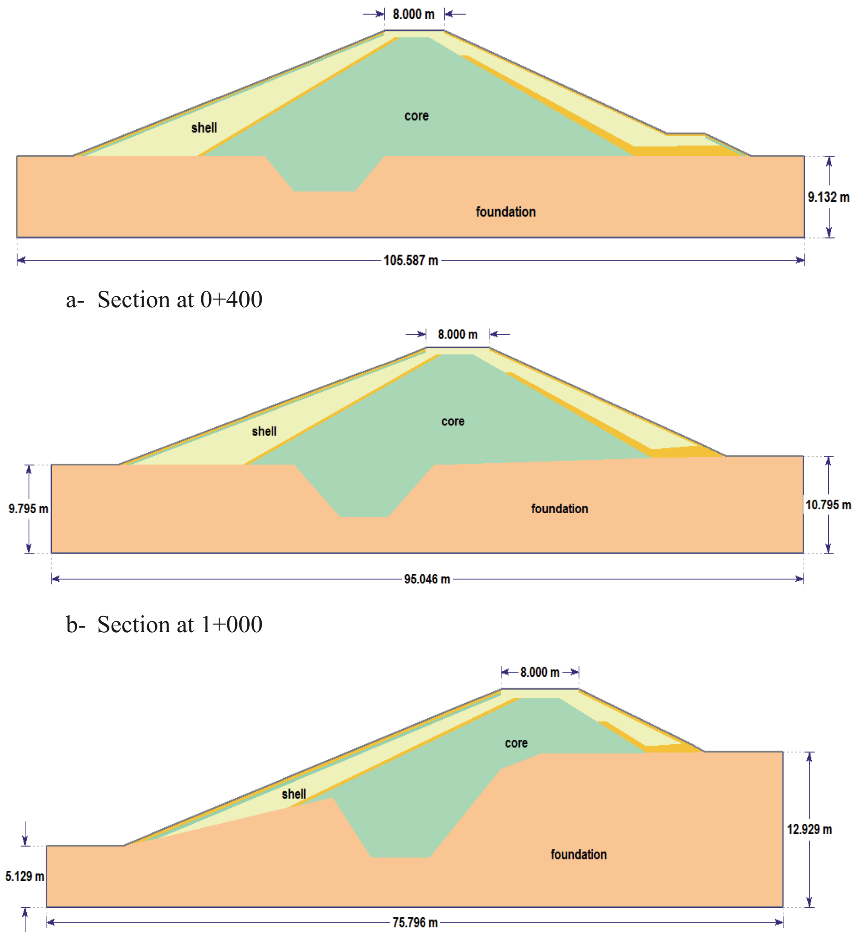

a- Section at 0+400

b- Section at 1+000

c- Section at 1+100

Figure (5.5) Cross Sections at Different Distance along Length of Mandali Dam

5.3.1.1 Normal Reservoir Level:

The water level in the upstream for the first case of normal operation is considered as 180.0 m.a.s.l and bed level of dam 170.0 m.a.s.l. Figures (5.6)and (5.7) show computed locations of free surface and flow vectors. The Figure indicates that free surface is constructed form several discontinuous surfaces because the rate of water movement is different in each material within the dam body. Furthermore, the free surface elevation drops from (179.8m) to (174.8m) at the boundary of diaphragm, which reflects the efficiency of the diaphragm as anti seepage device.

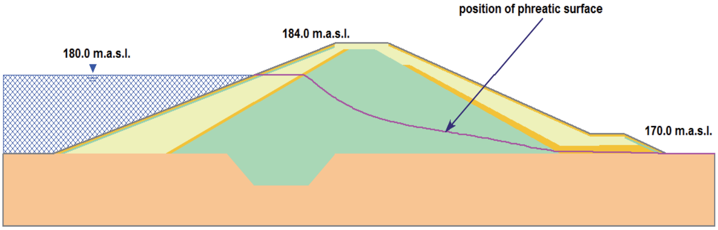

Figure (5.6) Computed Location of Phreatic Surface for Normal Water Level(180.0m.a.s.l.)

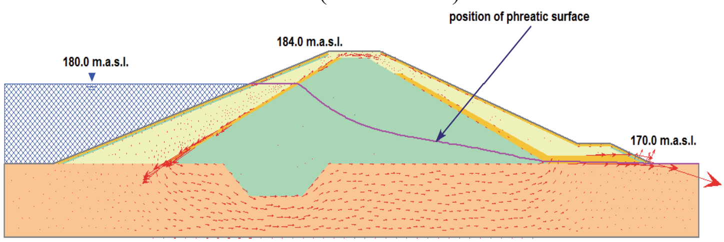

Figure (5.7) Computed Flow Vectors for Normal Water Level(180.0m.a.s.l.)

The water level in the upstream for the second case of normal operation is considered as 180.0 m.a.s.l and bed level for upstream of dam 171.0 m.a.s.l a. and downstream 172.0 m.a.s.l.. Figures (5.8)and (5.9) show computed location of free surface and flow vectors. The Figure indicates that the free surface elevation drops from (180.0m) to (176.0m) at the boundary of diaphragm.

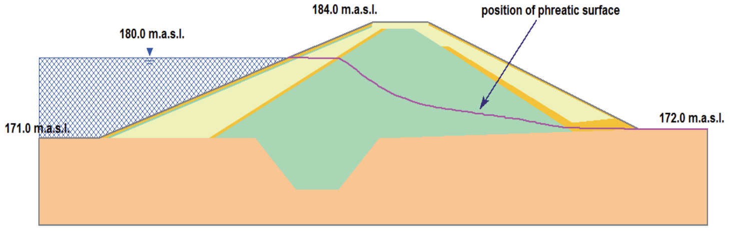

Figure (5.8) Computed Location of Phreatic Surface for Normal Water Level(180.0m.a.s.l.)

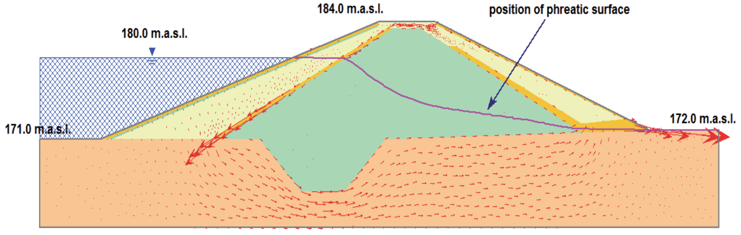

Figure (5.9) Computed Flow Vectors for Normal Water Level(180.0m.a.s.l.)

The water level in the upstream for the third case of normal operation is considered as 180.0 m.a.s.l and bed level for upstream of the dam 171.0 m.a.s.l a. and for the downstream 178.8 m.a.s.l. Figures (5.10) and (5.11) show computed location of free surface and flow vectors.

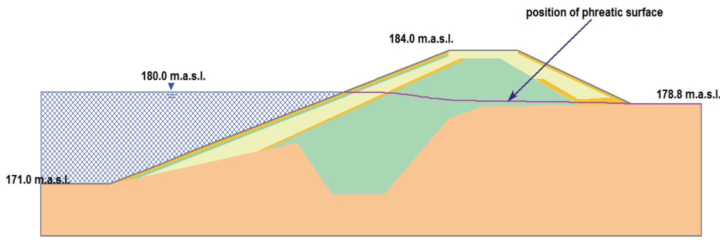

Figure (5.10) computed location of phreatic surface for normal water level(180.0m.a.s.l.)

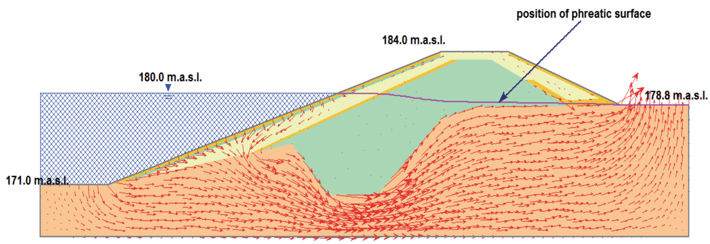

Figure (5.11) computed flow vectors for normal water level(180.0m.a.s.l.)

5.3.1.2 Maximum Reservoir Level

In this case, the water level in the upstream is considered at its maximum (i.e. 182.5m.a.s.l) and will be used for three sections. For the first section, Figures (5.12)and (5.13) show computed locations of the free surface in the shell and core for this water condition and flow vectors.

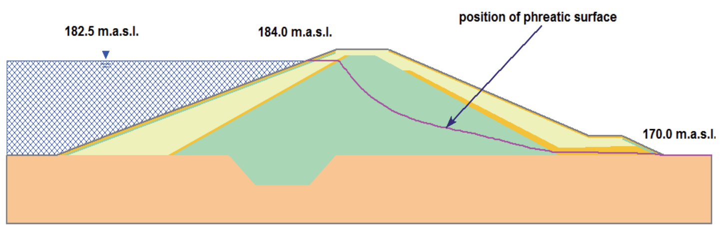

Figure (5.12) Computed Location of Phreatic Surface for Maximum Water Level(182.5m.a.s.l.)

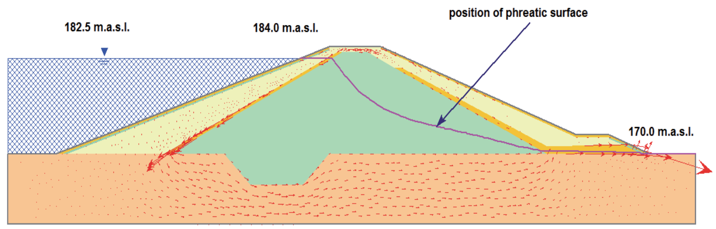

Figure (5.13) Computed Flow Vectors for Maximum Water Level(182.5m.a.s.l.)

For the second section figures (5.14)and (5.15) shows the computed locations of the free surface in the shell and core for this water condition and flow vectors.

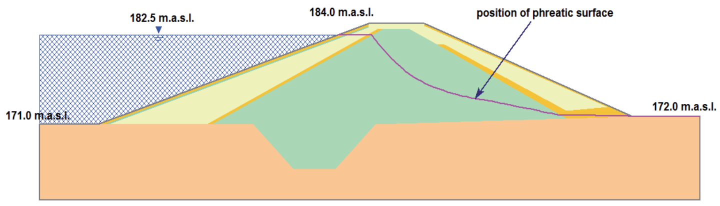

Figure (5.14) Computed Location of Phreatic Surface for Maximum Water Level(182.5m.a.s.l.)

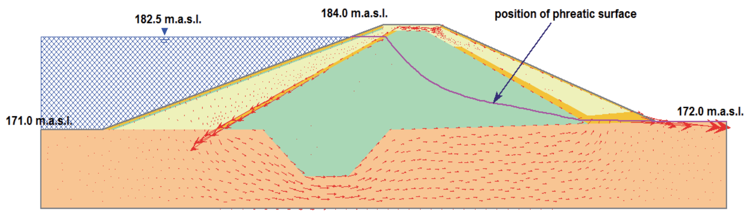

Figure (5.15) Computed Flow Vectors for Maximum Water Level(182.5m.a.s.l.)

For the third section Figures (5.16) and (5.17) show computed locations of the free surface in the shell and core for this water condition and flow vectors.

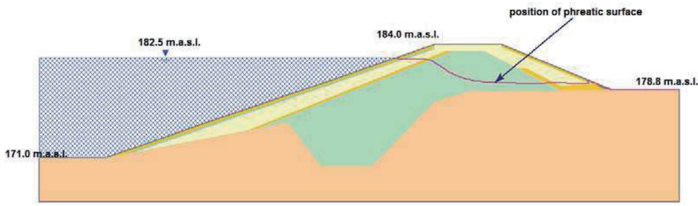

Figure (5.16) computed location of phreatic surface for maximum water level(182.5m.a.s.l.)

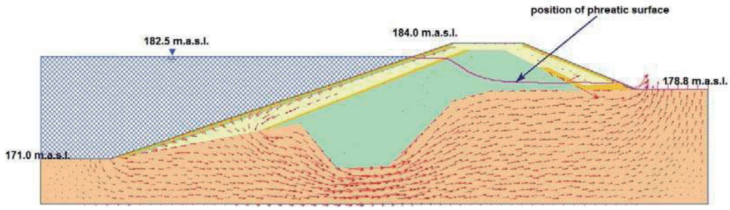

Figure (5.17) computed flow vectors for for maximum water level(182.5m.a.s.l.)

5.3.1.3 Minimum Reservoir Level

The water level is considered as 173.0 m.a.s.l. in the upstream side. For the first section the computed location of the free surface is corresponding to such a water condition and flow vectors which is shown in Figures (5.18) and (5.19). It can be noticed that a free surface is relatively horizontal in the shell and extension of the free surface in the core with a small drop near the junction of the core and diaphragm.

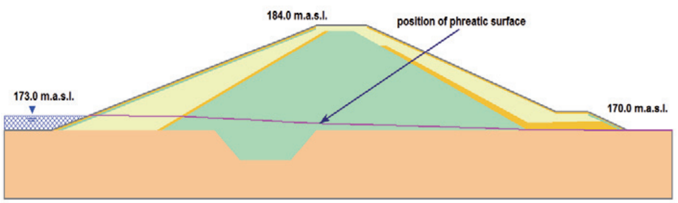

Figure (5.18) Computed Location of Phreatic Surface for Minimum Water Level(173.0m.a.s.l.)

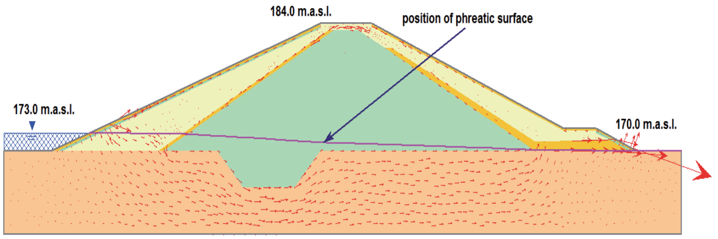

Figure (5.19) Computed Flow Vectors for Minimum Water Level(170.0m.a.s.l.)

For the second section the computed location of the free surface is corresponding to such a water condition and flow vectors which is shown in Figures (5.20) and (5.21).

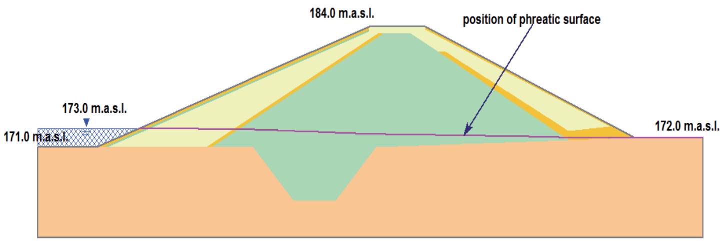

Figure (5.20) Computed Location of Phreatic Surface for Minimum Water Level(173.0m.a.s.l.)

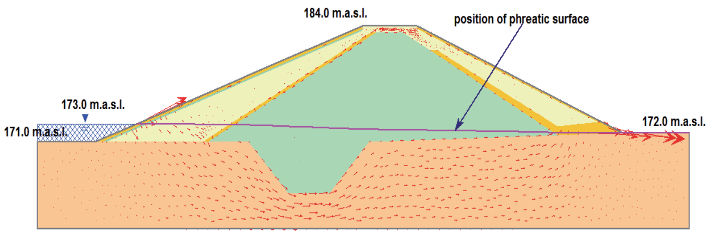

Figure (5.21) Computed Flow Vectors for Minimum Water Level(170.0m.a.s.l.)

For the third section the computed location of the free surface is corresponding to such a water condition and flow vectors which is shown in Figure (5.22)and (5.23).

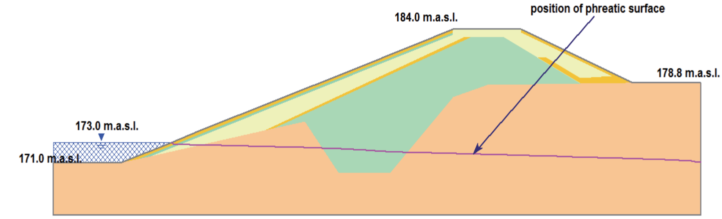

Figure (5.22) Computed Location of Phreatic Surface for Minimum Water Level(173.0m.a.s.l.)

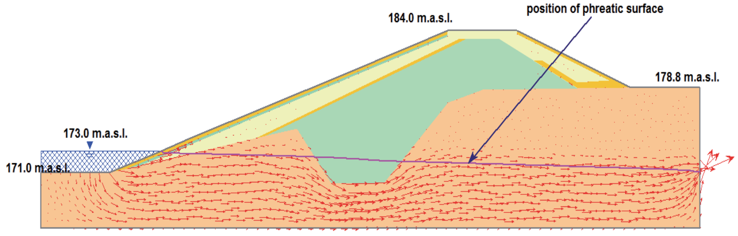

Figure (5.23) Computed Flow Vectors for Minimum Water Level(173.0m.a.s.l.)

5.3.2 Stability Analysis Results and Discussion

5.3.2.1 The Designer Stability Analysis of Mandali Dam

The designer has analyzed the stability of the dam in the channel portion where the height of the dam is about (14.0 m) (the maximum height). The analysis is accomplished according to the following methods **(Directorate General of Dams and Reservoire,(2004))**:

- Slip surface method.
- The ordinary slice method with earthquake.

For upstream, two slip surfaces are assumed the first passes the shell only, while the second passes through the core and the foundation. Steady seepage case is checked for downstream slope by two failure planes. One failure plane is assumed for rapid drawdown case as shown in Figures (5.24) and (5.25).

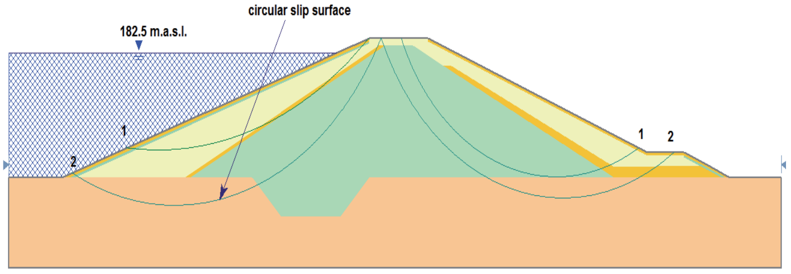

Figure (5.24) Slip Planes U/S and D/S Stability Checking Proposed by Designer

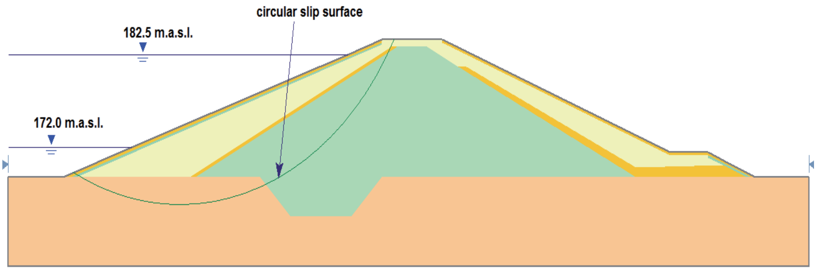

Figure (5.25) Deep Failure plane for Rapid Drawdown Case Proposed by Designer

According to the above-mentioned methods of analysis, slip surface of a certain shape and location is to be assumed and the value for the factor of safety is then to be obtained for that surface. In addition to this pre-asumption, which is in most cases not in the safe side, the ordinary method neglects completely the effects of the interslice forces. This assumption gives an underestimated value for the factor of safety and violates Newton's second law of action and reaction at the slice interfaces.

The results of the designer analysis (values of factor of safety to each shape of slip surface) for different water conditions are shown in Table(5.2) according to the slip surface method and they will be discussed and compared with the results of the present analysis in the following paragraphs.

Table (5.2) Factor of Safety for Stability of Side slope Presented by the Designer of Mandali Dam**(Directorate General of Dams and Reservoire,(2004))**

case	Type of slip surface	upstream side slope	downstream side slope
Full reservoir	Circular slip surface	1.52	-
Full reservoir+ Earth quake		1.23	-
End of construction		2.30	2.90
Steady seepage		-	2.74
Steady seepage+ Earthquake		-	1.54
Partial drawdown		1.97	-

(-) refer to unknown value

5.3.3 Methods of Solution Used in the Present Analysis

The computer program **(SLIDE V.6.0)** has been utilized to analyze the stability of the Mandali Dam. The loading conditions considered in the present analysis are, to some similar to those studied by the designer. The limit equilibrium method (LEM) ,according to Morgenstern-price presented by the computer program **(SLIDE V.6.0)** is applied to define the potential slip surface and to calculate the factor of safety of the dam slopes. The failure area is assumed and divided into a number of sections. The equilibrium of each section was considered and finally a factor of safety for the assumed slip surface was determined, hence, the consideration of the equilibrium of the whole mass. The potential slip surface and factor of safety are iteratively determined until a critical slip surface and minimum factor of safety have been found.

The slip surface types used in the present analysis are circular slip surfaces and non-circular slip surfaces (polygonal).The surface definition and search method used are encountered in the block search. The analysis method used is the limit equilibrium method (LEM) according to Morgenstern-price. The strength model used in the present analysis, is Mohr-Coulomb.

After reviewing the methods and scenario, which are used in the present analysis, the stability of the dam side slope is investigated under different conditions as follows:

5.3.3.1 End of Construction Condition:

Stability at the end of construction is the most critical for embankments constructed of plastic materials. Immediately on completion of embankment there would be construction pore pressure due to consolidation of fill under the embankment load there would be no water loads. The values of the factor of safety was obtained by the designer based on the slip surfaces method and according to the circular slip surface method.

According to the present analysis of slope stability, using program **(SLIDE V.6.0),** the most critical slip surfaces in the upstream and downstream for these loading conditions for each possible slip surfaces are shown in Figures (5.26), and (5.27).

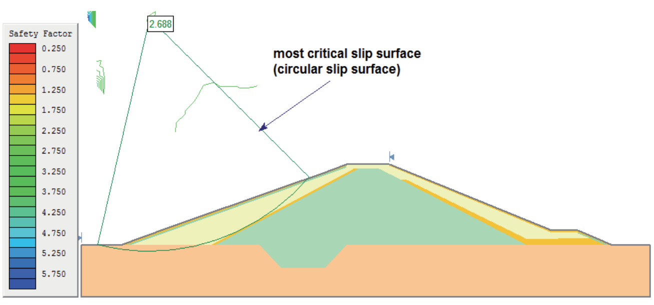

Figure (5.26) Location and Value of the Most Critical Slip Surface (Circular Slip Surface) Obtained in the Present Work, FOS = 2.688

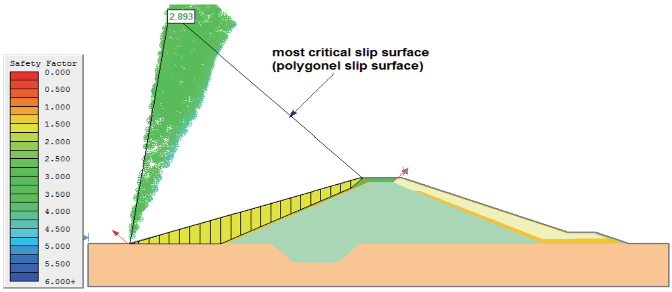

Figure (5.27) Location and Value of the Most Critical Slip Surface (Polygonel Slip Surface) Obtained in the Present Work, FOS = 2.893

Table (5.3)show the results obtained by the designer and compared with the results of the present by using program **(SLIDE V.6.0)**

Table (5.3) Factor of Safety Obtained by Designer and in the Present Work for End of Construction Condation

Condition	results of the present research			results of the designer	
	Method used	Type of slip surface		Method used	Type of slip surface
		circular	Non circular (polygonal)		circular
upstream	Morgenster n-price	**2.688**	**2.893**	Slip surface	**2.30**
downstream		**2.285**	**2.755**		**2.90**

From Table(5.3), the shape and location of the most critical slip surface are different from those presumed by designer,so it can be noticed that the values of factor of safety are slightly more than those found by the designer.

5.3.3.2 Minimum Reservoir Level Condition:

According to the present analysis of the slope stability, using program **(SLIDE V.6.0),** the most critical slip surfaces in the upstream and downstream for these loading conditions for each possible slip surfaces are shown in Figures (5.28), and (5.29).

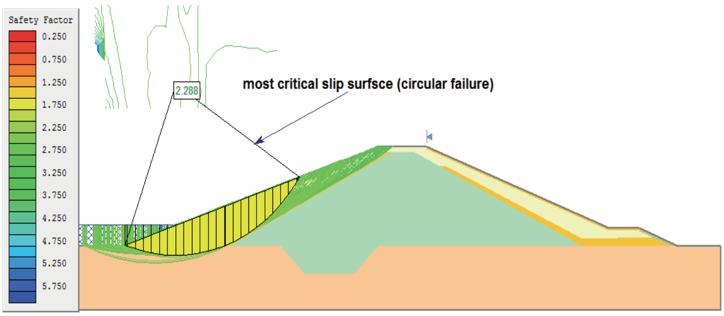

Figure (5.28) Location and Value of the Most Critical Slip Surface (Circular Slip Surface) Obtained in the Present Work, FOS = 2.288

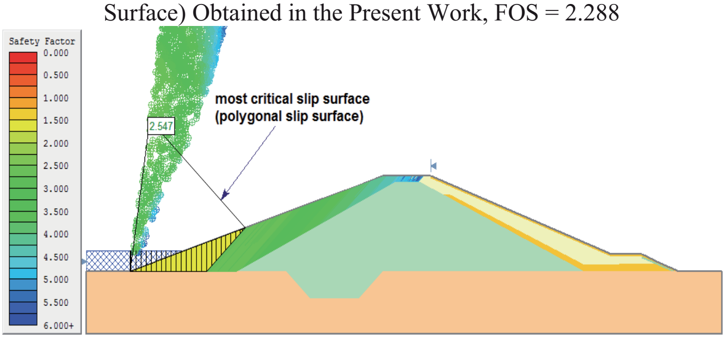

Figure (5.29) Location and Value of the Most Critical Slip Surface (Polygonel Slip Surface) Obtained in the Present Work, FOS = 2.547

The values of factor of safety obtained in the present work for upstream and downstream for two slip surface circular slip surfaces and non-circular slip surfaces (polygonal) are shown in Table (5.4).

Table (5.4) Factor of Safety Obtained in the Present Work for Minimum Reservoir Level Condition

Condition	results of the present research		
	Method used	Type of slip surface	
		circular	Non circular (polygonal)
upstream	Morgenstern-price	**2.288**	**2.547**
downstream		**2.882**	**2.717**

5.3.3.3 Minimum Reservoir Level with Seismic Effects:

The seismic load condition has been studied to investigate the stability of the Mandali Dam under this condition. The designer investigated the seismic effects on the dam due to an earthquake of about (0.07g) lateral acceleration. The inertia forces due to this proposed acceleration is assumed to act at each slice centroid. The dam is considered to be at the end of the construction stage and before filling the reservoir.

In the present work, the position and the shape of most critical slip surface for minimum water level with seismic effects for circular and polygonal slip surfaces are shown in Figures (5.30) and,(5.31) respectively. The seismic load coefficient used in this analysis is the same as that used by designer.

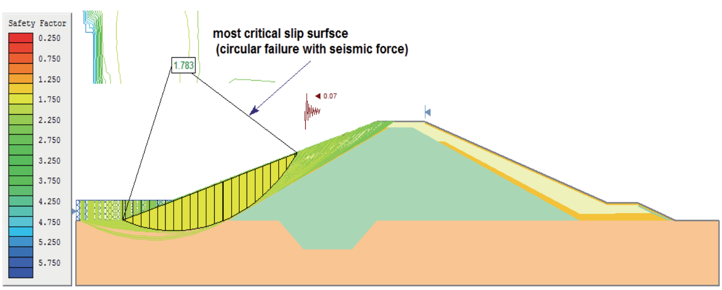

Figure (5.30) Location and Value of the Most Critical Slip Surface (Circular Slip Surface) for Minimum Water Level with Seismic Effect (0.07), FOS = 1.783.

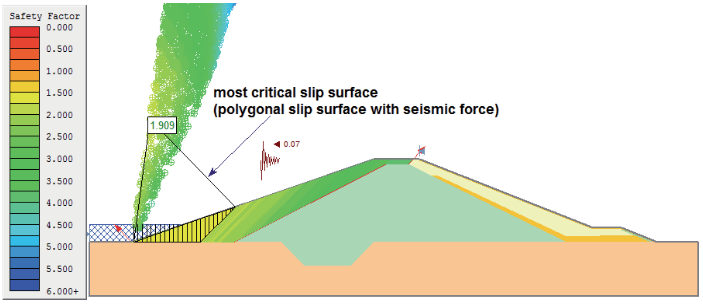

Figure (5.31) Location and Value of the Most Critical Slip Surface (Polygonal Slip Surface) for Minimum Water Level with Seismic Effect (0.07), FOS = 1.909

The values of the factor of safety obtained in the present work by using program **(SLIDE)** for upstream and downstream which includes two slip surface circular and non-circular slip surfaces (polygonal)are shown in Table (5.5).

Table (5.5)the Values of Factor of Safety Obtained in the Present Work.

Condition	results of the present research		
	Method used	Type of slip surface	
		circular	Non circular polygonal
upstream	Morgenster n-price	**1.783**	**1.909**
downstream		**1.866**	**1.971**

5.3.3.4 Maximum Reservoir Level condition:

In this loading condition, the water level in the upstream is assumed to be maximum (182.50 m). The values of the factor of safety that obtained by the designer are based on the slip surfaces method and according to the circular slip surface method.

The most critical slip surfaces, as determined by the present analysis, for this water condition are circular slip surfaces that pass close to the upper surface of the upstream slope and polygonal slip surface that passes close to toe of the dam in upstream are shown in Figure (5.32)and(5.33). The slip surface is shown in Figures (5.34)and(5.35), from the Figures it can be noted that the mode of the critical failure for this loading condition is almost a local failure in the upper face of the upstream and downstream (shell).

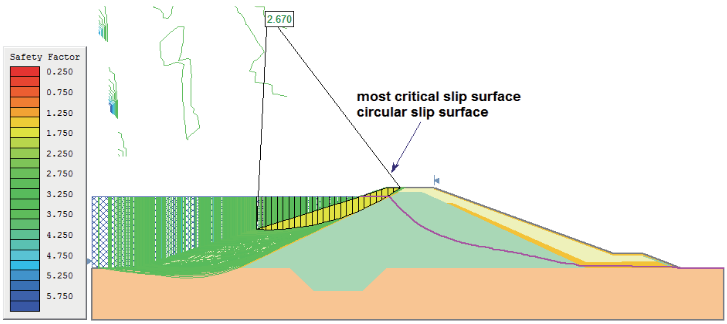

Figure (5.32) the Most Critical Slip Surface (Circular Slip Surface) in Upstream Side for Maximum Water Level in Reservoir

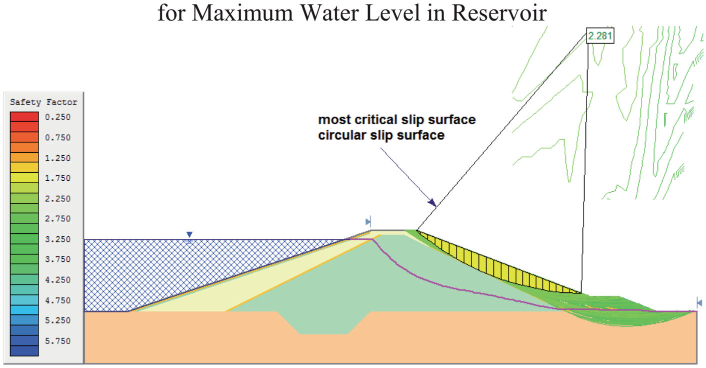

Figure (5.33) the Most Critical Slip Surface (Circular Slip Surface) in Downstream Side for Maximum Water Level in Reservoir

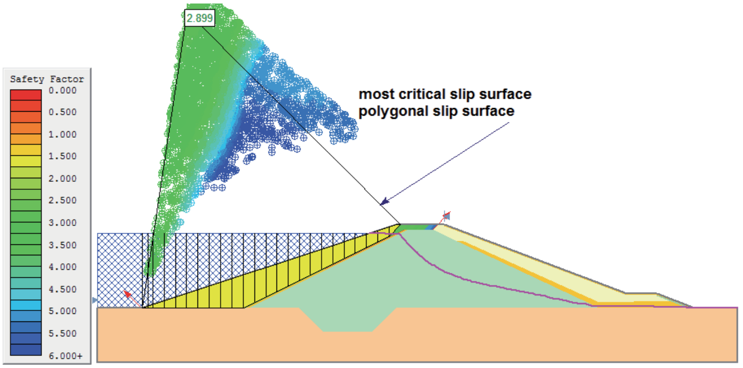

Figure (5.34) the Most Critical Slip Surface (Polygonal Slip Surface) in Upstream Side for Maximum Water Level in Reservoir.

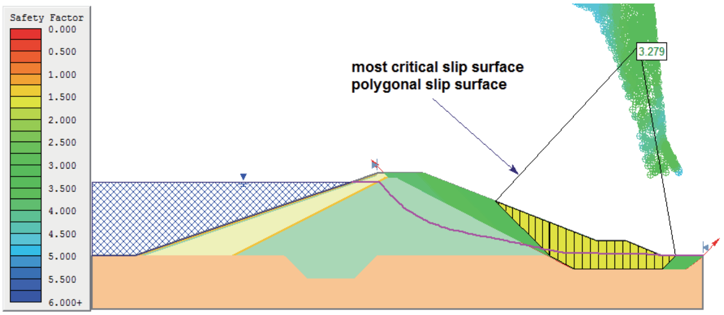

Figure (5.35) the Most Critical Slip Surface (Polygonal Slip Surface) in Downstream Side for Maximum Water Level in Reservoir.

Table (5.6) shows the results obtained by the designer and compared with the present results by using program **(SLIDE V.6.0)** for upstream and downstream under maximum reservoir level condation.

Table (5.6) Factor of Safety Obtained by Designer and in the Present Work for Maximum Reservoir Level condation

<table>
<tr><th rowspan="3">Condition</th><th colspan="3">results of the present research</th><th colspan="2">results of the designer</th></tr>
<tr><th rowspan="2">Method used</th><th colspan="2">Type of slip surface</th><th rowspan="2">Method used</th><th>Type of slip surface</th></tr>
<tr><th>circular</th><th>Non circular (polygonal)</th><th>circular</th></tr>
<tr><td>upstream</td><td rowspan="2">Morgenstern-price</td><td>2.670</td><td>2.889</td><td rowspan="2">Slip surface</td><td>1.52</td></tr>
<tr><td>downstream</td><td>2.281</td><td>3.279</td><td>2.74</td></tr>
</table>

From Table(5.6), it can be noticed that the values of factor of safety are slightly more than those found by the designer because the factor of safety depened on the shape and the location of the most critical slip surface and its difference from those presumed by designer.

5.3.3.5 Maximum Reservoir Level with Seismic Effects:

The seismic load condition has been studied to investigate the stability of the Mandali Dam under this condition. The designer investigated the seismic effects on the dam due to an earthquake of about (0.07g) lateral acceleration.

In the present research the position and the shape of most critical slip surface for maximum water level with seismic effects for circular and polygonal slip surfaces upstream and downstream are shown in Figures (5.36),(5.37),(5.38) and(5.39), respectively. The seismic load coefficient used in this analysis is the same as that used by designer.

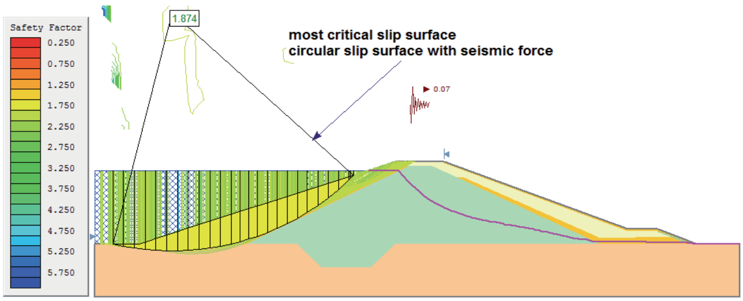

Figure (5.36) Most Critical Slip Surface (Circular Slip Surface) in Upstream Side for Maximum Water Level in Reservoir with Seismic Force

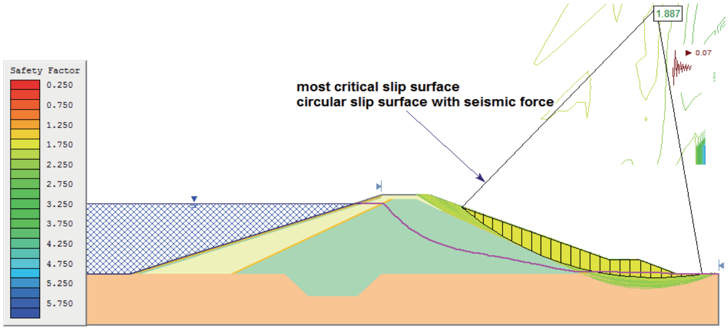

Figure (5.37) Most Critical Slip Surface (Circular Slip Surface) in Downstream Side for Maximum Water Level in Reservoir with Seismic Force

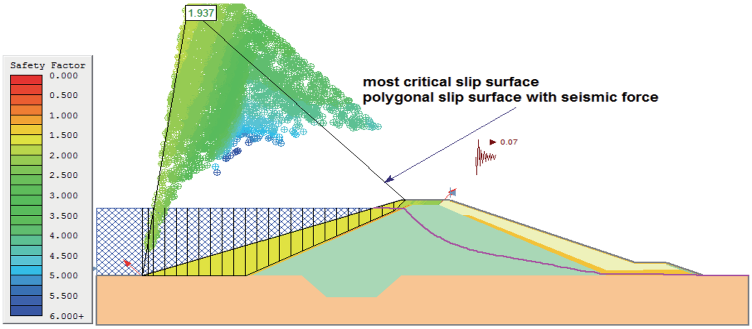

Figure (5.38) Most Critical Slip Surface (Polygonal Slip Surface) in Upstream Side for Maximum Water Level in Reservoir with Seismic Force

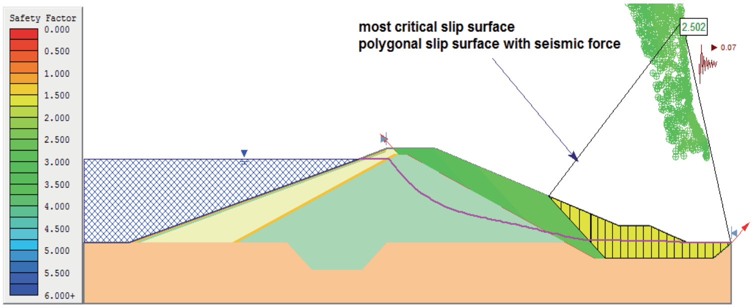

Figure (5.39) Most Critical Slip Surface (Polygonal Slip Surface) in Downstream Side for Maximum Water Level in Reservoir with Seismic Force

Table (5.76)show the results obtained by the designer and compared with the present results by using program **(SLIDE V.6.0)** for upstream and downstream under Maximum Reservoir Level with seismic force condation(0.07).

Table (5.7) Factor of Safety Obtained by Designer and in the Present Work for Maximum Reservoir Level with Seismic Force Condation

Condition	results of the present research			results of the designer	
	Method used	Type of slip surface		Method used	Type of slip surface
		circular	Non circular polygonal		circular
upstream	Morgenstern-price	**1.874**	**2.502**	ordinary	**1.23**
downstream		**1.887**	**1.937**		**1.54**

5.3.3.6 Rapid Drawdown Condition

Stability analysis during rapid drawdown is an important consideration in the design of embankment dams. During rapid drawdown, the stabilizing effect of the water on the upstream face is lost, but the pore-water pressures within the embankment may remain high. As a result, the stability of the upstream face of the dam can be much reduced. The dissipation of pore-water pressure in the embankment is largely influenced by the permeability and the storage characteristic of the embankment materials. Highly permeable materials drain quickly during rapid drawdown, but low permeability materials take a long time to drain.

Generally, sudden drawdown stability computations are performed for conditions occurring when the water level adjacent to the slope is lowered rapidly. For the analysis purposes, it is assumed that drawdown is very fast, and no drainage occurs in materials with low permeability, thus the term "Sudden" drawdown. Materials with values of permeability greater than 10^{-4} cm/sec can be assumed to drain during drawdown, and drained strengths are used for these materials [**U.S Army Corps of Engineers, (2003a)**].

Excess pore pressure refers to changes in pore pressure within the soil due to rapidly drawdown of pounded water in the upstream side conditions (undrained loading). Materials with low permeability such as clays, may exhibit this behavior. With the so-called "B-bar" method, the change in pore pressure is assumed to be directly proportional to the change in vertical stress. The excess pore pressure is given by :

$$\Delta u = \bar{B}\,\Delta\sigma_V \qquad \text{. . . . .} \quad (5.1)$$

where:

Δu = excess pore water pressure caused by drawdown condition.

$\bar{B}$ = (B-bar) overall pore pressure coefficient for earth fill material.

$\Delta \sigma_V$ = change in vertical effective stress.

From equation (5.1), it can be noted that the value of the excess pore pressure is dependent on the value of (B-bar) coefficient. The value of (B-bar) coefficient is dependent on the type of soil and properties of soil. If (B-bar) coefficient is defined about 0, the soil is free to drain and no excess pore water pressure is developed in upstream side. If (B-bar) coefficient is defined about 1, the undrained condition is applied and excess pore pressure is developed in upstream side. The value of (B-bar) coefficient close to 1then it represents the critical condition of rapid drawdown in upstream side and should be selected to any soils which have low permeability.

The designer has analyzed the case of rapid drawdown of the reservoir water level from elevation (182.5 m to 172. 0 m). In the present analysis a greater range of rapid drawdown is investigated and it starts from maximum elevation of 182.5m to elevation of 172.0 m which is the same as that used by designer.

Table (5.8) shows the results obtained by the designer and compared with the present results by using program **(SLIDE V.6.0)** for upstream under rapid drawdown condition of the reservoir water level from elevation 182. m to 172.0m.

Table (5.8) Factor of Safety Obtained by Designer and in the Present Work for Rapid Drawdown Condition of the Reservoir Water Level from Elevation 182.5 m to 172. 0 m

<table>
<tr><th rowspan="3">Condition</th><th colspan="2">results of the present research</th><th colspan="2">results of the designer</th></tr>
<tr><th rowspan="2">Method used</th><th>Type of slip surface</th><th rowspan="2">Method used</th><th>Type of slip surface</th></tr>
<tr><th>circular</th><th>circular</th></tr>
<tr><td>Upstream before drawdown</td><td rowspan="2">Morgenstern-price</td><td>2.983</td><td rowspan="2">ordinary</td><td>-</td></tr>
<tr><td>Upstream with drawdown</td><td>1.837</td><td>1.97</td></tr>
</table>

(-) refer to unknown value

Figure (5.40) shows the value and location of most critical slip surface for steady state condition (before drawdown). Figure (5.41) shows the value and location of most critical slip surface for rapid drawdown condition from EL. 182.5 m to EL. 172.0 m. Figures (5.42),(5.43),(5.44),(5.45),(5.46) and (5.47) show the value and location of most critical slip surface for rapid drawdown condition with seismic load effect for one and two direction for three different values of seismic coefficient, namely, (0.05, 0.07, and 0.09) acoording to scismic zoning factor**(Directorate General of Dams and Reservoire,(2004))**.

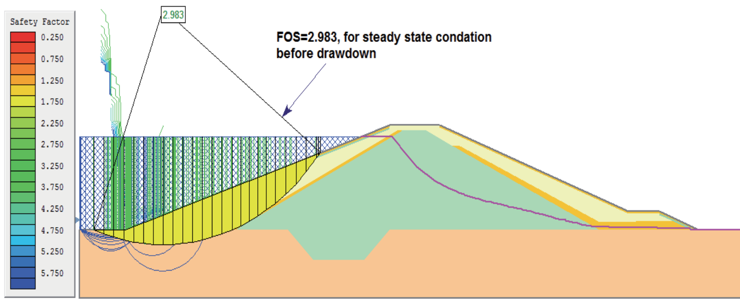

Figure (5.40) the Most Critical Slip Surface for Steady State Condition, before Drawdown, FOS = 2.983

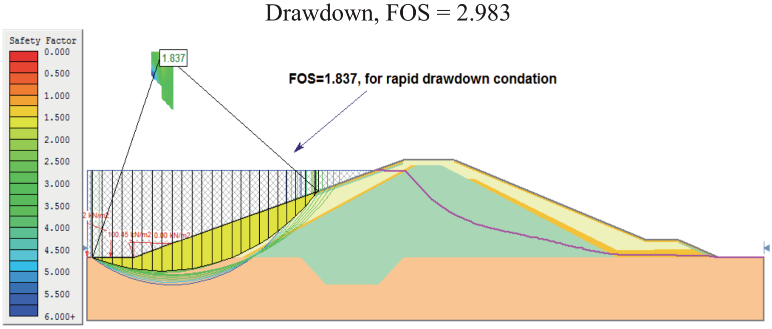

Figure (5.41) the Most Critical Slip Surface for Rapid Drawdown Condition from EL. 182.5 m to EL. 172.0 m, FOS = 1.837

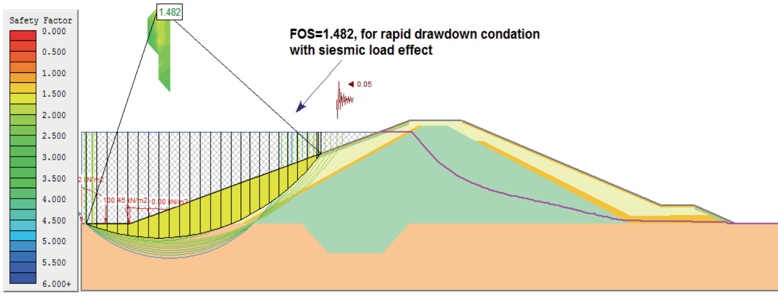

Figure (5.42) the Most Critical Slip Surface for Rapid Drawdown Condition with Seismic Load Effect (0.05) in One Directions, FOS = 1.482.

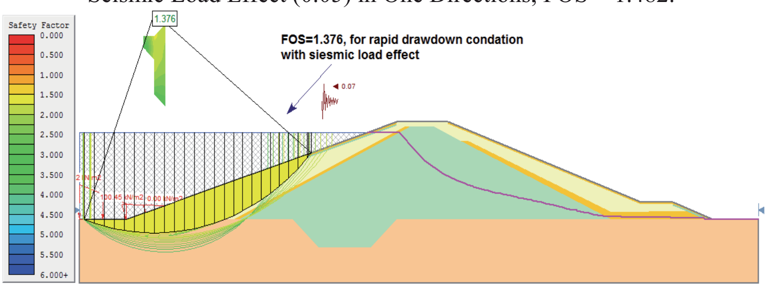

Figure (5.43) the Most Critical Slip Surface for Rapid Drawdown Condition with Seismic Load Effect (0.07) in One Directions, FOS = 1.376

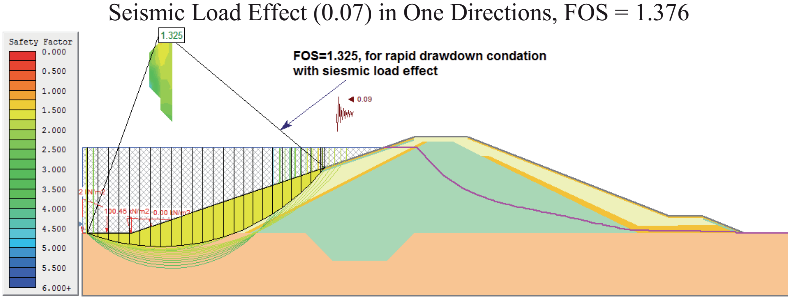

Figure (5.44) the Most Critical Slip Surface for Rapid Drawdown Condition with Seismic Load Effect (0.09) in One Directions, FOS = 1.325

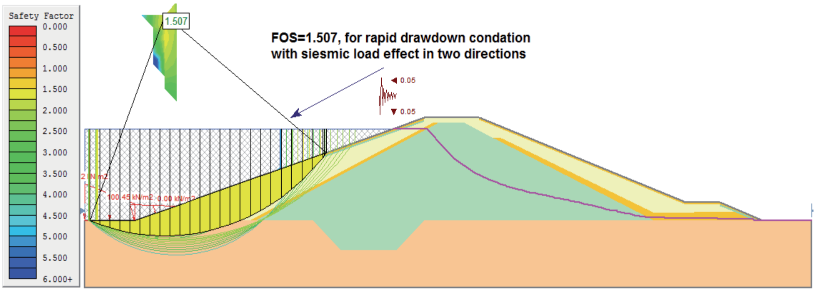

Figure (5.45) the Most Critical Slip Surface for Rapid Drawdown Condition with Seismic Load effect (0.05) in Two Directions, FOS = 1.507

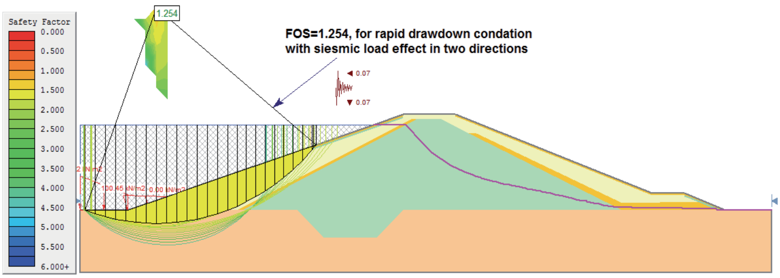

Figure (5.46) the Most Critical Slip Surface for Rapid Drawdown Condition with Seismic Load Effect (0.07) in Two Directions, FOS = 1.254.

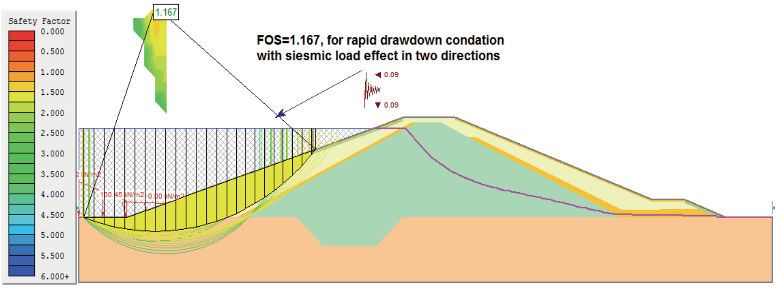

Figure (5.47) the Most Critical Slip Surface for Rapid Drawdown Condition with Seismic Load Effect (0.09) in Two Directions, FOS = 1.167.

5.4 Probabilistic Analysis of Zoned Earth Dams:

Probabilistic approaches become more and more popular for the design of embankments and dams in recent years as they provide a degree of safety, which corresponds to the specific structure. From the results of most critical slip surfaces for upstream and downstream side slopes for the Mandali Dam, it can be observed that the most critical slip surfaces in most cases are located at the shell of the dam in upstream and downstream. For these reasons, material properties for the shell of the dam will be defined as random variables (cohesion, unit weight, angle of internal friction), and load (seismic load).

Table (5.9) contains variables that were defined as random variables in the shell of the dam in this part of analysis.

Table (5.9) Input Data for Probabilistic Analysis and Variables that are Defined as Random Variables in the Shell of Dam, n = 3000.

Random variables	Distribution	Mean value	Minimum value	Maximum value	Standard deviation
Cohesion (kN/m^2)	Normal	0	0	20	3.333
Angle of internal friction(degree)	Normal	44	34	54	3.333
Unit weight(kN/m^3)	Normal	18.6	15.6	21.6	1
Seismic load coefficient	Normal	0.07	0	0.14	0.0233

Results of probabilistic analysis of stability of the upstream and downstream sides are shown in table (5.10)

Table (5.10) Results of Probabilistic Analysis for Uupstream and Downstream Side

Results of probabilistic analysis		
	downstream	upstream
Factor of Safety, deterministic	1.886	1.872
Factor of Safety, mean	1.910	1.958
Factor of Safety, standard deviation	0.134	0.251
Factor of Safety, minimum	1.570	1.355
Factor of Safety, maximum	2.368	3.067
Probability of Failure	0.00 % (0 failed surfaces / 3000 valid surfaces)	0.00 % (0 failed surfaces / 3000 valid surfaces)
Reliability index (assuming normal distribution)	6.744	3.806
Reliability index (assuming lognormal distribution)	9.136	5.185

It can be observed from the Table that the probability of failure is equal to zero which means that for all failed surface, of the 3000 valid surface for slip surface, the factor of the sefety more than 1.

Figures (5.48) and (5.49), present the sensitivity analysis of parameters that affect the factor of safety for upstream and downstream sides, respectively. From these Figures, it can be observed that the values of FOS are very sensitive to the value of seismic load more than that to the other variables.

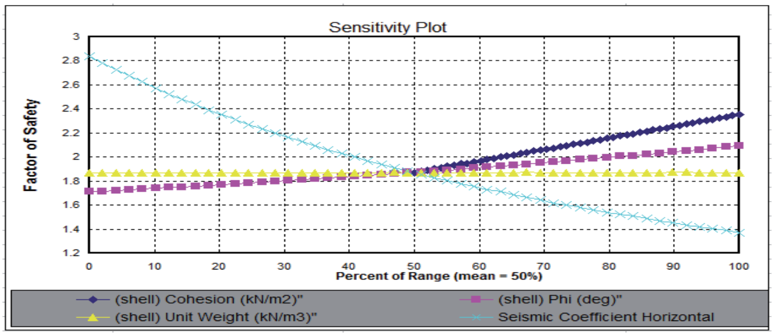

Figure (5.48) Sensitivity Analysis Plot of Parameters that Affect FOS for Upstream Side of Dam (shell).

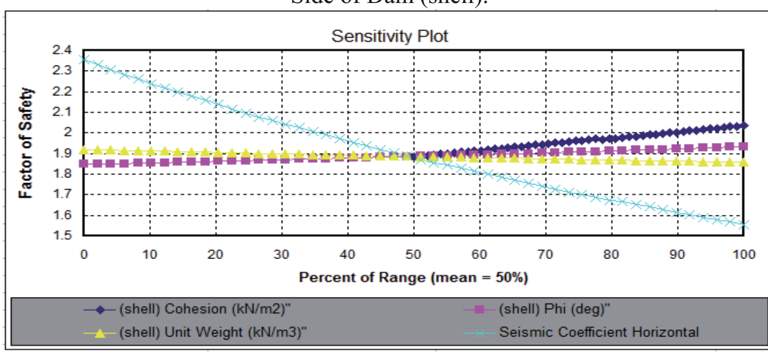

Figure (5.49) Sensitivity Analyses Plot of Parameters that Affect FOS for Downstream Side of Dam (shell).

Figures (5.50), and (5.51) show the determination coefficient between FOS and seismic load coefficient of the shell of dam in upstream side and downstream side

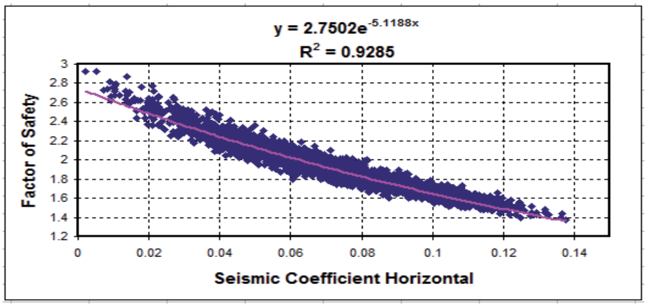

Figure (5.50) the Determination Coefficient between FOS and Seismic Load Coefficient of the Shell of Dam in Upstream Side.

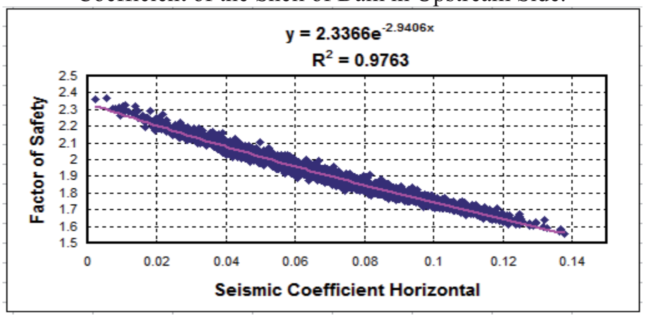

Figure (5.51) the Determination Coefficient between FOS and Seismic Load Coefficient of the Shell of Dam in Downstream Side.

From the high determination between the FOS and parameter (seismic load coefficient) for stability of upstream and downstream sides, proposed equations have been made to represent real correlation between FOS and this parameter.

Equations (5.2), is proposed for use to calculate the factor of safety of upstream sides of Mandali Dam.

$$FOS = 2.7502\ e^{-5.118x} \qquad [0 \le x \le 0.14] \qquad \text{- - - - - (5.3)}$$

$R^2 = 0.9285$

where:

FOS = factor of safety for upstream side

a = seismic load coefficient (shell).

Equations (5.3) is proposed for use to calculate the minimum factor of safety of downstream sides of Mandali Dam.

FOS = 2.3366 $e^{-2.9406x}$ $[0 \leq x \leq 0.14]$ - - - - - (5.4)

$R^2 = 0.9763$

where:

FOS = factor of safety for downstream side.

a = seismic load coefficient (shell).

Note: These proposed equations are obtained by using the facilities which provided with **SLIDE** program by using 3000 input data

5.5 Transient Groundwater Analysis:

A transient groundwater analysis may be important when there is a pore pressure -dependent change in time. This will occur when groundwater boundary conditions change and the permeability of the material is low. In this case, it will take a finite amount of time to reach steady state flow conditions. The transient pore pressures may have a large effect on slope stability.

This research will describe how to perform a transient groundwater analysis in ***Slide*** using finite elements and describe how this affects the slope stability. Calculations in this part will take ten stages for different time (10, 50, 100, 500, 10000, 30000, 50000, 70000, 90000, and 100000hours).

Figures (5.52) and(5.53) show the discharge section and straight line with ten points taken inside the body of the dam to show the effect of transient groundwater with time of pressure head for each stage.

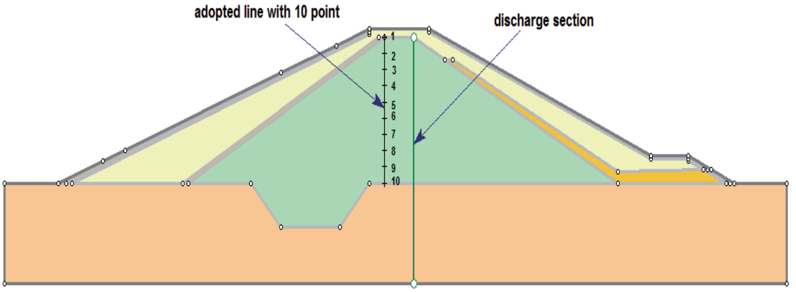

Figure (5.52) Body of Dam with Adopted Line and Discharge Section

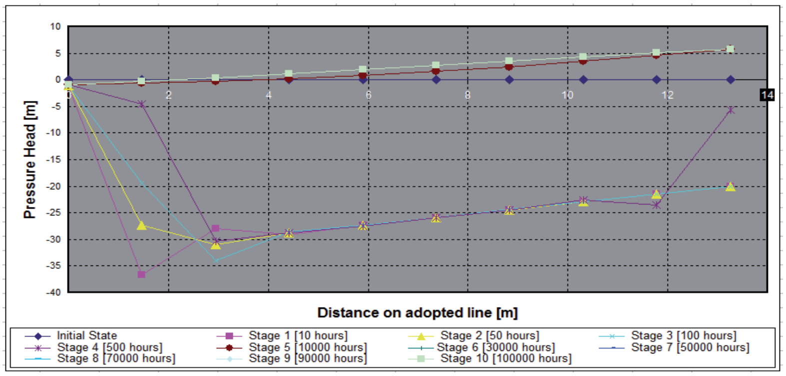

Figure (5.53)Pressure Head with Distance on Adopted Line.

Figures below shows how rapid rise in water level at the left edge has induced high pore pressure along the left flank gradually then reaching to steady state condition.

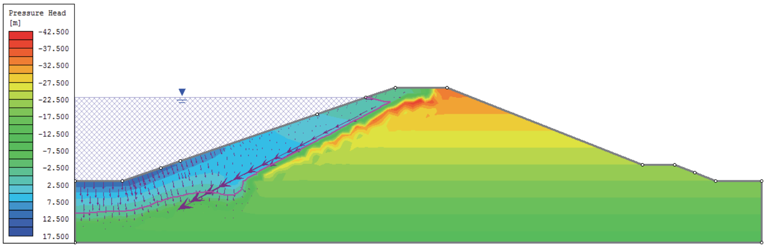

Figure (5.54) a Transient Groundwater (Stage 1at Time 10 hours)

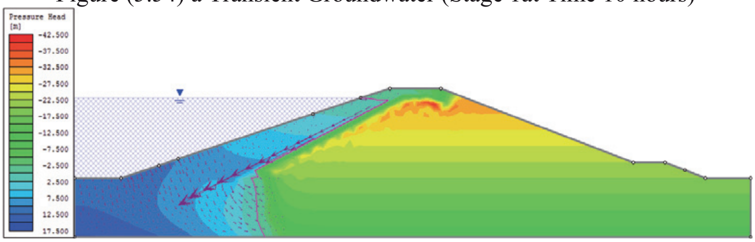

Figure (5.55) a Transient Groundwater (Stage 2 at Time 50 hours)

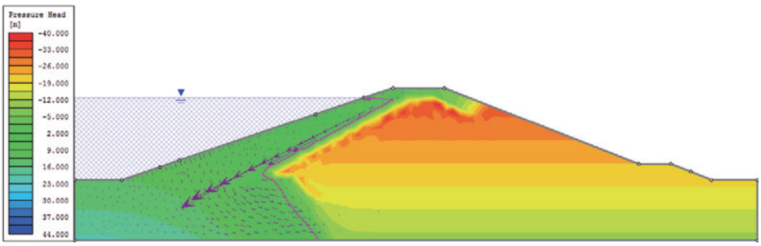

Figure (5.56) a Transient Groundwater (Stage 3 at Time 100 hours)

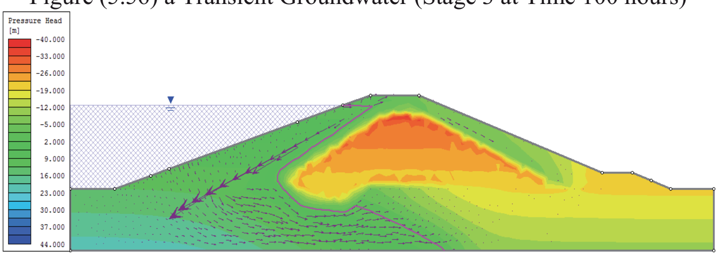

Figure (5.57) a Transient Groundwater (Stage 4 at Time 500 hours)

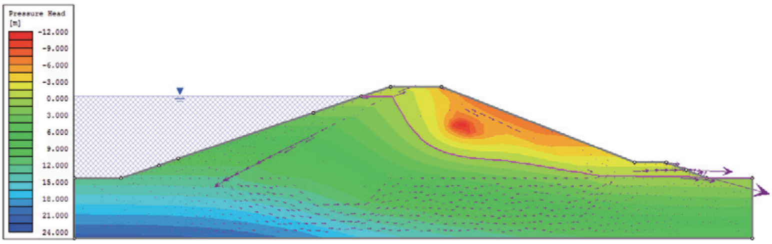

Figure (5.58) a Transient Groundwater (Stage 5 at Time10000 hours)

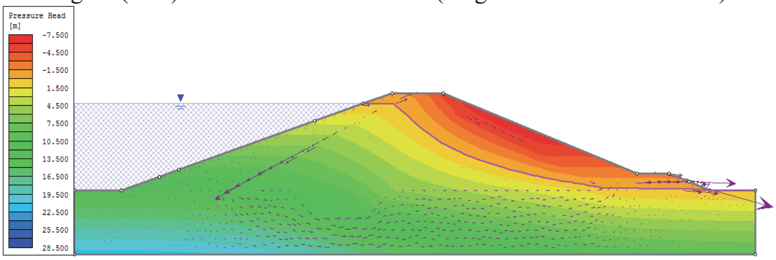

Figure (5.59) a Transient Groundwater (Stage 6 at Time 30000 hours)

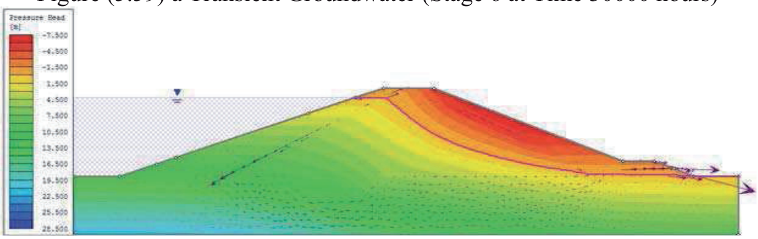

Figure (5.60) a Transient Groundwater (Stage 7 at Time 50000 hours)

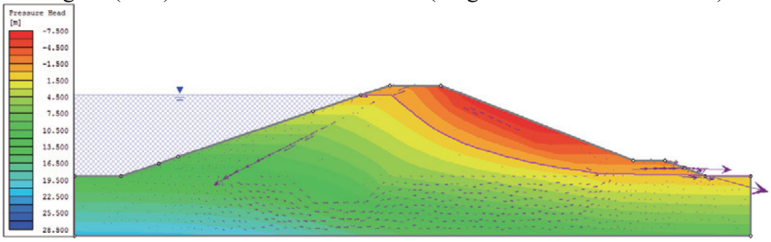

Figure (5.61) a Transient Groundwater (Stage 8 at Time 70000 hours)

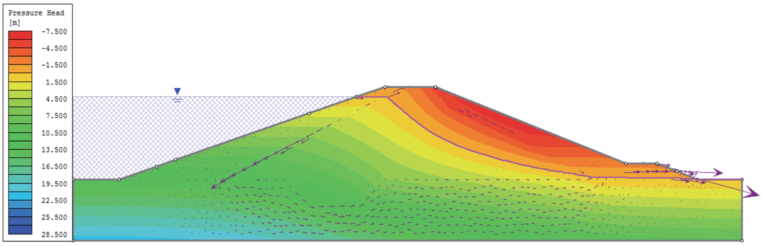

Figure (5.62) a Transient Groundwater (Stage 9 at Time 90000hours)

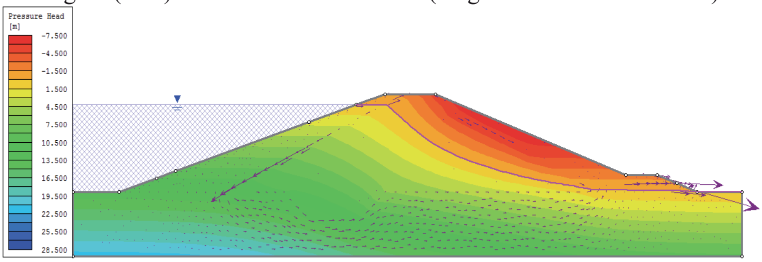

Figure (5.63) a Transient Groundwater (Stage 10 at Time 100000hours)

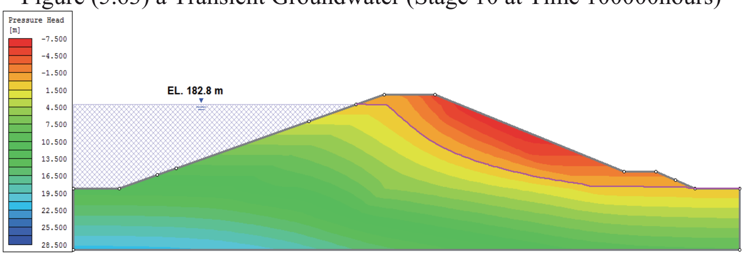

Figure (5.64) Steady State Condition

It can be observed from the figures that the phreatic surface from stage 7 to 10 remains constant whicht means that in time 50000 hours it will be reaching the steady state condition.

Table (5.11) Show the Change in the Value of Discharge for Each Stage.

Number of stage	**Time(hours)**	**Discharge(m^3/h)**
1	10	0
2	50	$5.99*10^{-6}$
3	100	$2.343*10^{-5}$
4	500	0.07965
5	10000	0.05433
6	30000	0.05430
7	50000	0.05427
8	70000	0.05427
9	90000	0.05427
10	100000	0.05427

From the Table, it can be observed that the value of discharge constant when the time equal 50000 hours when the dam reachs to the steady state condition.

The results of the present research, for deterministic analysis of the factor of safety for loading condition (end constraction, minimum water level, and maximum water level) for upstream and downstream and the effect of seismic force of factor of safety are acceptable. The mimimum of factor of safety will happen in upstream for rapid drawdown condition with seismic force effect. From probabilistic analysis the probabilty of failure is equal to zero and factor of safety are very sensitive to seismic force more than any other parameter.

Chapter Six

Conclusions and Recommendations

6.1 Conclusions

In this chapter, the main conclusions which can be drawn from the results of this study are summarized below:

1. The **SLIDE** computer program is suitable for modelling a complex geometry of earth dams than any other applicable methods; the modelling is very close to the realities of zoned earth dams.
2. The factor of safety increases for the following:
   - Decreased of the water level of reservoir.
   - It increases between (0.83% -15.40%) for horizontal drain, (2.03% -15.53%) for toe drain and (12.09% -16.428%) for chimney drain when water level decreased.
   - Increase prorate (67.78%) for the increase in the value of cohesion of soil.
   - Increase prorate (57.95%) for the increase in the value of angle of internal friction.
3. The factor of safety decreases for the following:
   - Decrease prorate (6.32%) for the increase in the value of unit weight of soil.
   - Decrease prorate (6.192%) for the increase in the value of distributed load.
   - Decrease prorate (28.67%) for the increase in the value of the seismic load coefficients.
   - Decrease prorate (48.754%) for the increase of the drawdown ratio for rapid drawdown condition.

4. The value of the factor of safety is more sensitive to the values of the angle of internal friction, seismic force and cohesion of soil than to those of other parameters.
5. Probabilistic analysis results make a guide to any designer of earthen dams to check reliability index and degree of confidence of design.
6. The stability of the upstream side slope is dramatically decreasing during a rapid drawdown. It can be concluded that the critical degree of FOS during the rapid drawdown can be considered at the drawdown ratio of 0.78, not until the emptying.
7. In the case study (Mandali Dam), the factor of safety for upstream and downstream for all considered condition are acceptable.
8. In the case study (Mandali Dam), the upstream slope is still stable during a rapid drawdown and the minimum value obtained for FOS is about 1.167 during the rapid drawdown and seismic load coefficient 0.09.
9. The factor of safety of Mandali Dam are very sensitive to seismic force more than any other parameter proposed equations have been made to represent real correlation between FOS and seismic force

   $FOS = 2.7502\, e^{-5.118x}$ $[0 \le x \le 0.14]$ (for upstream side)

   $R^2 = 0.9285$

   $FOS = 2.3366\, e^{-2.9406x}$ $[0 \le x \le 0.14]$ (for downstream side)

   $R^2 = 0.9763$

10. Transient groundwater analysis results make a guide at time (50000 hours) Mandali Dam reaches to steady state condition.

6.2 Recommendations for Future studies:

Based on the results obtained during assessing this work, the following recommendations are suggested for further studies:

1. The analysis can be modified further if three dimensional analysis of the seepage problem under transient conditions and three dimensional analysis for slope stability are considered.
2. Studying the effect of external loading on slope stability, such as waves in downstream.

1. Al-Bataineh, N., (2006), "**Slope Stability Analysis Using 2D and 3D Methods"** M.S. Dissertation, The Graduate Faculty of The University of Akron.

2. Al- Jairry H. H., (2010), **"2D-Flow Analysis Through Zoned Earth Dam Using Finit Element Approach"**, Building and Construction Department, University of Technology, Baghdad

3. Al-Jorany, A.N., (1996), **"Slope Stability Analysis"**, Ph.D. Dissertation, Department of Civil Engineering, University of Baghdad.

4. Al- Labban S.N.,(2007), "**Seepage Analysis of Earth Dams by Finit Element ",**M Sc. The College of Engineering of University of Kufa

5. Al-Qaisi, K.A., (1999), "**Analysis of earth dam by finite element method**", M.Sc. Dissertation, Department of Civil Engineering, University of Baghdad.

6. Arora K. R., (2007) "**Irrigation, Water Power and Water Resources Engineering**", Standard Publishers Distributers, Delhi, India.

7. Aryal K.P.,(2006) **"Slope Stability Evaluation by Limit Equilibrium and Finit Element Method**", Department of Civil and Transport Engineering Geotechnical Division Trondheim Norwag

8. Baker R., (1980). **"Determination of the Critical Slip Surface in Slope Stability Computations"**, International Journal for Numerical and Analytical Methods in Geomechanics, Vol.4.

9. Desai, C.S and Sherman, W.C., (1971), "**Unconfined transient seepage in sloping banks**", Journal of the Soil Mechanics and Foundations Division, ASCE, Vol.97, No.SM2, pp.357-373.

10. Directorate General of Dams and Reservoirs, (2004) **" Mandali Dam Project-Geological Report"** Ministry of water Resources.

11. Duncan, J. M. and Stephen, G. W., (2005), "**Soil Strength and Slope Stability"** John Wily and Sons, Hoboken, New Jersey.

12. Elouni M.R. and Kheder K., (2006) **"Reliabilty Analysis of Earth Dams: Case Elhouareb Dam- Kairouan- Tunisia",** Institut National Agronomiquede, Tunis, Tunisia and Institute Superieur Etudes Technologiquesde, Nabeul, Tunisia.

13. Fredlund, D.J and Krahn, J. (1977). "Comparison of Slope Stability Methods of Analysis", Canadian Geotechnical Journal, Vol.14, No. 3.

14. Fredlund M.D., Fredlund D.G. and Hung V.Q.,(2001) "**Seepage Modelling in Saturated Unsaturated Soil System ",** President of soil vision System L.td Sasatoon,sask,Canada , University of Saskatchewan, Sakatoon,Sask,Canada

15. Freeze, R.A. and Cherry, J.A. (1979), **"Groundwater",** Prentice-Hall, Inc. Englewood Cliffs, New Jersey.

16. Harr, M. E., (1962), "**Groundwater and Seepage**", McGraw-Hill Book Company, New York.

17. Janbu, N. (1973). "**Slope Stability Computations**," Embankment Dam Engineering - Casagrande Volume, John Wiley and Sons, N.Y.

18. Kamanbedast A. and Delvari A., (2012), **"Analysis of Earth Dam: Seepage and Stability Using Ansys and Geo-Studio Software",** Department of Agriculture, Ahwas Branch, Islamic Azad University, Azhad, Iran and Shoshtar Branch, Islamic Azad University, Iran.

19. Karami A. and Roozbahani M.,(2010) **"Reliability Analysis of Earth Dam, Case of Kalan Dam- Malayer, Iran ",** Department of Civil Engineering Technical and Vocational School of Sama, Malayer Branch, Iran.

20. Kassa N.A., (2009) **"Probabilistic Safety Analysis of Earth Dams"**, Submitted to Facculty of Civil Engineering of Technischc University Dresden.

21. Khan F. and Malik A. (2013). **"Probability and Sensitivity Analysis of the Slope Stability of Naulong Dam"**, Pak. J. Engg. & Appl. Sci. , Vol.13. (P. 54-64)

22. Khattab S.A.A., (2008), **"Stability Analysis of Mosul Dam under Saturated and Unsaturated Soil Condition",** Mosul University, Civil Engineering Department, Mosul

23. Lakehal R., Djemili L. and Houichi L., (2011) **"Nomograms for Calculation the Factor of Homegeneous Earth Dams in Long- Term Stability "**, Department of Hydraulics, Badhi Mokhtar University, Annaba,2300Annaba, Algeria and Department of Hydraulics, Hadjlakhdar University, Batna, Algeria.

24. Lambe, T.W. and Whitman, R.V., (1969), "**Soil mechanics**", John Wily and Sons, New York.

25. Li, G.C. and Desai, C.S., (1983), "**Stress and seepage analysis of earth dams**", Journal of Geotechnical Engineering, ASCE, Vol.109, No.7, pp.946-960.

26. Megan, R. S**., (2002),** "**Response of the Self-Potential Method to Changing Seepage Conditions in Embankment Dams"**M.AS. Dissertation, Department of Civil Engineering, University Of British Columbia.

27. Novak P.A. Moffat and Nalluri C., (2007) **"Hydraulic Structures",** School of Civil Engineering and Geosciences University Upon Tyne, UK and Formerly Department of Civil and Structural Engineering, UMIST, University of Manchester, UK (Fourth Edition)

28. Obaid, I. H., (2002), **"Stability of Zoned Earth Dam Coupled with Unsteady Drawdown"**, M.Sc. Dissertation, Department of Civil Engineering, University Of Babylon.

29. Pakhshandehroo Gholamreza, Vaghefi Mohammad and Hekmatzadeh Ali Reza, (2011) **" Three Dimensional Seepage Analysis in Mollasadra Dam after Its Impoundment"** Civil Engineering Department Faculty, Shiraz University, Iran, Shiraz. Civil Engineering Department Faculty, Persian Gulf University, Iran, Bushehr

30. Patel S.K. and Sanghvi C.S., (2012) **"Seismic Slope Stability Analysis of Kaswati Earth Dam",** Applied Mechanics Department and Prof. L.D. College of Engineering, Gujarat, India

31. Salgado F.M. and Byrne P.M. (1988), **"Evaluation of a three Dimension Method of Slope Stability Analysis",** Department of civil Engineering, The University of British, Columbia, Vancouver, B.C., Canada V6T 1W5.

32. Sherard J.L., Woodward R.J., Gizienski S.G. and Cleverger W.A. (1963) **" Earth and Earth Rock Dams",** John Wiley and Sons

33. Spencer, E., (1967). "**A Method of Analysis for the Stability of Embankments Assuming Parallel Inter-Slice Forces**", Geotechnique, Vol. 17, March, pp. 11-26.

34. Stephenson, D., (1978), **"Drawdown in embankments",** Geotechnique, Vol.28, No.3, pp.273-280.

35. Subuh, M. A., (2002), **“finite element solution for unconfined seepage problem with references to Al-Qadisiya Dam”** M.Sc. Dissertation, Department of Civil Engineering, University Of Babylon.

36. Taha Mohd Raihan, Khagehzaded M. and El-Shafie Ahmed, (2010) **“Slope Stability Assessment Using Optimization Techniques: an Overview”**, Civil and Structure Engineering Department, University Kebangsaan Malaysia.

37. Tran X. Tho, (2008) **“Stability Problems of an Earth Fill Dam in Rapid Drawdown Condition ”,** Grant Project, No.1/9066/02.

38.U.S. Army Crops of Engineers, (1986), **“Seepage principles”,** Manual, EM1110-2-1901, Chapter 4.

39.U.S. Army Crops of Engineers, (2003a), **“Slope Stability”,** Manual, EM1110-2-1902, Chapter 2.; Design Considerations.

40.U.S Army Corps of Engineers (2003b) “**Appendix G - Procedures and Examples for Rapid Drawdown”**. Engineering Manual, EM 1110-2-1902. Department of the U.S Army Corps of Engineers.

41.USBR, 2001, **“Safety Evaluation of Existing Dams”** (SEED) Manual, United States Bureau of Reclamation, Denver, Colorado.

42. Whitman, R.V. and Bailey, W.A., (1967), “**Use of computers for slope stability**”, Journal of Geotechnical Engineering, ASCE, Vol.93, No.SM4, pp.475-498.

43. Zhang Jianhong, Xu Qianjum and Chen Zuyu, (2000), **“ Seepage Analysis Based on The Unified Unsaturated Soil Theory ”,** 1 Department of Civil Engineering, Hong Kong University of Science and Technology, Clear Water Bay, Kowloon Hong Kong. 2 Department of Geotechnical Engineering, Wayne State University Detroit, MI, USA, 48202. 3 Department of Geotechnical Engineering, China Institute of Water Resources and Hydropower Research Beijing, P.R. China, 100044

44. Zienkiewicz, O.C., Mayer, P., and Cheung, Y.K., (1966), “**Solution of anisotropic seepage by finite elements”,** Journal of the Engineering Mechanics Division, ASCE, Vol.92, No.EM1, pp.111-120

APPENDIX- A

SLIDE V.6.0 COMPUTER PROGRAM

A-1 General

SLIDE V.6.0 is the most comprehensive slope stability analysis available, complete with sensitivity, probabilistic and back analysis capabilities. It is the only slope stability software to include built-in steady state unsaturated groundwater analysis capabilities using the finite element method. This program is product of **Rocscience** Inc., company.

SLIDE analyzes the stability of slip surfaces using vertical slice limit equilibrium methods (e.g. Bishop, Janbu, Spencer, etc). Individual slip surfaces can be analyzed, or search methods can be applied to locate the critical slip surface for a given slope. Deterministic (safety factor) or probabilistic (probability of failure) analyses can be carried out.

Features include:

- Analysis methods include Bishop, Janbu, Spencer, GLE / Morgenstern-Price.
- Probabilistic analysis – calculate probability of failure, reliability index and Sensitivity analysis.
- Groundwater – piezo surfaces, Ru factors, pore pressure grids, finite element groundwater analysis (see below), B-bar factor (excess pore pressure).
- Tension crack (dry or water filled).
- Critical surface search methods for circular or non-circular slip surfaces.
- Multiple materials.
- Anisotropic, non-linear Mohr-Coulomb materials.
- External loading – line, distributed or seismic.

- Support – soil nails, tiebacks, geotextiles, piles. Infinite strength (slip surface exclusion) zones.

A-2 SLIDE Model

The **SLIDE** program consists of 3 program modules:

- **MODEL**
- **COMPUTE**
- **INTERPRET**

MODEL is the pre-processing program used for entering and editing the model boundaries, loads, material properties, groundwater conditions, slip surface definition, and saving the input file.

MODEL, **COMPUTE** and **INTERPRET** will each run as standalone programs. They also interact with each other as illustrated in figure (A-1) below:

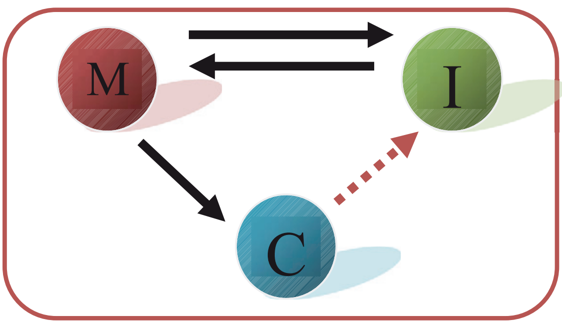

Figure (A-1) the Interact between (Model, Compute and Interpret) with Each Other in SLIDE Program.

The structure block of the input data is shown in Figure (A-2). This diagram describes the main features of the input data, and describes the model of groundwater and slope stability by using **SLIDE** program.

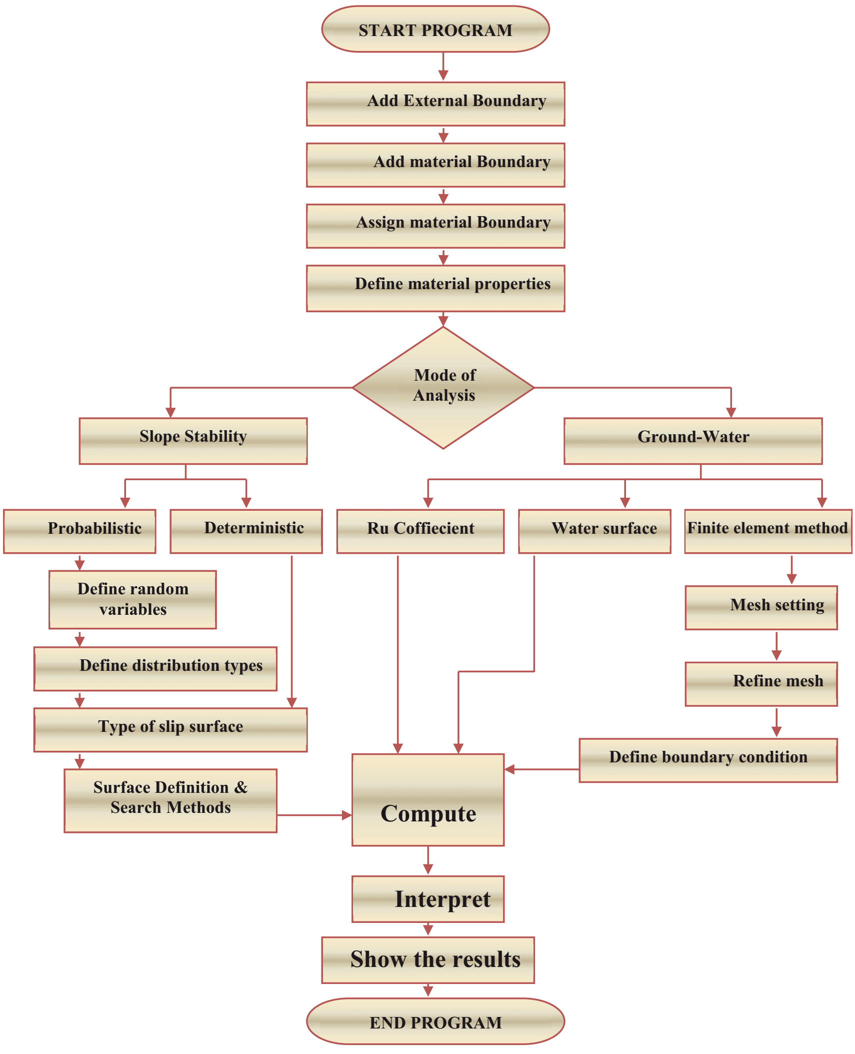

Figure (A-2) Structure Plocks of the Modeling by **SLIDE** Program for both, Seepage Analysis and Slope Stability Analysis.

Appendix- B

Step by Step Solution by SLIDE

APPENDIX- B

STEP BY STEP SOLUTION BY SLIDE

B.1 General.

The following paragraphs present step by step solution of examples problems that prementioned in Chapter four in part of parametric and drawdown analysis of slope stability analysis using **SLIDE** program.The first step show the effect of some design parameters on the stability of side slope of earth dams

B.2 General Example

Table (B.1), and (B.2) shows the input and output parameters of general example and the values of factor of safety that were found by using **SLIDE** program when the values of the angle of internal friction (ϕ = 10°, 20°, 25°,28°, 34°, and40°) and the value of cohesion of soil(c) and unit weight of soil (γ) decreasing and increasing

Table (B.1): the Factor of Safety for Different Values for Angle of Internal Friction of Soil when the Value of Cohesion (c) Decreasing and Increasing

Input Parameters				**Output Parameters**
Ex. No	**ϕ^o**	**c kPa**	**γ kN/m^3**	FOS by **SLIDE** Prog.
1	5	20	20	0.919
	10			1.069
	20			1.386
	25			1.559
	28			1.670
	34			1.910
	40			2.186
2	5	16	20	0.765
	10			0.915
	20			1.232
	25			1.405
	28			1.515
	34			1.756
				2.031
3	5	30	20	1.305
	10			1.455
	20			1.772
	25			1.945
	28			2.056
	34			2.297
	40			2.572

Table (B.2): the Factor of Safety for Different Values for Angle of Internal Friction of Soil when the Value of Unit Weight (γ) Decreasing and Increasing

Input Parameters				Output Parameters
Ex. No	ϕ^o	c kPa	γ kN/m^3	FOS by **SLIDE** Prog.
1	5	20	20	0.919
	10			1.069
	20			1.386
	25			1.559
	28			1.670
	34			1.910
	40			2.186
2	5	20	18	0.995
	10			1.134
	20			1.428
	25			1.589
	28			1.692
	34			1.915
	40			2.170
3	5	20	22	0.858
	10			1.016
	20			1.352
	25			1.535
	28			1.652
	34			1.906
	40			2.199

Table (B.3), and (B.4) shows the input and output parameters of general example and the values of factor of safety that were found by using **SLIDE** program when the values cohesion (c = 10, 20, 30, 40 and50 kPa) of and the value of angle of internal friction (ϕ), and unit weight of soil (γ) decreasing and increasing.

Table (B.3) the Factor of Safety for Different Values of Cohesion when the Value of Angle of Internal Friction (ϕ) Decreasing and Increasing.

Input Parameters				**Output Parameters**
Ex. No	**c kPa**	**ϕº**	**γ kN/m³**	FOS by **SLIDE** Prog.
1	10	28	20	1.283
	20			1.670
	25			1.863
	30			2.056
	40			2.442
	50			3.983
2	10	23	20	1.102
	20			1.489
	25			1.682
	30			1.875
	40			2.260
	50			3.802
3	10	34	20	1.523
	20			1.910
	25			2.104
	30			2.297
	40			2.683
	50			4.224

Table (B.4) the Factor of Safety for Different Values of Cohesion when the Value of Unit Weight (γ)Decreasing and Increasing

Input Parameters				Output Parameters
Ex. No	**c kPa**	**ϕ^o**	**γ kN/m^3**	FOS by **SLIDE** Prog.
1	10	28	20	1.283
	20			1.670
	25			1.863
	30			2.056
	40			2.442
	50			3.983
2	10	28	18	1.262
	20			1.692
	25			1.906
	30			2.121
	40			2.550
	50			2.979
3	10	28	22	1.300
	20			1.652
	25			1.827
	30			2.002
	40			2.353
	50			3.754

Table (B.5), and (B.6) shows the input and output parameters of general example and the values of factor of safety that were found by using **SLIDE** program when the values of unit weight of soil (γ =14, 16,18,20,22 and 23 kN/m^3) and the value of angle of internal friction (ϕ), and cohesion of soil(c) decreasing and increasing.

Table (B.5) the Factor of Safety for Different Values of Unit Weight of Soil when the Value of Cohesion Decreasing and Increasing

Input Parameters				Output Parameters
Ex. No	**γ kN/m³**	**c kPa**	**ϕ°**	FOS by **SLIDE** Prog.
1	14	20	28	1.755
	16			1.719
	18			1.692
	20			1.670
	22			1.652
	23			1.644
2	14	16	28	1.533
	16			1.526
	18			1.520
	20			1.515
	22			1.511
	23			1.510
3	14	30	28	2.308
	16			2.203
	18			2.121
	20			2.056
	22			2.002
	23			1.979

Table (B.6) the Factor of Safety for Different Values of Unit Weight of Soil when the Value of Angle of Internal Friction (ϕ) Decreasing and Increasing.

Input Parameters				Output Parameters
Ex. No	γ kN/m	**C** kPa	ϕ^{o} 3	FOS by **SLIDE** Prog.
	14			1.755
	16			1.719
1	18	20	28	1.692
	20			1.670
	22			1.652
	23			1.644
	14			1.624
	16			1.568
2	18	20	23	1.524
	20			1.489
	22			1.460
	23			1.448
	14			1.928
	16			1.921
3	18	20	34	1.915
	20			1.910
	22			1.906
	23			1.905

Table (B.7), (B.8) and (B.9) shows the input and output parameters of general example and the values of factor of safety that were found by using **SLIDE** program when the values of seismic force coefficients (0.05, 0.07, 0.1, 0.13, 0.15 and 0.2) and the value of angle of internal friction (ϕ), cohesion of soil(c) and unit weight of soil (γ) decreasing and increasing. It can be observed from the table that the factor of safety decreases with the increase of seismic force coefficients.

Table (B.7) the Factor of Safety for Different Values of Seismic Force Coefficients and when the Value of Angle of Internal Friction Decreasing and Increasing

Input Parameters					**Output Parameters**
Ex. No	seismic force coefficients	ϕ^o	**C kPa**	**γ kN/m**	FOS by **SLIDE** Prog.
1	0.05	28	20	20	1.460
	0.07				1.389
	0.1				1.293
	0.13				1.207
	0.15				1.255
	0.2				1.042
2	0.05	23	20	20	1.303
	0.07				1.241
	0.1				1.156
	0.13				1.081
	0.15				1.035
	0.2				0.936
3	0.05	34	20	20	1.667
	0.07				1.585
	0.1				1.474
	0.13				1.375
	0.15				1.316
	0.2				1.184

Table (B.8) the Factor of Safety for Different Values of Seismic Force Coefficients and when the Value of Cohesion of Soil(c) Decreasing and Increasing

Input Parameters					Output Parameters
Ex. No	**seismic force coefficients**	**γ kN/m^3**	**C kPa**	**ϕ^o**	**FOS by SLIDE Prog.**
1	0.05	20	20	28	1.460
	0.07				1.389
	0.1				1.293
	0.13				1.207
	0.15				1.255
	0.2				1.042
2	0.05	20	16	28	1.323
	0.07				1.257
	0.1				1.169
	0.13				1.091
	0.15				1.044
	0.2				0.940
3	0.05	20	30	28	1.803
	0.07				1.717
	0.1				1.601
	0.13				1.498
	0.15				1.436
	0.2				1.299

Table (B.9) the Factor of Safety for Different Values of Seismic Force Coefficients and when the Value of Unit Weight of Soil (γ) Decreasing and Increasing

Input Parameters					**Output Parameters**
Ex. No	seismic force coefficients	ϕ^o	**C kPa**	**γ kN/m**	FOS by **SLIDE** Prog.
1	0.05	28	20	20	1.460
	0.07				1.389
	0.1				1.293
	0.13				1.207
	0.15				1.255
	0.2				1.042
2	0.05	28	20	18	1.479
	0.07				1.407
	0.1				1.310
	0.13				1.223
	0.15				1.171
	0.2				1.056
3	0.05	28	20	22	1.444
	0.07				1.374
	0.1				1.278
	0.13				1.194
	0.15				1.143
	0.2				1.030

Table (B.10) shows the input and output parameters of the general example and the values of the factor of safety were found by using **SLIDE** program when the values of the distributed load and the value of the cohesion of the soil(c) is decreasing or increasing. It can be observed from the table that the factor of safety

Table (B.10) Table (B.10) The Factor of Safety for Different Values of Distributed Load decreases with the increase of the distributed load

Input Parameters					Output Parameters
Ex. No	distributed load(**kN/m²**)	**C** **kPa**	**γ** **kN/m**	**ϕ^{o}** 3	FOS by **SLIDE** Prog.
1	0	20	20	28	1.744
	10				1.724
	20				1.705
	30				1.687
	40				1.670
	50				1.653
	60				1.636
2	0	10	20	28	1.551
	10				1.534
	20				1.519
	30				1.503
	40				1.489
	50				1.474
	60				1.460
3	0	30	20	28	1.936
	10				1.914
	20				1.892
	30				1.871
	40				1.850
	50				1.830
	60				1.811

Table (B.11) and (B.12) shows the input and output parameters of general example and the values of factor of safety that were found by using **SLIDE** program when the values of drawdown ratio (0.34, 0.45, 0.56, 0.67, and 1)and the value of angle of internal friction (ϕ) andcohesion of soil(c) decreasing and increasing.

Table (B.11) the Factor of Safety for Different Values of Cohesion of Soil with Drawdown Effect

Input Parameters					**Output Parameters**
Ex. No	drawdown ratio(D/H)	**C kPa**	**ϕº**	**γ kN/m**	FOS by **SLIDE** Prog.
1	0.34	20	28	20	2.689
	0.45				2.117
	0.56				1.753
	0.67				1.560
	1				1.522
2	0.34	10	28	20	2.376
	0.45				1.847
	0.56				1.510
	0.67				1.331
	1				1.295
3	0.34	30	28	20	3.003
	0.45				2.390
	0.56				1.998
	0.67				1.791
	1				1.750

Table (B.12) the Factor of Safety for Different Values of Internal Friction of Soil with Drawdown Effect

Input Parameters					Output Parameters
Ex. No	drawdown ratio(D/H)	**C kPa**	**ϕº**	**γ kN/m**	FOS by **SLIDE** Prog.
1	0.34	20	28	20	2.689
	0.45				2.117
	0.56				1.753
	0.67				1.560
	1				1.522
2	0.34	20	22	20	2.193
	0.45				1.740
	0.56				1.450
	0.67				1.296
	1				1.266
3	0.34	20	34	20	3.243
	0.45				2.541
	0.56				2.094
	0.67				1.857
	1				1.810

APPENDIX- C

RESULTS OF SLIDE PROGRAM
(MANDALI DAM AS A CASE STUDY)

C.1 General

Hydraulic structures such as dams, weirs, barrages, regulators,.etc., may either be founded on impervious solid rock or on a pervious foundation. Whenever such structure is founded on a pervious foundation, it is subjected to seepage of water beneath the structures, in addition to all other forces to which it will be subjected when founded on an impervious foundation.

In Iraq, most of these hydraulic structures are founded to be on pervious layers which do allow seepage beneath them, such as the Mandali dam. Mandali dam project it's one of the projects of the Ministry of Water Resources Republic of Iraq had been Produced by Rafidain General Company for dam construction.

C.2 Details of Field Works

The geological investigations were carried on in the site selected for construction of Mandali dam, investigation had been carried out through drilling (4) holes different depth along the dam axis, performing field tests in drill holes ,excavation of test pits in construction materials borrow area and alithologic section along the dam axis was prepared based on the succession of lithologic units encountered in drill holes as shown in figures (C.1) and (C.2). **(Directorate General of Dams and Reservoire,(2004))**.

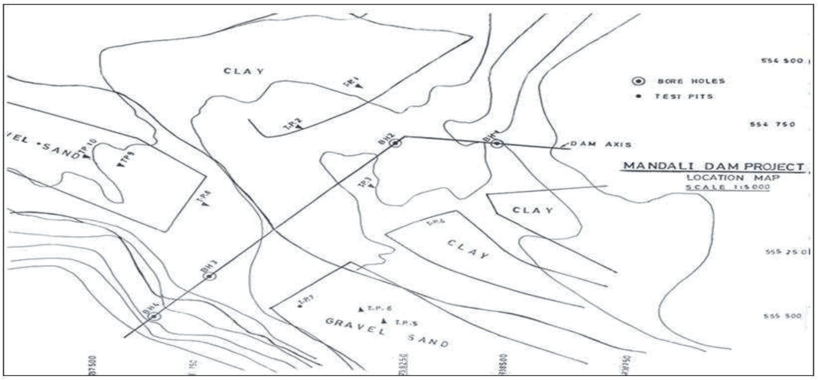

Figure (C.1) the Location Map of Mandali Dam**(Directorate General of Dams and Reservoir,(2004)).**

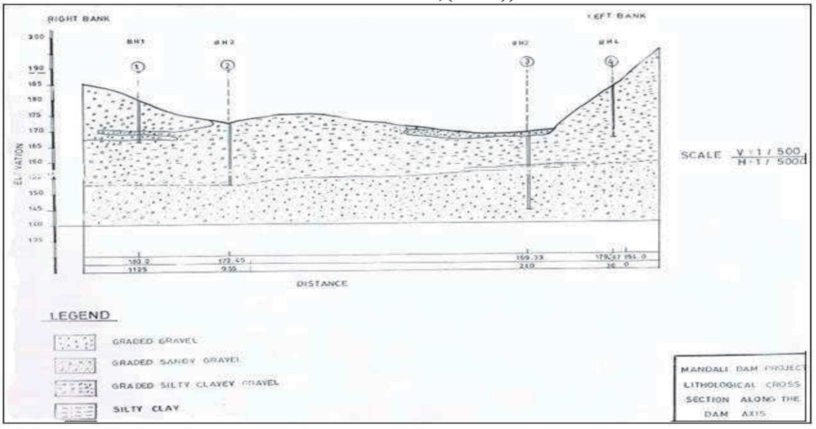

Figure (C.2) Alithologic Section along the Mandali Dam Axis**(Directorate General of Dams and Reservoir,(2004))**.

C.3Results and Discussion

C.3.1 Seepage Analysis Results

For first section the figures (C.2), (C.3) show contour maps for total head and pressure head distributions throughout the dam body at normal operation conditions.

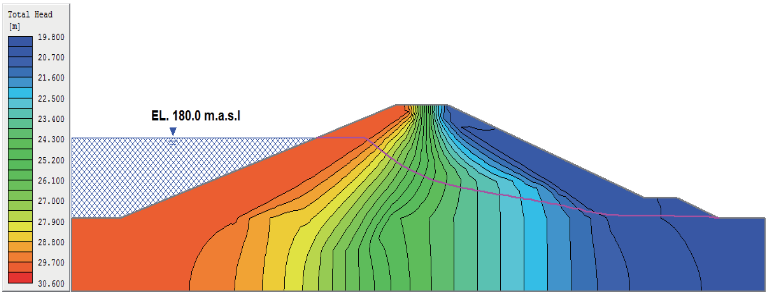

Figure (C.3) Computed Contour Maps for Total Head Distribution for Normal Water Level (180.0m.a.s.l.) First Case

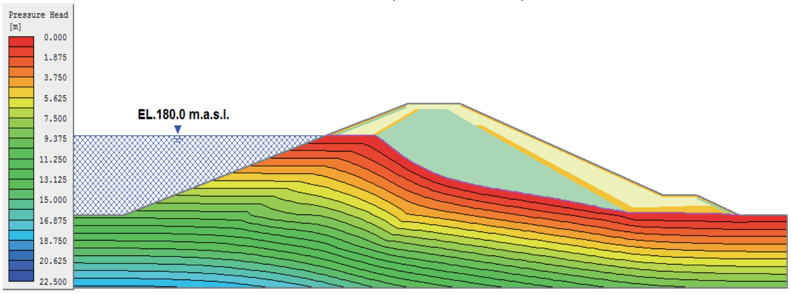

Figure (C.4) Computed Contour Maps for Pressure Head Distribution for Normal Water Level (180.0m.a.s.l.) First Case

For second section the figures (C.5) and (C.6) show contour maps for total head and pressure head distributions throughout the dam body at normal operation conditions.

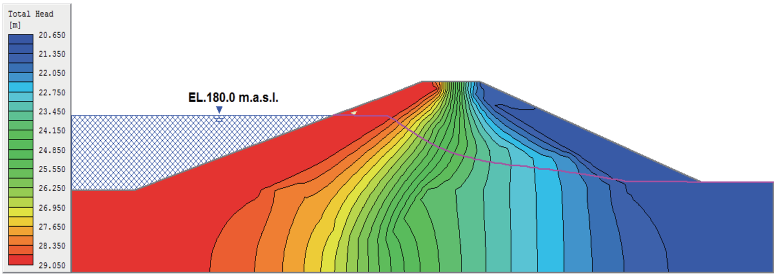

Figure (C.5) Computed Contour Maps for Total Head Distribution for Normal Water Level(180.0m.a.s.l.) Second Case

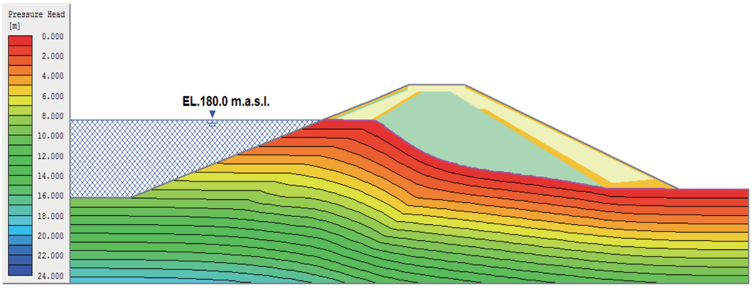

Figure (C.6) Computed Contour Maps for Pressure Head Distribution for Normal Water Level (180.0m.a.s.l.) Second Case

For second section the figures (C.7) and (C.8) show contour maps for total head and pressure head distributions throughout the dam body at normal operation conditions.

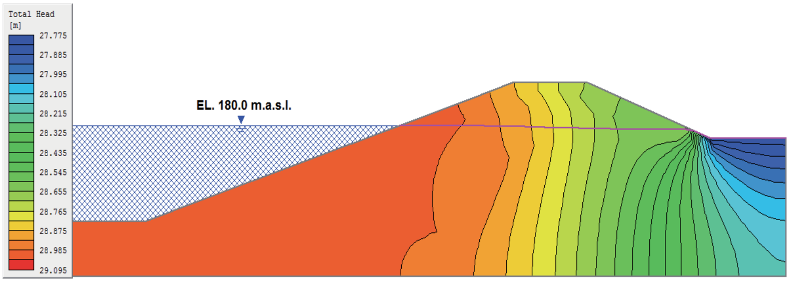

Figure (C.7) Computed Contour Maps for Total Head Distribution for Normal Water Level (180.0m.a.s.l.) Third Case

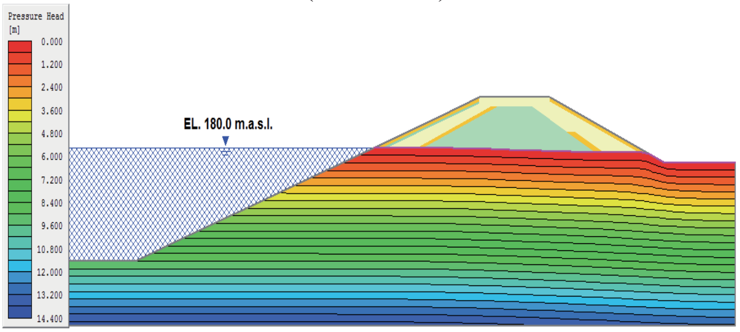

Figure (C.8) Computed Contour Maps for Pressure Head Distribution for Normal Water Level (180.0m. a.s.l.) Third Case

The head and pressure distributions for maximum water level for first section are demonstrated in Figures (C.9) and (C.10), respectively

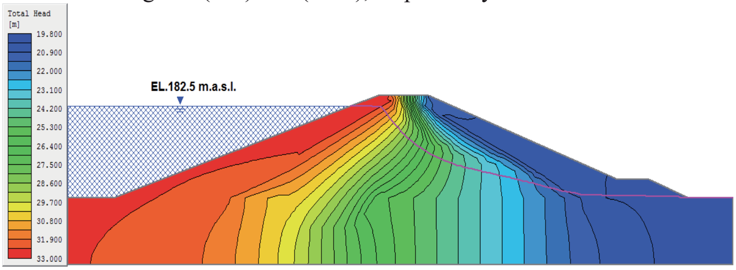

Figure (C.9) Computed Contour Maps for Total Head Distribution for Maximum Water Level(182.5m.a.s) First Case

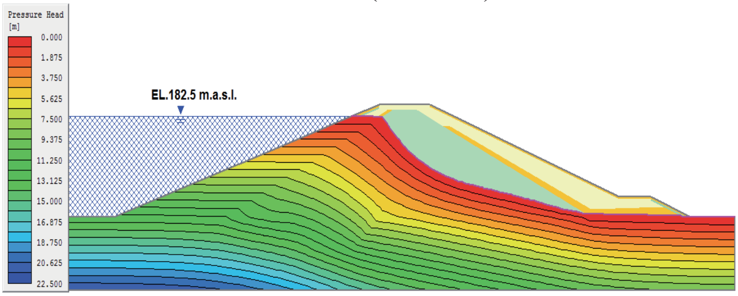

Figure (C.10) Computed Contour Maps for Pressure Head Distribution for Maximum Water Level (182.5m.a.s.l.) First Case

The head and pressure distributions for second section are demonstrated in Figures (C.11) and (C.12), respectively.

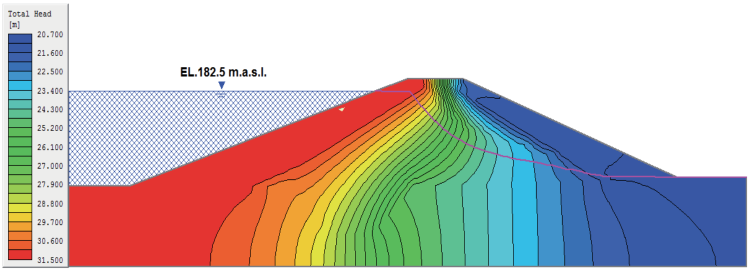

Figure (C.11) Computed Contour Maps for Total Head Distribution for Maximum Water Level (182.5m.a.s) Second Case

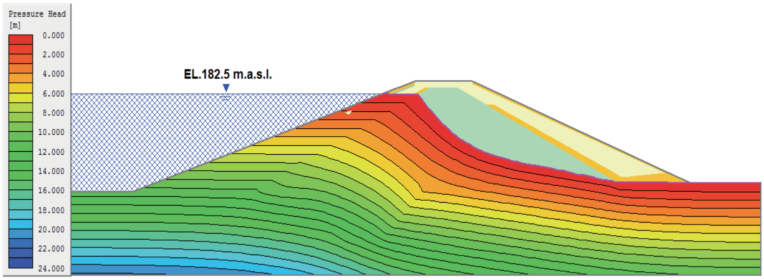

Figure (C.12) Computed Contour Maps for Pressure Head Distribution for Maximum Water level (182.5m.a.s.l.) Second Case

The head and pressure distributions for third section are demonstrated in Figures (C.13) and (C.14), respectively.

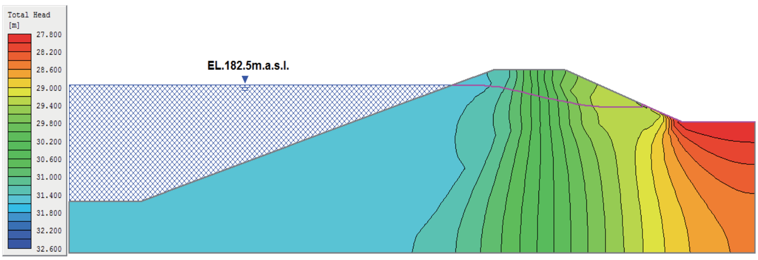

Figure (C.13) Computed Contour Maps for Total Head Distribution for Maximum Water Level (182.5m.a.s)

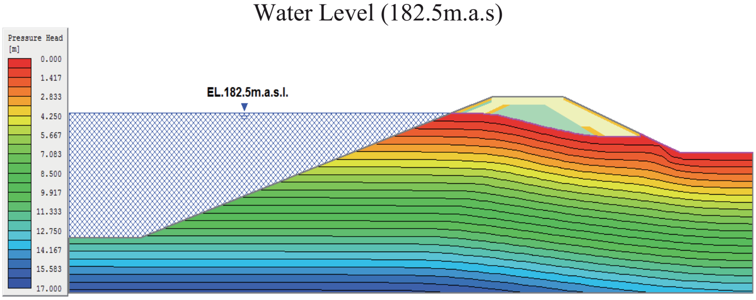

Figure (C.14) Computed Contour Maps for Pressure Head Distribution for Maximum Water Level (182.5m.a.s.l.)

For first section the figures (C.15) and (C.16) display the total head and pressure head distributions due to the minimum water level in reservoir.

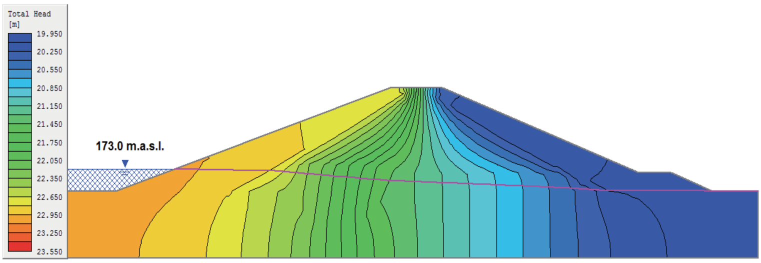

Figure (C.15) Computed Contour Maps for Total Head Distribution for Minimum Water Level(170.0m.a.s)

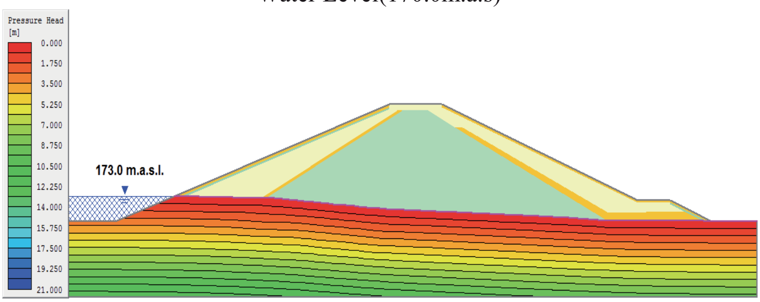

Figure (C.16) Computed Contour Maps for Pressure Head Distribution for Minimum Water Level (170.0m.a.s.l.)

For second section the Figures (C.17) and (C.18) display the total head and pressure head distributions due to the minimum water level in reservoir

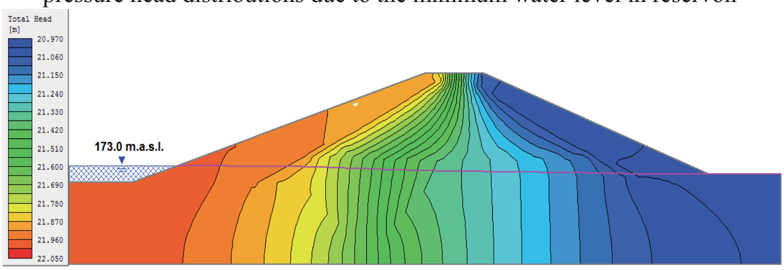

Figure (C.17) Computed Contour Maps for Total Head Distribution for Minimum Water Level(170.0m.a.s)

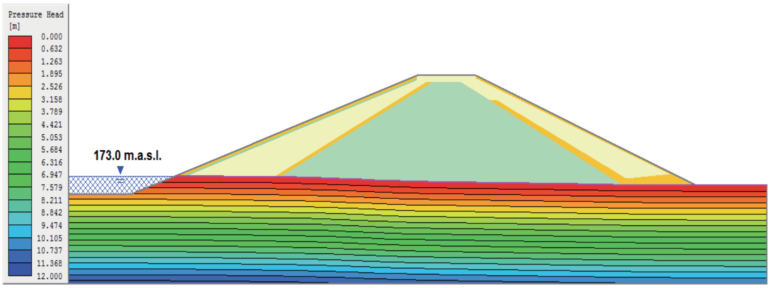

Figure (C.18) Computed Contour Maps for Pressure Head Distribution for Minimum Water Level (170.0m.a.s.l.)

For third section the Figures (C.19) and (C.20) display the total head and pressure head distributions due to the minimum water level in reservoir.

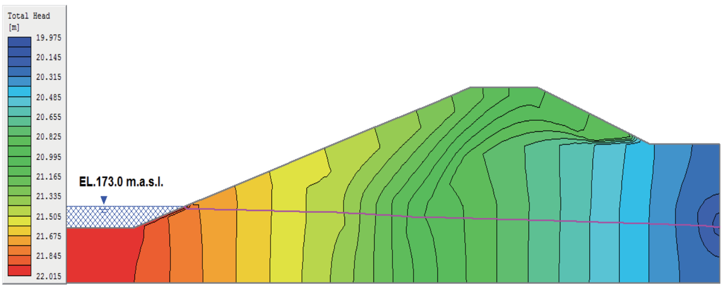

Figure (C.19) Computed Contour Maps for Total Head Distribution for Minimum Water Level(170.0m.a.s)

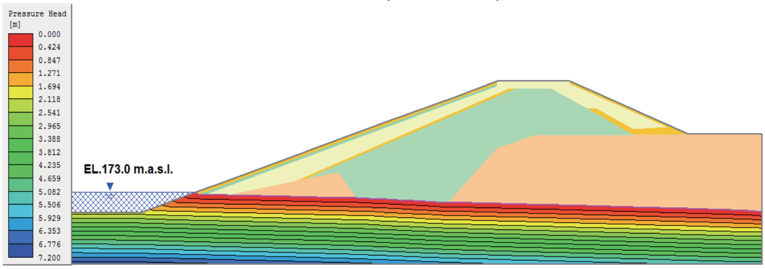

Figure (C.20) Computed Contour Maps for Pressure Head Distribution for Minimum Water Level(170.0m.a.s.l.)

الخلاصة

في هذا البحث تم استخدام طريقة العناصر المحددة بأستخدام البرنامج التحليلي SLIDE (version 6.0) وبالاعتماد على نظريتي التحليل: الحتمي والاحتمالي لتحليل أستقرارية الميل الجانبي للسدود الترابية تحت تأثير الأحمال المختلفة. طريقة الاتزان المحدد تبعا ل(Bishop and Morgenstern-Price) استخدامة بواسطة برنامج الحاسوب, واستخدم هذا البرنامج لتعريف وتحديد سطح الفشل وحساب عامل الأمان للميول الجانبية في السد. وجرت دراسة تأثيرات عناصر التصميم الأساسية والأحمال المؤثرة على قيمة معامل الأمان.

التحليل الحتمي يتضمن معاملات سطح الماء (موقع السطح الحر للماء مع تاثير انواع من المبازل، خطوط الجريان) و خواص التربة (معاملات قوة القص) والأحمال الديناميكية المؤثرة (الهبوط المفاجئ وقوة الهزة الأرضية والاحمال المنتشره) والتحليل الاحتمالي يتضمن (احتمالية الفشل وتحليل الحساسيه(sensitivity analysis)). والنتائج التي أستحصلت من التحليل الحتمي اوضحت ان معامل الامان يقل بنسبة بنسبة (6.32%) مع زيادة كثافة التربه و بنسبة (28.67%) مع زيادة معامل الهزه الارضيه وبنسبة (48.754%)مع زيادة نسبة النزول المفاجئ. معامل الامان يزداد بين (15.40% - 0.83%) للمبزل الافقي و (15.53% -2.03%) للمبزل الامامي و(16.428% -12.09%) للمبزل العمودي وبنسبة (67.78%) مع زيادة تماسك التربه وبنسبة (57.95%)مع زيادة زاوية الاحتكاك الداخلي للتربه.

اما التحليل الاحتمالي فان النتائج أوجدت بأن احتمالية الفشل تساوي(55.2 %) وتأثير معاملات التصميم بتحليل الحساسية لكلّ المتغيرات التي لَها تأثيراتُ ملموسة على استقرارية السد. وجد ان استقرارية الميل الجانبي للسد في المقدمة تتناقص تدريجيا في حالة انخفاض مستوى الماء في مقدمة السد من بدء الانخفاض وحتى وصوله الى نسبة (0.78) من الارتفاع, التي عندها تحصل اخطر حالات عدم الاستقرار,. في حالة السد الممنطق(zoned)(آخذين سد مندلي كحالة تطبيقية) استخدمت نظرية العناصر المحددة لحل مسالة الترشح وإيجاد موقع السطح الحر للجريان وتوزيع ضغط الماء المسامي داخل جسم السد لثلاث مقاطع و لثلاث حالات مختلفة للتحميل، وهي مستوى ماء المقدمة الاعظم والاعتيادي والاخفض كذلك تمت دراسة أستقرارية الميل الجانبي تحت ظروف مختلفة للتحميل . لقد بينت النتائج المستحصلة من التحليل بان الحالة الحرجة ستحصل في مقدمة السد في حالة تزامن الخفض السريع لماء المقدم مع الهزة الارضية ، لكن السد سيكون قريبا من حالة السلامة في ظل الحالتين الاخريين المعتبرة(الخفض السريع لماء المقدم مع الهزة الارضية) ، حيث بلغت اقل قيمة لمعامل الامان (1,167)لمعامل هزة ارضيه (0.09). انتقال الماء خلال السد مع الزمن اوضح انه عند زمن (50000 hours, 6 years) سد مندلي يصل لحالة الجريان المنتظم